

Short Wavelength Accelerators (I)

Guoxing Xia
Cockcroft Institute and the University of Manchester

Part I

- ✧ Particle accelerators
- ✧ Why short wavelength accelerators?
- ✧ Why plasmas?
- ✧ Why lasers?
- ✧ Laser wakefield accelerators (LWFA)
 - ❖ Electron acceleration from LWFA
 - ❖ Radiation sources
 - ❖ Proton/ion acceleration
- ✧ Conclusions

Parts II

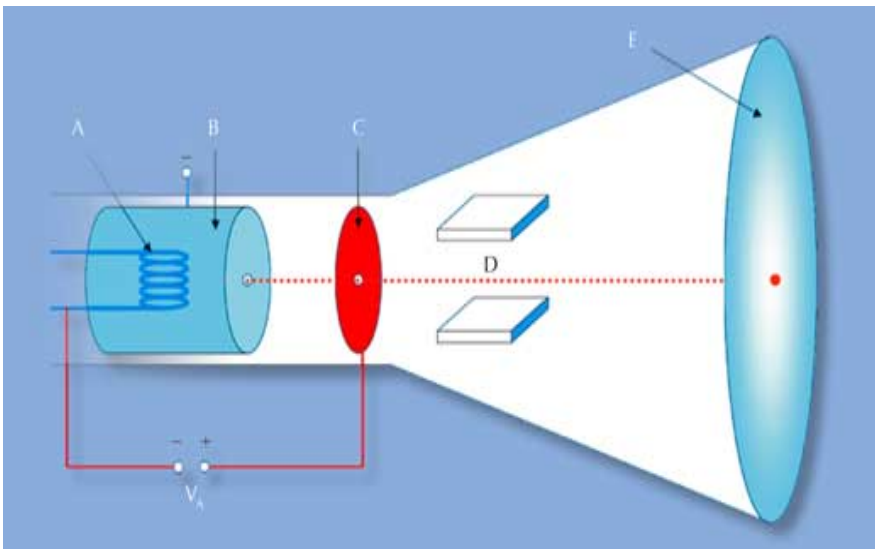
- ✧ Beams from conventional accelerators
- ✧ Plasma wakefield accelerators (PWFA)
 - ❖ Electron driven PWFA
 - ❖ Positron driven PWFA
 - ❖ Proton driven PWFA
- ✧ Dielectrics in accelerators
 - ❖ Laser driven dielectric accelerators
 - ❖ Beam driven dielectric accelerators
- ✧ Conclusions and future perspectives

Learning objectives-Lecture I

- ? Motivations for short wavelength accelerators
- ? How laser-plasma acceleration works
- ? Limitations of laser-plasma accelerators
- ? Applications of laser-plasma accelerators

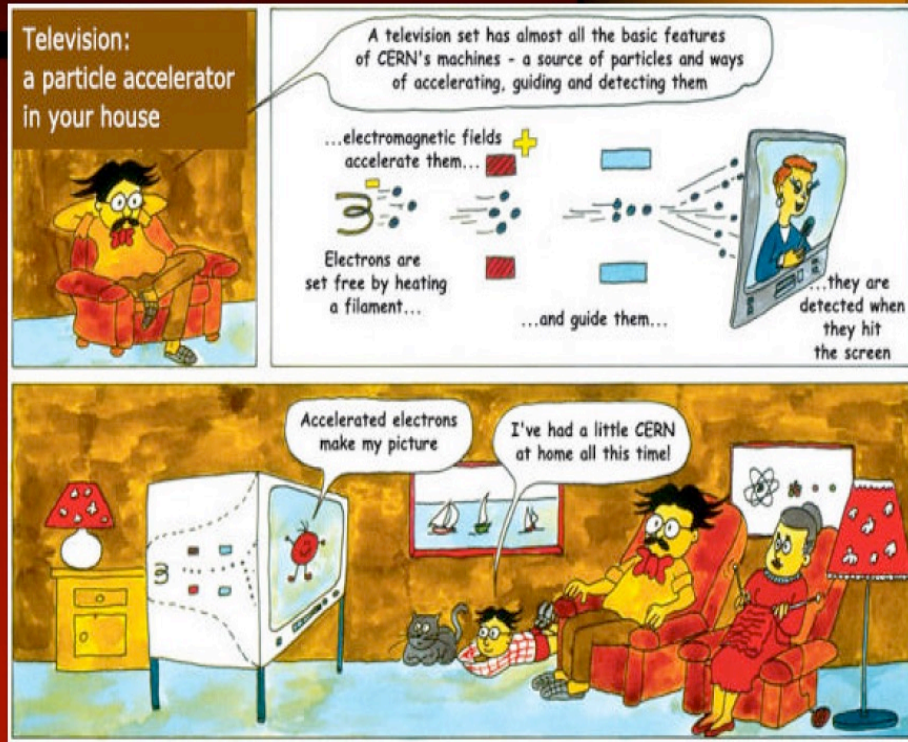
Particle accelerators

- A **particle accelerator** is a device that uses electromagnetic fields to propel charged particles to high speeds and to contain them as beams.
- An ordinary CRT television set is a simple form of accelerator.



Principle of Accelerators:

A particle accelerators in your house



Particle accelerators

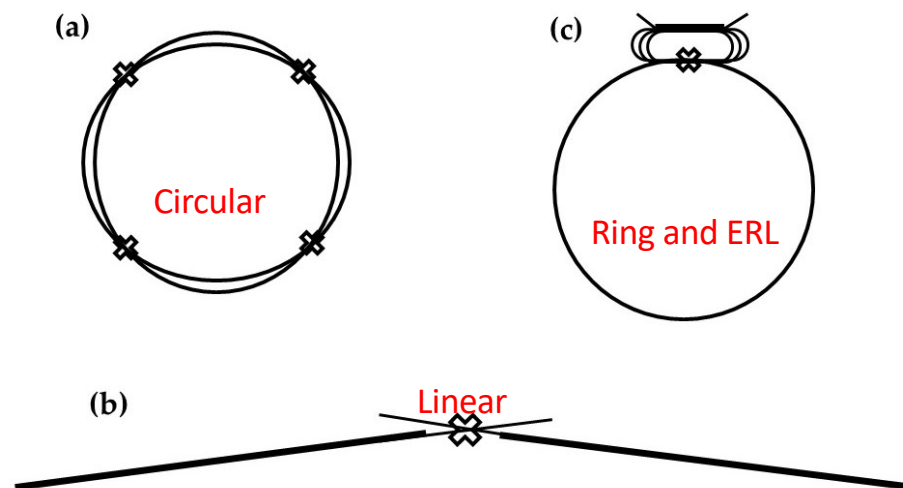
- Particle accelerators are unique instruments in physics research and many applications
- Provide well-focused, high-intensity beams of electrons, positrons, protons, antiprotons, muons, ions, photons, etc.
- Nobel prizes awarded for advancements in accelerator science and technology
 - Cockcroft and Walton, 1932 (HV accelerator)
 - Lawrence and Livingston, 1939 (cyclotron)
 - Van der Meer, 1985 (stochastic cooling)
- A quarter of the most acclaimed physics discoveries since 1939 using particle accelerators^[1]



[1] Haussecker and Chao (2011), Physics in Perspective, 13 (2), 146.

Colliders

- There are about 140 accelerators of all types worldwide for fundamental research
- Among these, the most complex and technologically advanced are high energy accelerators, especially colliders for nuclear and particle physics



Energy and luminosity

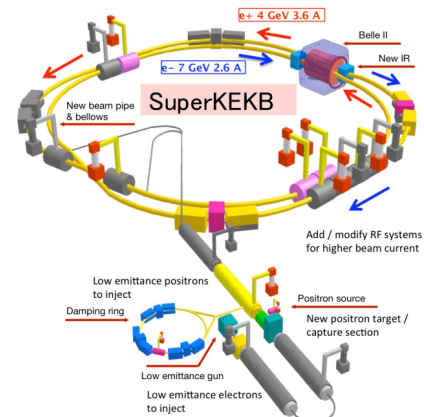
- For head-on collisions of two ultra-relativistic particles with equal energy E , the center-of-mass energy (E_{cme}) is given by $2E$
- For unequal particle energies, the center-of-mass energy is $2\sqrt{E_1 E_2}$
- For stationary target resulting $\sqrt{2Emc^2}$
- The highest cosmic rays observed on Earth reaching $E \sim 10^{21}$ eV, i.e. a million PeV (1 million $\times 10^{15}$ eV)
- The LHC achieves $E_{\text{cme}} = 14$ TeV or 0.014 PeV

Energy and luminosity

- The exploration of rare particle physics phenomena at the energy frontier requires not only the high energy, but also a sufficiently large number of detectable reactions, $N_{reaction}$
- This number is given by the product of the cross-section of the reaction under study, σ , and the time integral over the instantaneous collider luminosity, L , *i.e.* $N_{reaction} = \sigma \int L(t) dt$
- Colliders with bunched beams of particles with Gaussian distributions containing equal numbers of particles colliding head on, the luminosity is given by

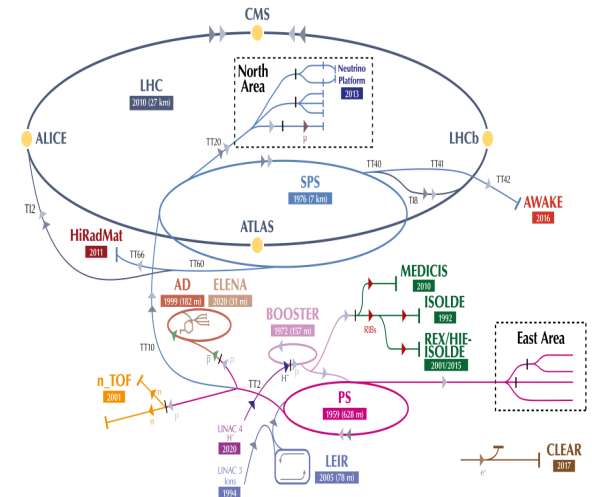
$$L = f_{rep} n_b \frac{N^2}{4\pi\sigma_x^* \sigma_y^*}$$

Colliders (1964-)



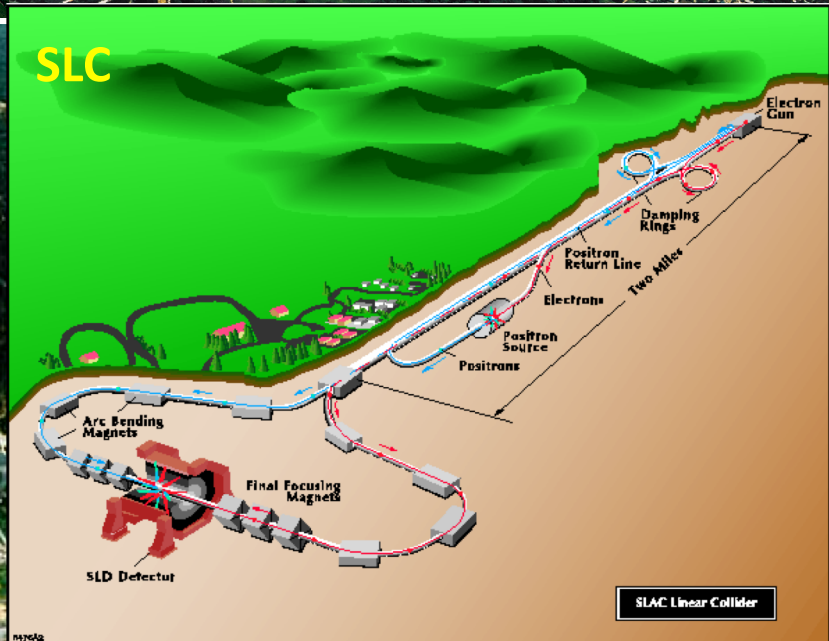
Colliders	Species	E_{cm} , GeV	C , m	\mathcal{L} , 10^{32}	Years	Host lab, country
AdA	e^+e^-	0.5	4.1	10^{-7}	1964	Frascati/Orsay
VEP-1	e^-e^-	0.32	2.7	5×10^{-5}	1964-68	Novosibirsk, USSR
CBX	e^-e^-	1.0	11.8	2×10^{-4}	1965-68	Stanford, USA
VEPP-2	e^+e^-	1.34	11.5	4×10^{-4}	1966-70	Novosibirsk, USSR
ACO	e^+e^-	1.08	22	0.001	1967-72	Orsay, France
ADONE	e^+e^-	3.0	105	0.006	1969-93	Frascati, Italy
CEA	e^+e^-	6.0	226	0.8×10^{-4}	1971-73	Cambridge, USA
ISR	pp	62.8	943	1.4	1971-80	CERN
SPEAR	e^+e^-	8.4	234	0.12	1972-90	SLAC, USA
DORIS	e^+e^-	11.2	289	0.33	1973-93	DESY, Germany
VEPP-2M	e^+e^-	1.4	18	0.05	1974-2000	Novosibirsk, USSR
VEPP-3	e^+e^-	3.1	74	2×10^{-5}	1974-75	Novosibirsk, USSR
DCI	e^+e^-	3.6	94.6	0.02	1977-84	Orsay, France
PETRA	e^+e^-	46.8	2304	0.24	1978-86	DESY, Germany
CESR	e^+e^-	12	768	13	1979-2008	Cornell, USA
PEP	e^+e^-	30	2200	0.6	1980-90	SLAC, USA
SppS	$p\bar{p}$	910	6911	0.06	1981-90	CERN
TRISTAN	e^+e^-	64	3018	0.4	1987-95	KEK, Japan
Tevatron	$p\bar{p}$	1960	6283	4.3	1987-2011	Fermilab, USA
SLC	e^+e^-	100	2920	0.025	1989-98	SLAC, USA
LEP	e^+e^-	209.2	26659	1	1989-2000	CERN
HERA	ep	30+920	6336	0.75	1992-2007	DESY, Germany
PEP-II	e^+e^-	3.1+9	2200	120	1999-2008	SLAC, USA
KEKB	e^+e^-	3.5+8.0	3016	210	1999-2010	KEK, Japan
VEPP-4M	e^+e^-	12	366	0.22	1979-	Novosibirsk, Russia
BEPC-I/II	e^+e^-	4.6	238	10	1989-	IHEP, China
DAΦNE	e^+e^-	1.02	98	4.5	1997-	Frascati, Italy
RHIC	p, i	510	3834	2.5	2000-	BNL, USA
LHC	p, i	13600	26659	210	2009-	CERN
VEPP2000	e^+e^-	2.0	24	0.4	2010-	Novosibirsk, Russia
S-KEKB	e^+e^-	7+4	3016	6000*	2018-	KEK, Japan
NICA	p, i	13	503	1*	2024(tbd)	JINR, Russia
EIC	ep	10+275	3834	105*	2032(tbd)	BNL, USA
Proposals	Species	E_{cm} , TeV	C , km	\mathcal{L}^* , 10^{35}	Years	Host lab, country
FCCee	e^+e^-	0.24	91	0.5	n/a	CERN
CEPC	e^+e^-	0.24	100	0.5	n/a	China
ILC-0.25	e^+e^-	0.25	20.5	0.14	n/a	Japan
CLIC-0.38	e^+e^-	0.38	11	0.15	n/a	CERN
ILC-1	e^+e^-	1	38	0.5	n/a	Japan
LHeC	ep	0.06+7	9+26.7	0.08	n/a	CERN
CLIC-3	e^+e^-	3	50	0.6	n/a	CERN
MC-3	$\mu^+\mu^-$	3	4.5	0.18	n/a	n/a
MC-14	$\mu^+\mu^-$	14	14	4	n/a	n/a
WFA-15	e^+e^-	15	12	5	n/a	n/a
WFA-30	e^+e^-	30	20	32	n/a	n/a
FCChh	pp	100	91	3	n/a	CERN
SPPC	pp	125	100	1.3	n/a	IHEP, China

Table 1: Past, present and several proposed future particle colliders: their particle species, center of mass energy E_{cm} , circumference or length C , maximum peak luminosity \mathcal{L} per interaction point, years of luminosity operation, and host labs. (i is for ions; luminosity is in units of $\text{cm}^{-2}\text{s}^{-1}$, * design; see also text.)

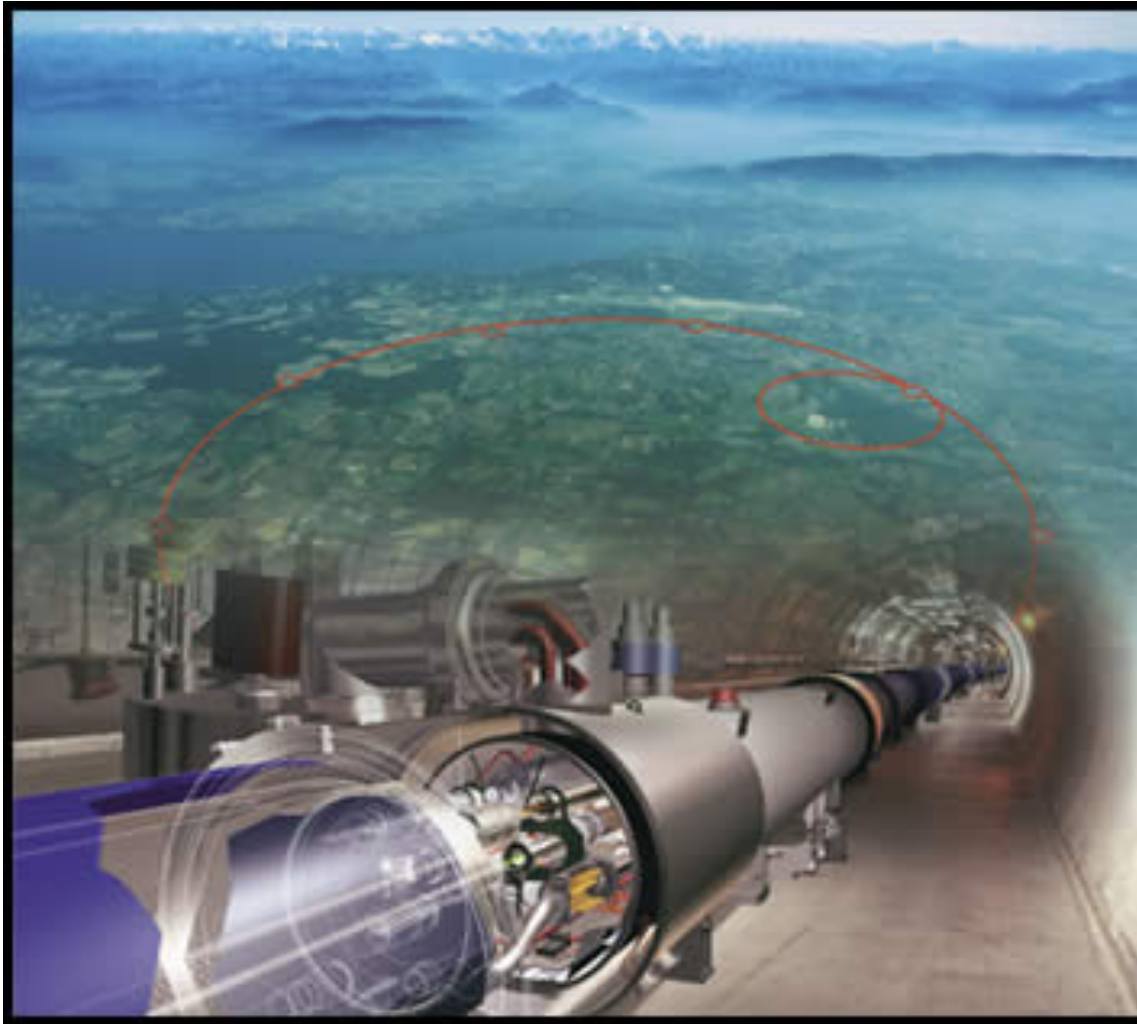


LHC

Giant machines

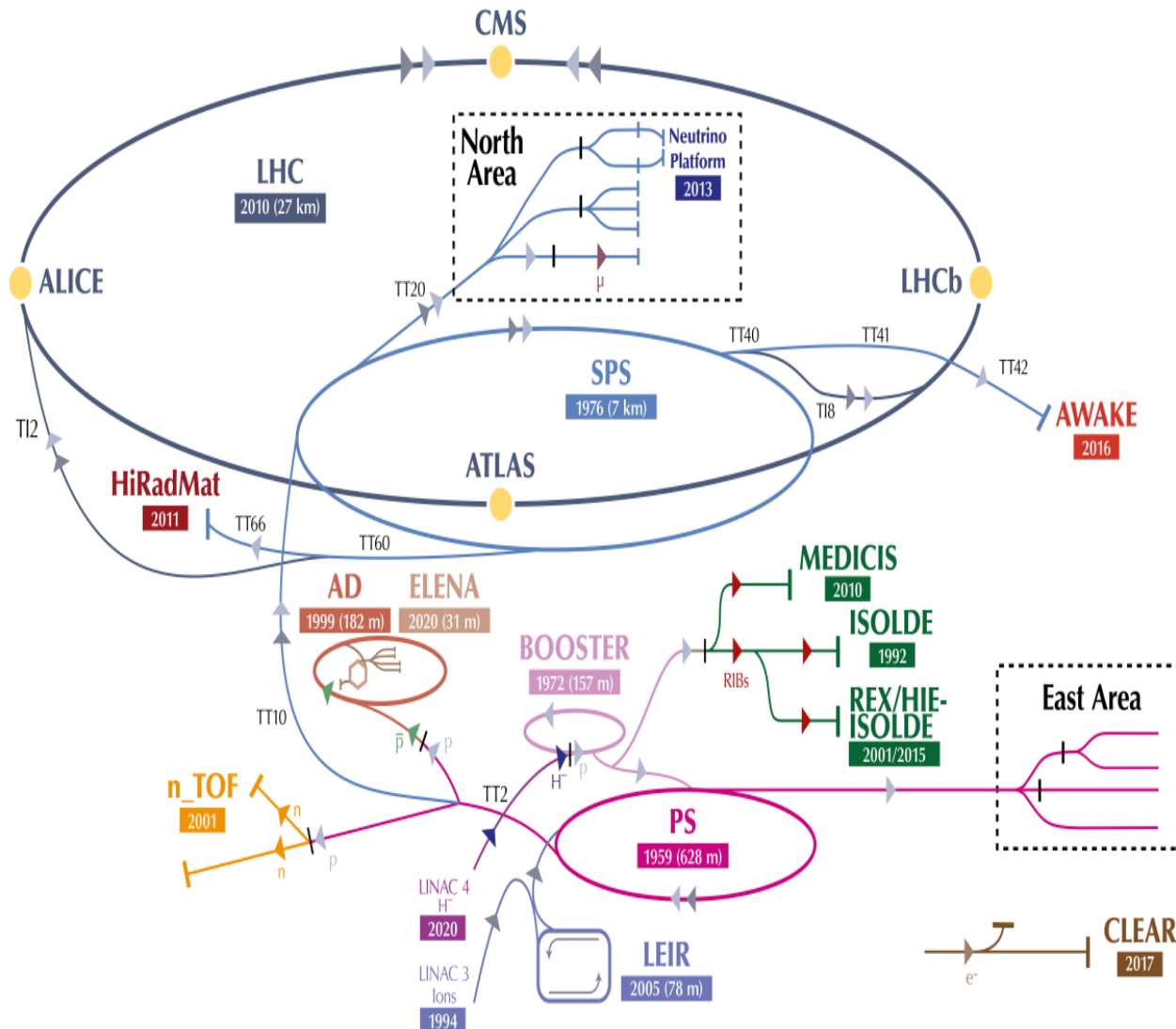


World biggest machine



- **LHC**: the world biggest accelerator, both in energy and size
- Grand start-up and perfect function at injection energy in September 2008
- An electrical fault halted the machine running
- First collisions in late 2009 (2.36 TeV)
- 7 TeV collisions in March 2010
- Higg bosons have been found in July 2012 !
- Record beam energy 6.5 TeV in April 2015
- LHC achieved CoM collision energy 13.6 TeV in 2022

Complex machine



The human's curiosity on the micro-world has always the driven force behind the development of the particle accelerators. The history of accelerators is a continuous upgrade for higher energy and better performance !

Then, what is the future (sustainable) of this technology, especially for the HEP machines?

Solutions:

Short wavelength accelerators

Motivations

- Sizes and costs reach the limit
- Traditional accelerators
 - Gradient: <100 MV/m limited by material breakdown
 - RF frequency range, 10s MHz to 10s GHz
 - Thus large facilities for energy frontier machines
- To shrink the facility one needs higher gradient:
 - Higher frequency to avoid breakdown:
 - L band (1.3 GHz) \Rightarrow S band (3 GHz) \Rightarrow C band (4-8 GHz)
 - X band (11 GHz) \Rightarrow Ku band (15 GHz) \Rightarrow W band (100 GHz)
 - To go further \Rightarrow optical frequency (~ 100 THz)
- How about using material already broken down (plasmas)?
- How about using higher breakdown materials (e.g. dielectrics?)

Motivations

- For a given peak power P of the RF, the electric fields E in structure increases as wavelength reduced by

$$E \sim P^{1/2} / \lambda$$

- The increase in breakdown fields is predicted to scale as from $f^{1/4}$ to $f^{7/8}$.

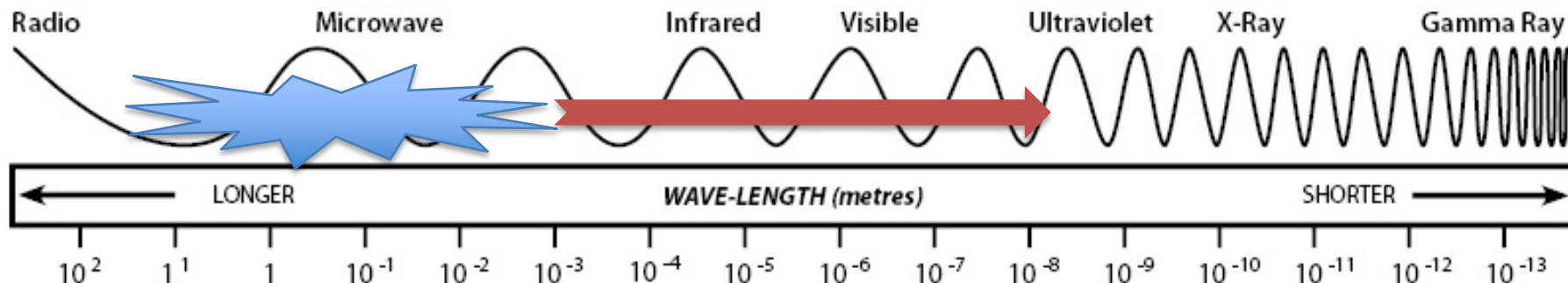
T. Katsouleas, AIP Proceedings 807 (2006)

THE ELECTRO MAGNETIC SPECTRUM

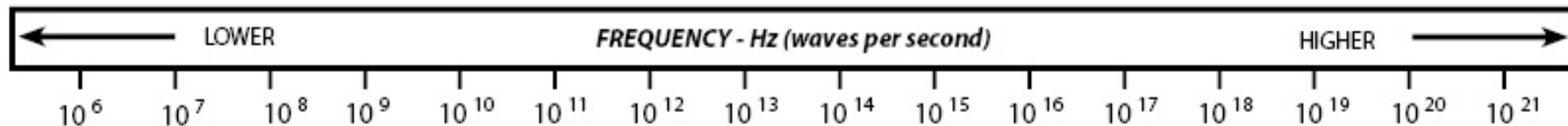
1 metre = 100cm 1 cm = 10mm 1 millimetre = 1000 microns 1 micron = 1000 nanometres (nm) - one nanometre is one billionth of a metre

$$10^{-5} = 0.00001 \quad 10^5 = 100,000$$

WAVE (type)



APPROXIMATE equivalent size to:



Electromagnetic Radiation detected by the human eye is called visible light and falls approximately between 700 and 400 nanometres

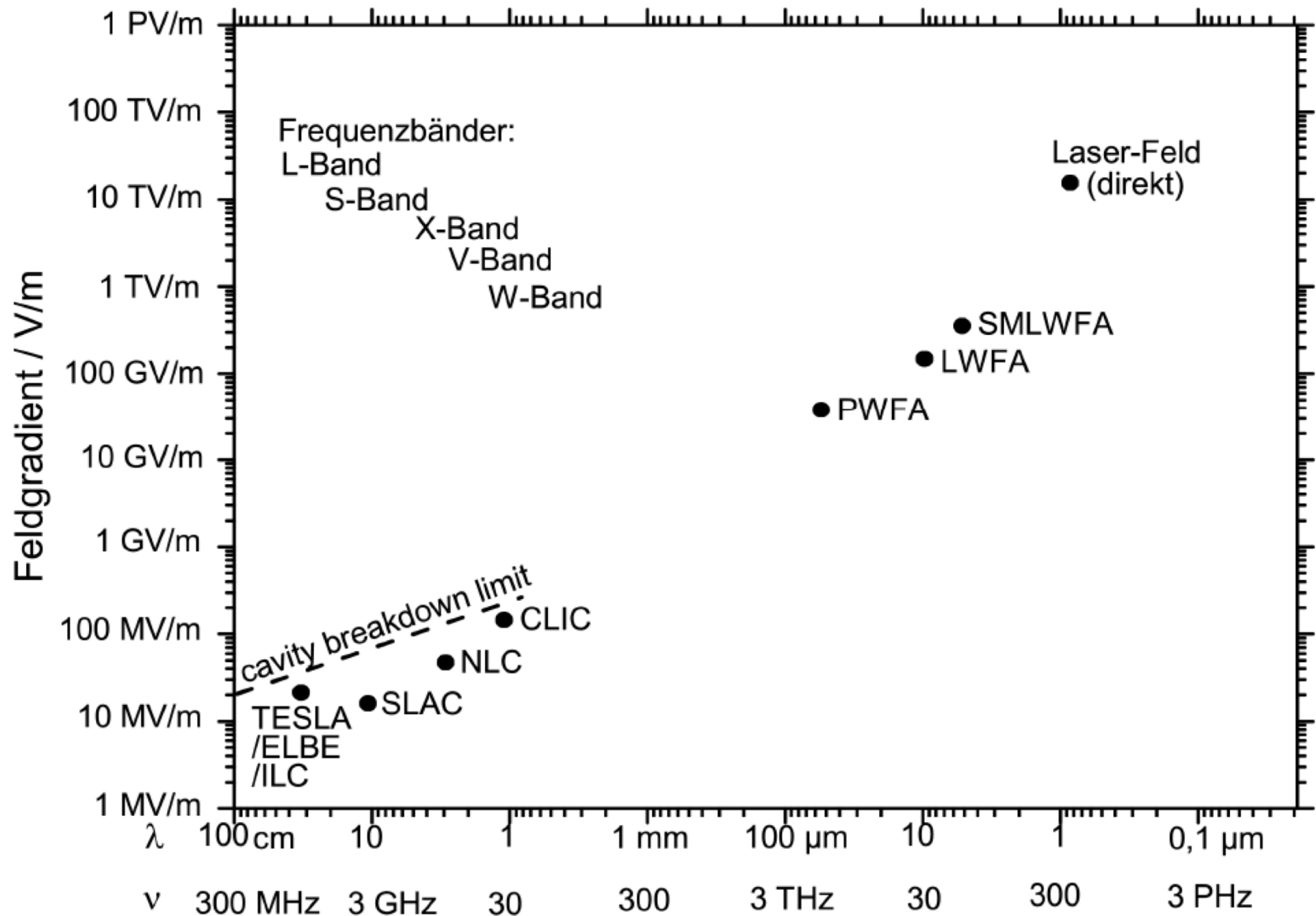


© Copyright ColourTherapy Healing 2010 - www.colourtherapyhealing.com

Frequency bands

Frequency band	Frequency range (GHz)	Wavelength range (cm)
L band	1–2	15–30
S band	2–4	7.5–15
C band	4–8	3.75–7.5
X band	8–12	2.5–3.75
Ku band	12–18	1.67–2.5
K band	18–27	1.11–1.67
Ka band	27–40	0.75–1.11
V band	40–75	0.4–0.75
W band	75–110	0.27–0.4

Gradient vs. wavelength



Comparison

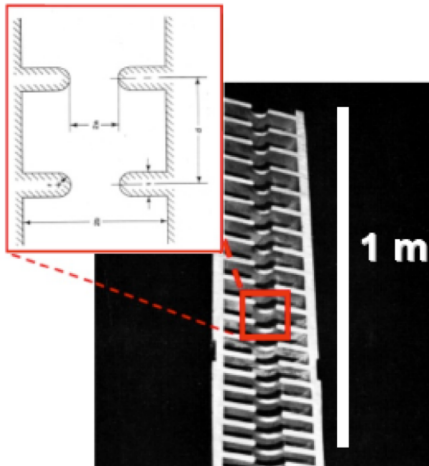
Conventional Accelerator

Copper Structure with irises

Powered by microwaves

Energy Gain 20 MV/m

Structure Diameter 10cm



Plasma Accelerator

Ionized Gas

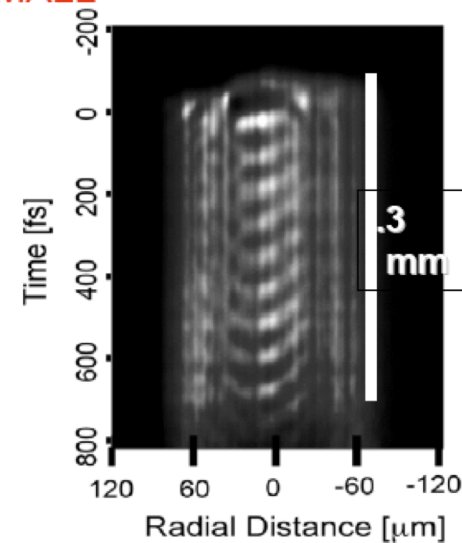
Lifetime, few picoseconds

*Powered by a Laser or
electron beam pulse*

Energy Gain 20 GV/m

Diameter 0.1-1 mm

BIG PHYSICS BECOMES SMALL



M.Downer U.Tex

Why plasmas?

Long term future of High-Energy physics requires the need for new high-gradient technology

Gradients from 1 GeV/m to 200 GeV/m are possible from relativistic plasma waves

Conventional Accelerators

- Limited by peak power and breakdown
- 20-50 MeV/m

Plasma

- No breakdown limit
- 10-200 GeV/m

Brief history-plasma based accelerators

- Concept on laser-plasma based acceleration was proposed by [Tajima & Dawson in 1979](#).
- The key idea was to excite **large amplitude plasma electron waves by using short pulse laser (LWFA)** in high density plasma.
- However, there was no such laser in that era, and beat wave could excite the plasma waves as well.
- In 1985, P. Chen et al. proposed to use electron bunch to excite the plasma wave (**PWFA**) and this idea was confirmed by [Rosenzweig et al.\(1988\)](#).
- In 1992, [Kitagawa et al.](#) succeeded in electron acceleration by using **PBWA** (Plasma Beat wave) method.
- In 1995, [Nakajima et al.](#) succeeded to accelerate electrons up to 100 MeV by using **LWFA** method.
- In 1985, [Mourou et al.](#) invented the **CPA** (Chirped Pulse Amplification) method to generate ultrashort, intense lasers and was put in practical use around 1995.

1st paper on plasma accelerator

VOLUME 43, NUMBER 4

PHYSICAL REVIEW LETTERS

23 JULY 1979



Laser Electron Accelerator

T. Tajima and J. M. Dawson

Department of Physics, University of California, Los Angeles, California 90024

(Received 9 March 1979)



An intense electromagnetic pulse can create a weak of plasma oscillations through the action of the nonlinear ponderomotive force. Electrons trapped in the wake can be accelerated to high energy. Existing glass lasers of power density 10^{18}W/cm^2 shone on plasmas of densities 10^{18}cm^{-3} can yield gigaelectronvolts of electron energy per centimeter of acceleration distance. This acceleration mechanism is demonstrated through computer simulation. Applications to accelerators and pulsers are examined.

Collective plasma accelerators have recently received considerable theoretical and experimental investigation. Earlier Fermi¹ and McMillan² considered cosmic-ray particle acceleration by moving magnetic fields¹ or electromagnetic waves.² In terms of the realizable laboratory technology for collective accelerators,

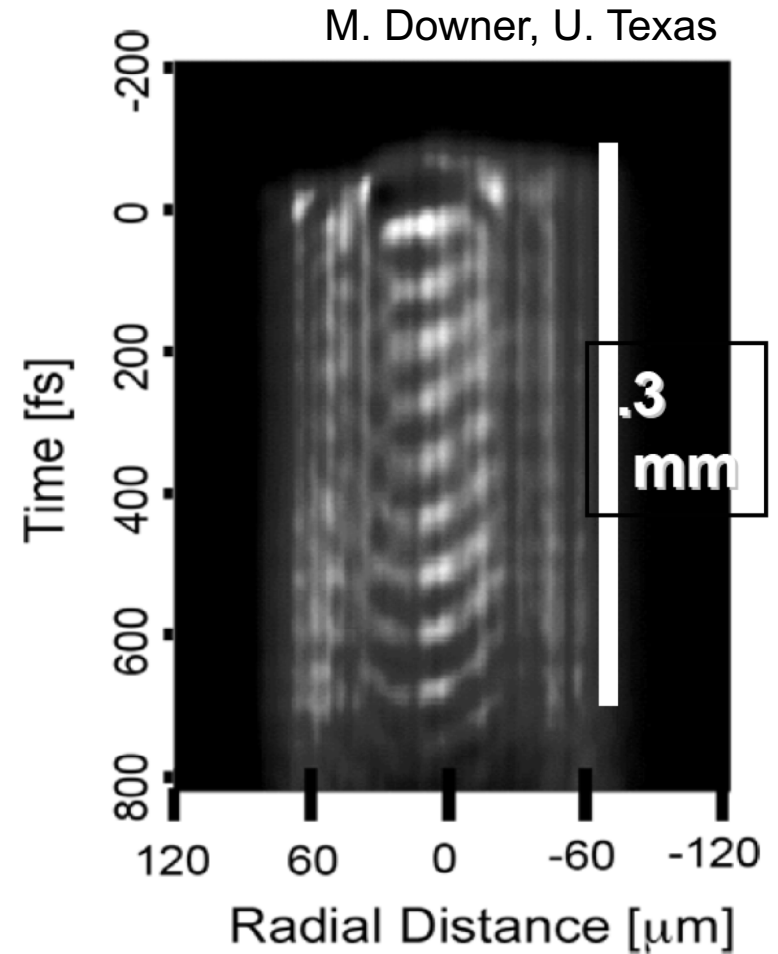
the wavelength of the plasma waves in the wake:

$$L_1 = \lambda_w/2 = \pi c/\omega_p. \quad (2)$$

An alternative way of exciting the plasmon is to inject two laser beams with slightly different frequencies (with frequency difference $\Delta\omega \sim \omega_p$) so that the beat distance of the packet becomes

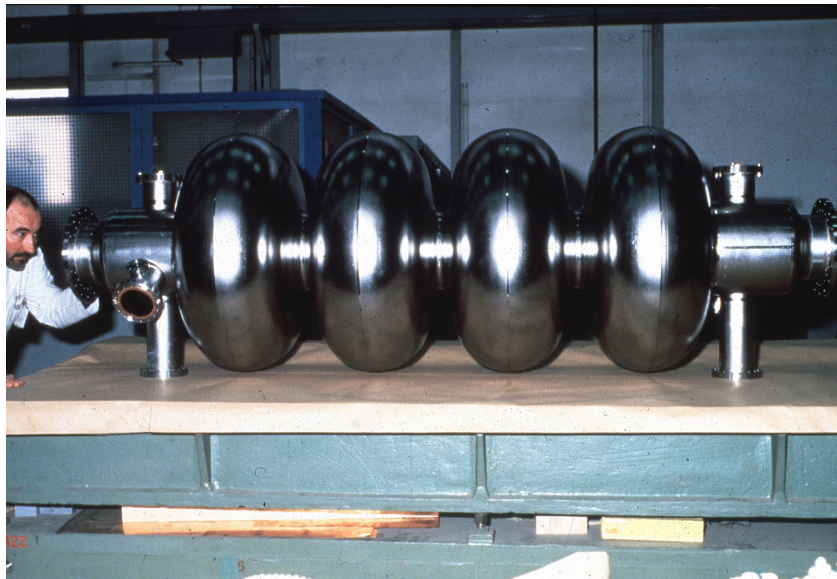
Accelerating field in plasma is **3-4 orders of magnitude** higher than conventional accelerators!

Our dream



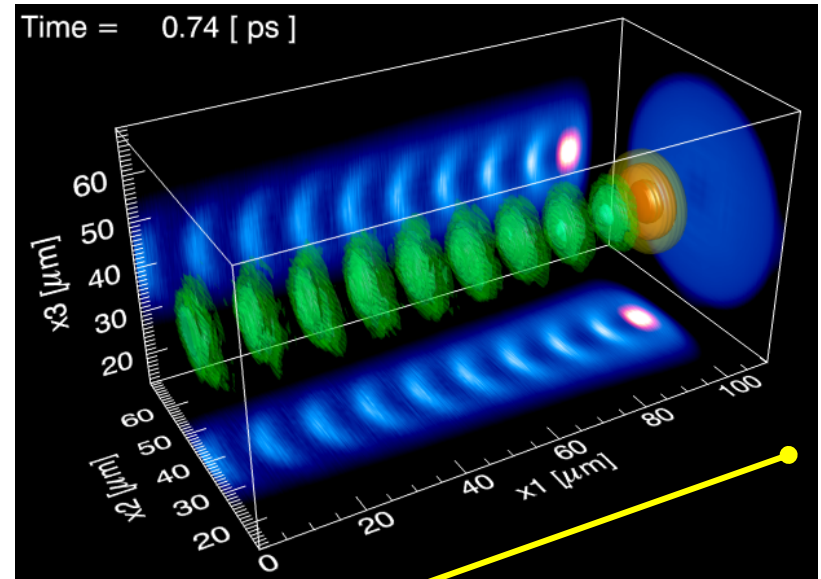
Conventional accelerator limitations

$E\text{-field}_{\max} \approx \text{few } 10 \text{ MeV /meter (Breakdown)}$
 $R > R_{\min}$ Synchrotron radiation



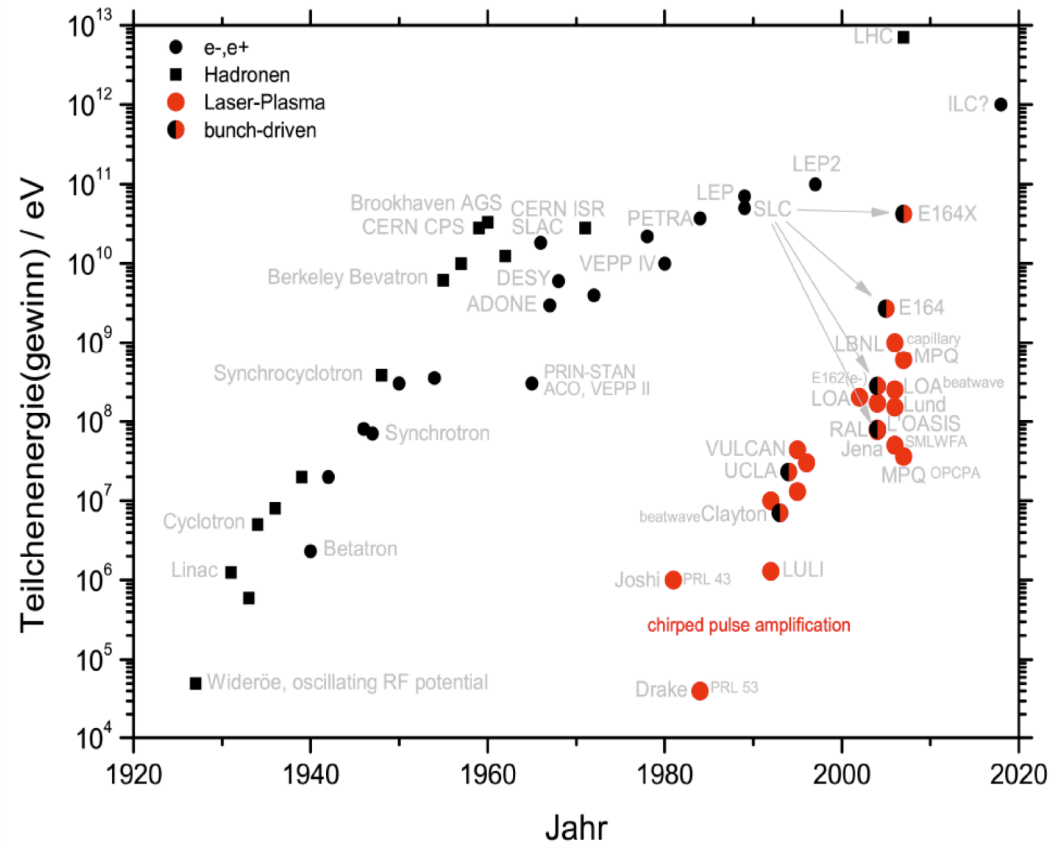
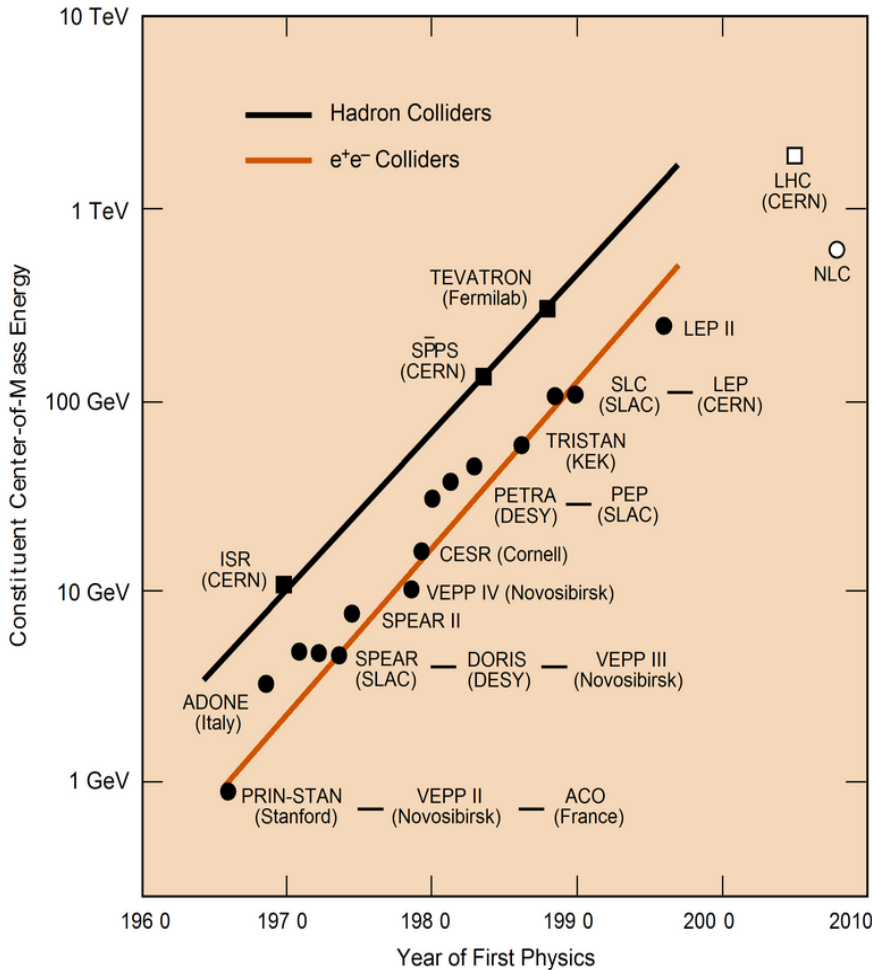
1 m
RF cavity

Courtesy of W. Mori & L. da Silva

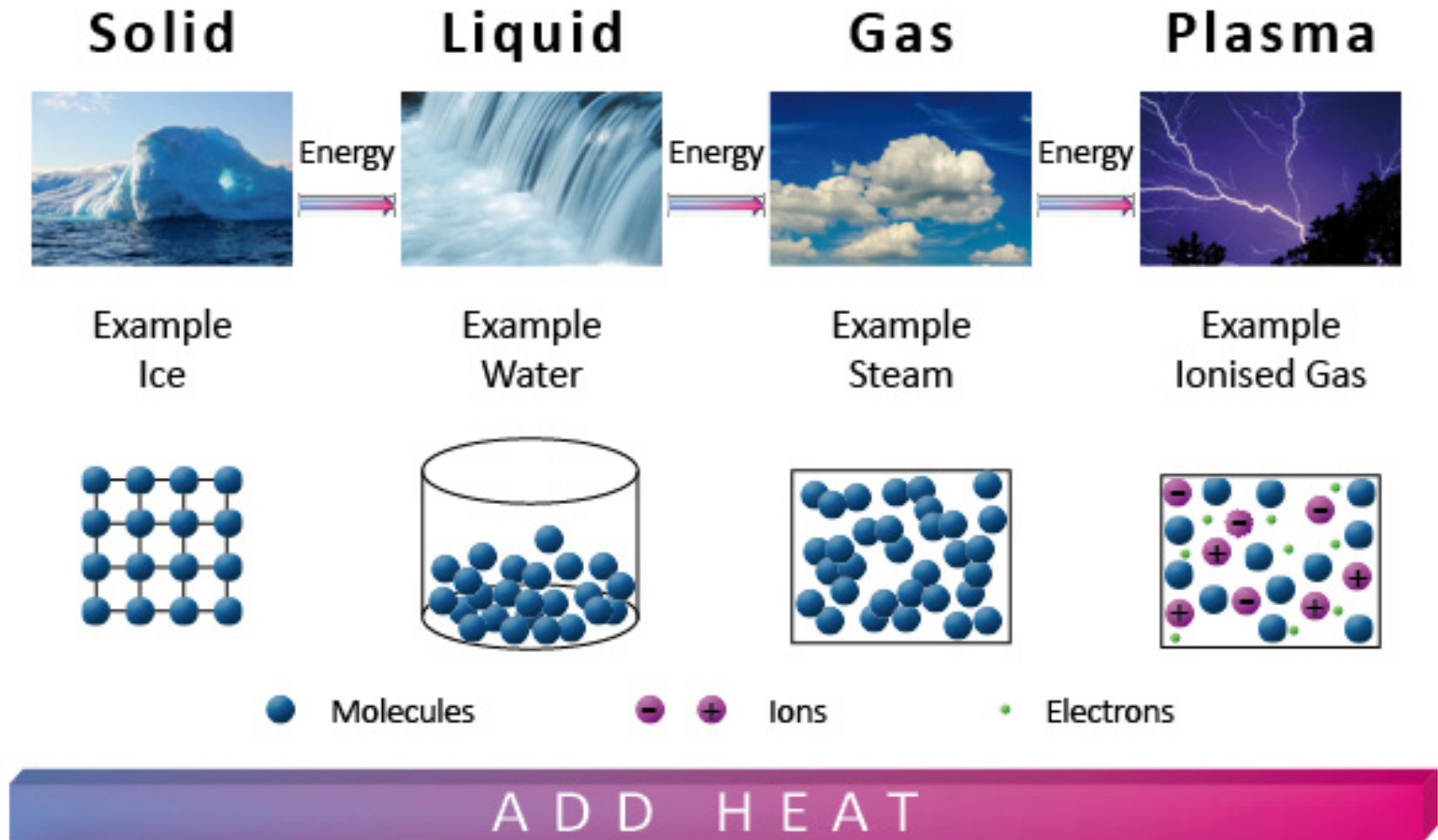


100 μm
Plasma cavity

New Livingston plot



What is plasma?



What is plasma?

- What is a plasma?

Plasma is loosely described as an electrically neutral medium of unbound positive and negative particles (i.e. the overall charge of a plasma is roughly zero).

- Quasi-neutrality

Number of densities of electrons n_e , and ions n_i , with charge state Z are locally balanced $n_e \approx Zn_i$

- Breakdown medium (no further breakdown)

Free electrons + ions

Types of plasmas

Type	Electron density n_e (cm ⁻³)	Temperature T_e (eV*)
Stars	10^{26}	2×10^3
Laser fusion	10^{25}	3×10^3
Magnetic fusion	10^{15}	10^3
Laser-produced	$10^{18} - 10^{24}$	$10^2 - 10^3$
Discharges	10^{12}	1-10
Ionosphere	10^6	0.1
ISM	1	10^{-2}

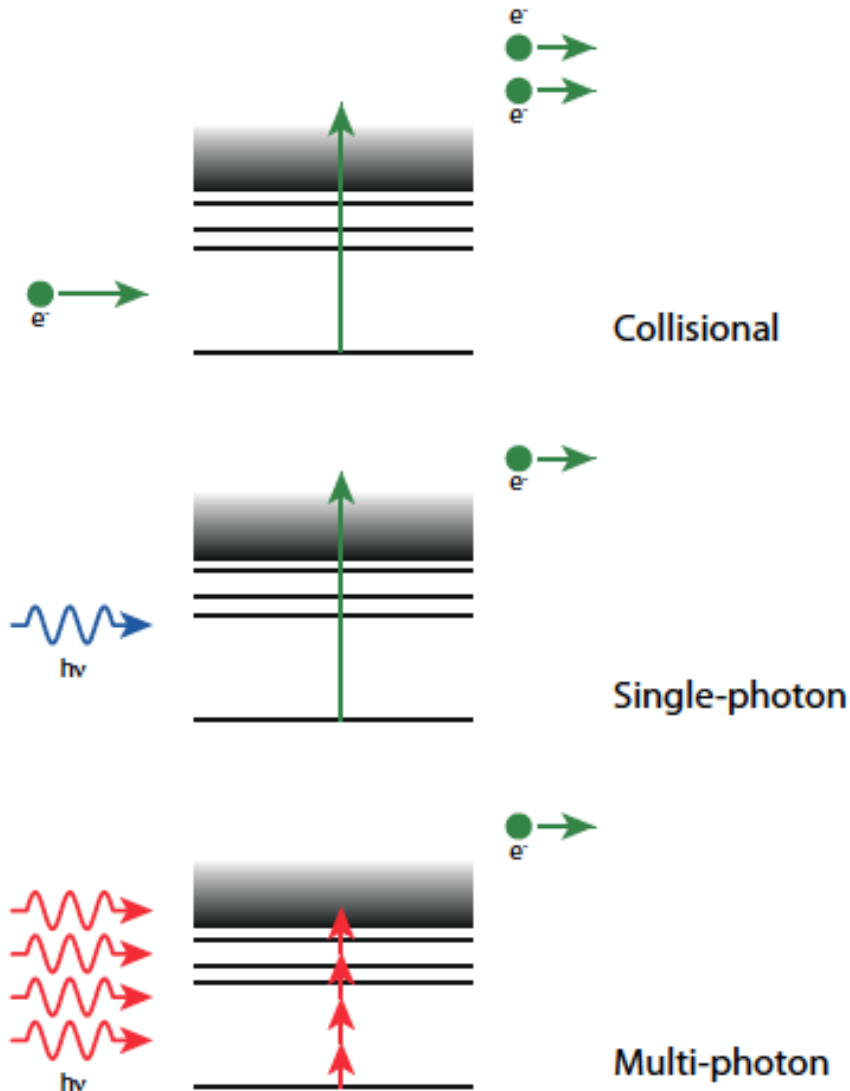
Specifications of plasmas

* 1 eV=11600 K

Plasma sources

- Gas ionization to plasma
- Several ways to produce plasma
- Lasers, RF (DC) field, particle beams can be used to produce plasmas
 - Collisional ionization
 - Single photon ionization
 - Multi-photon ionization

Plasma sources



Ionization of gas into plasma

Components in plasmas:

Electrons

Ions

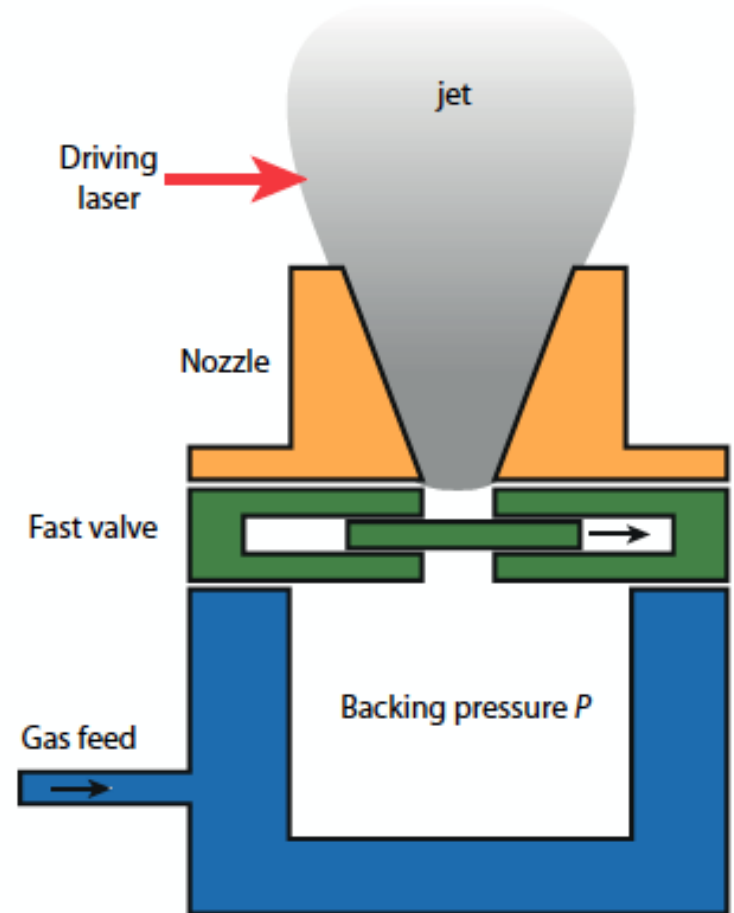
Atoms (molecules)-not ionized

Plasma sources in use

- Supersonic gas jet (LWFA)
- Gas cell based source (LWFA+PWFA)
- Capillary discharge waveguide (LWFA+PWFA)
- Heat pipe ovens (PWFA)
- Others (helicon RF plasma source)

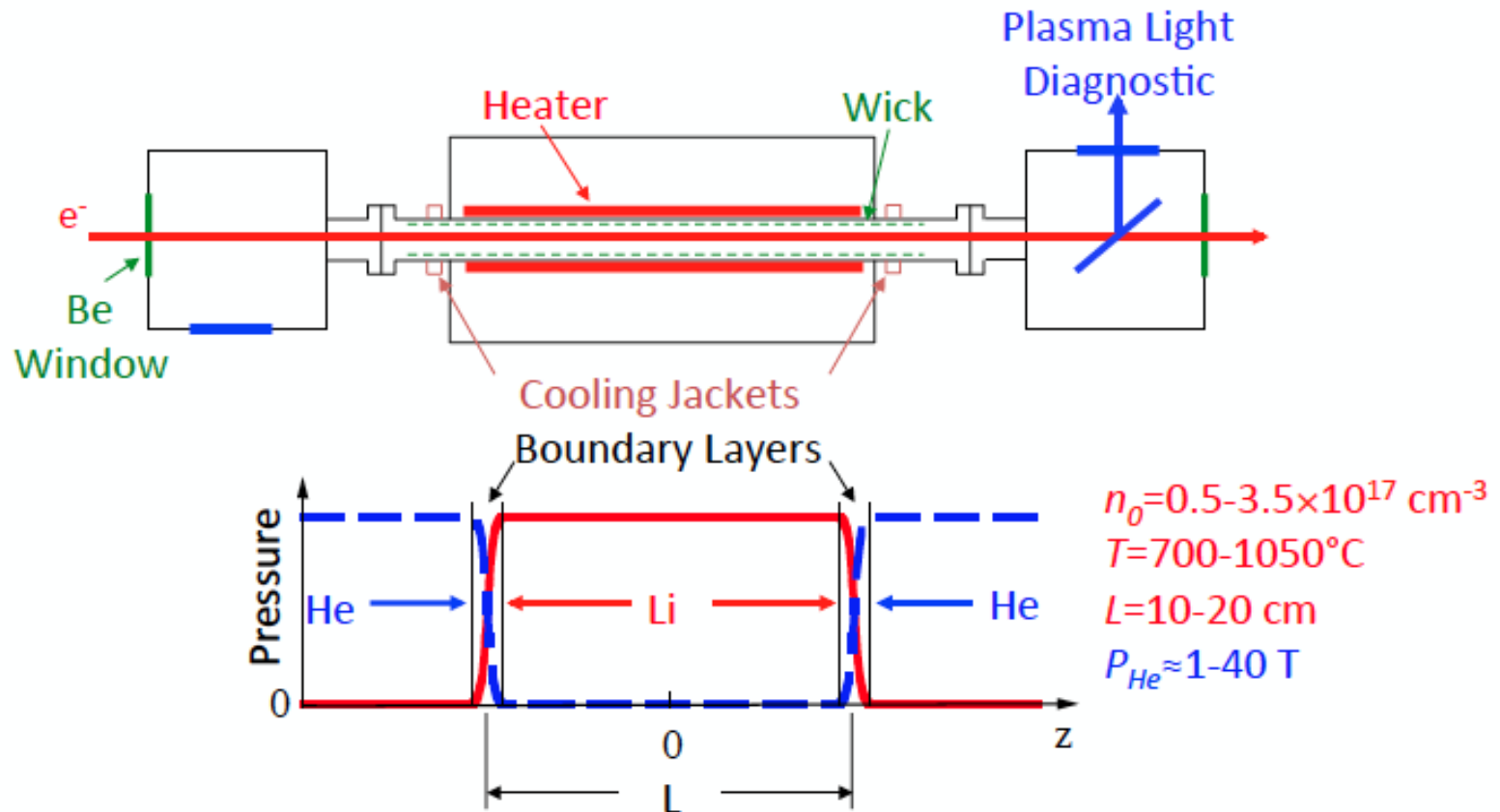
Supersonic gas jet

- ▶ Supersonic nozzles provide near-flat-top density profile for laser wakefield experiments
- ▶ Plasma density controlled by varying backing pressure behind jet -
 - Typically 10 - 100 bar depending on nozzle diameter and desired density
- ▶ n_e typically $10^{17} - 10^{20} \text{ cm}^{-3}$
- ▶ Length typically few mm
 - larger nozzle diameters give lower densities (fortuitously matched to increase in dephasing length)



S. Hooker, talk at CERN CAS, 2014

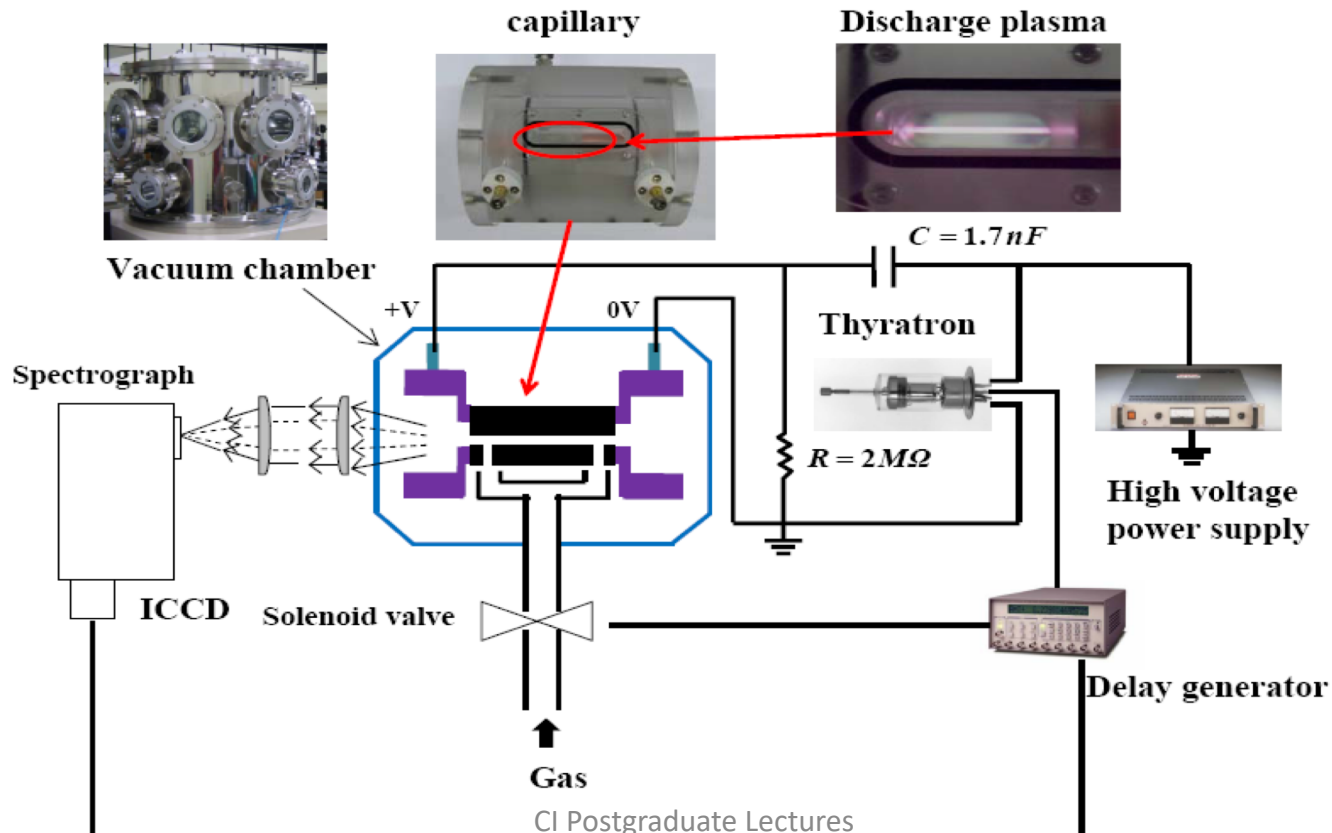
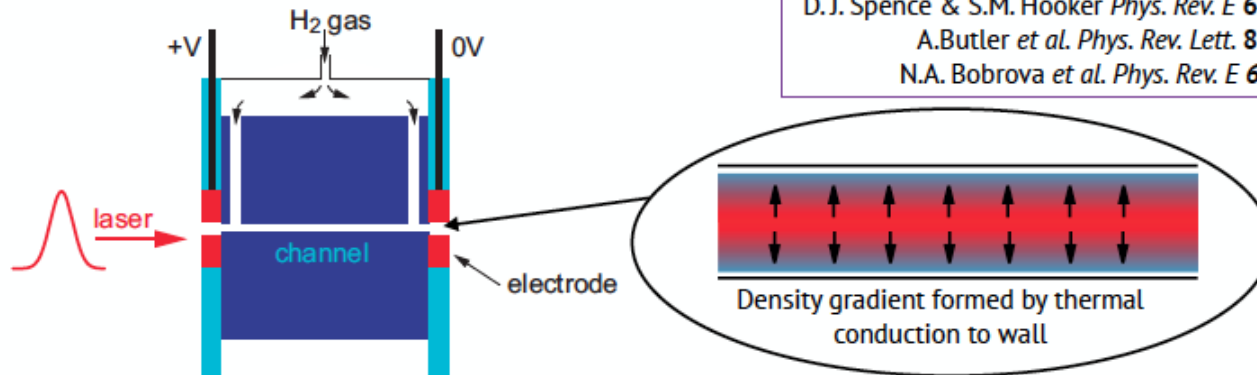
Heat pipe oven



P. Muggli *et al.* *IEEE Trans. Plasm. Sci.* **27** 791 (1999)

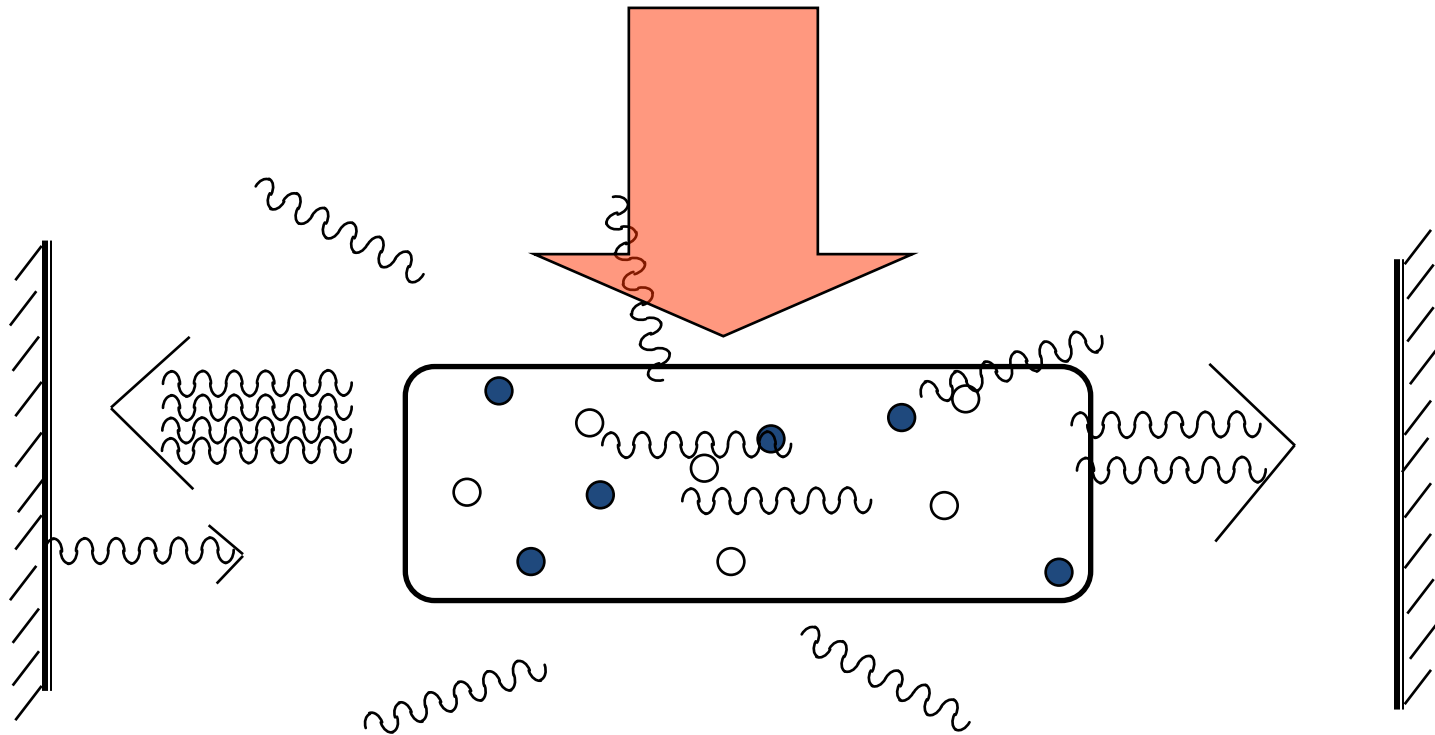
Discharge plasma source

D.J. Spence & S.M. Hooker *Phys. Rev. E* **63** 015401 (2000)
 A. Butler *et al. Phys. Rev. Lett.* **89** 185003 (2002)
 N.A. Bobrova *et al. Phys. Rev. E* **65** 016407 (2002)



Lasers

Light amplification in an optical cavity

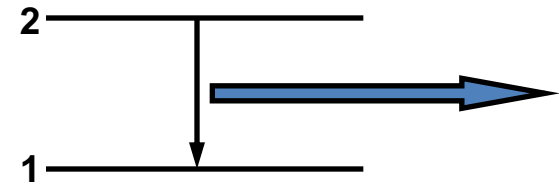


Light Amplification by Stimulated Emission of Radiation (LASER)

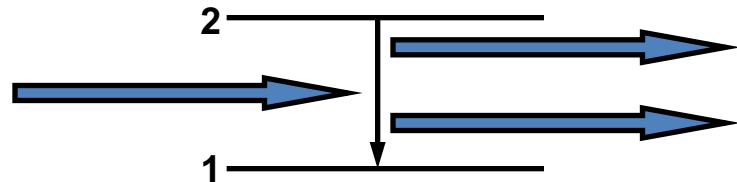
Three processes

Three basic processes:

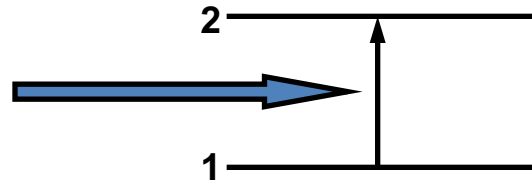
Spontaneous Emission



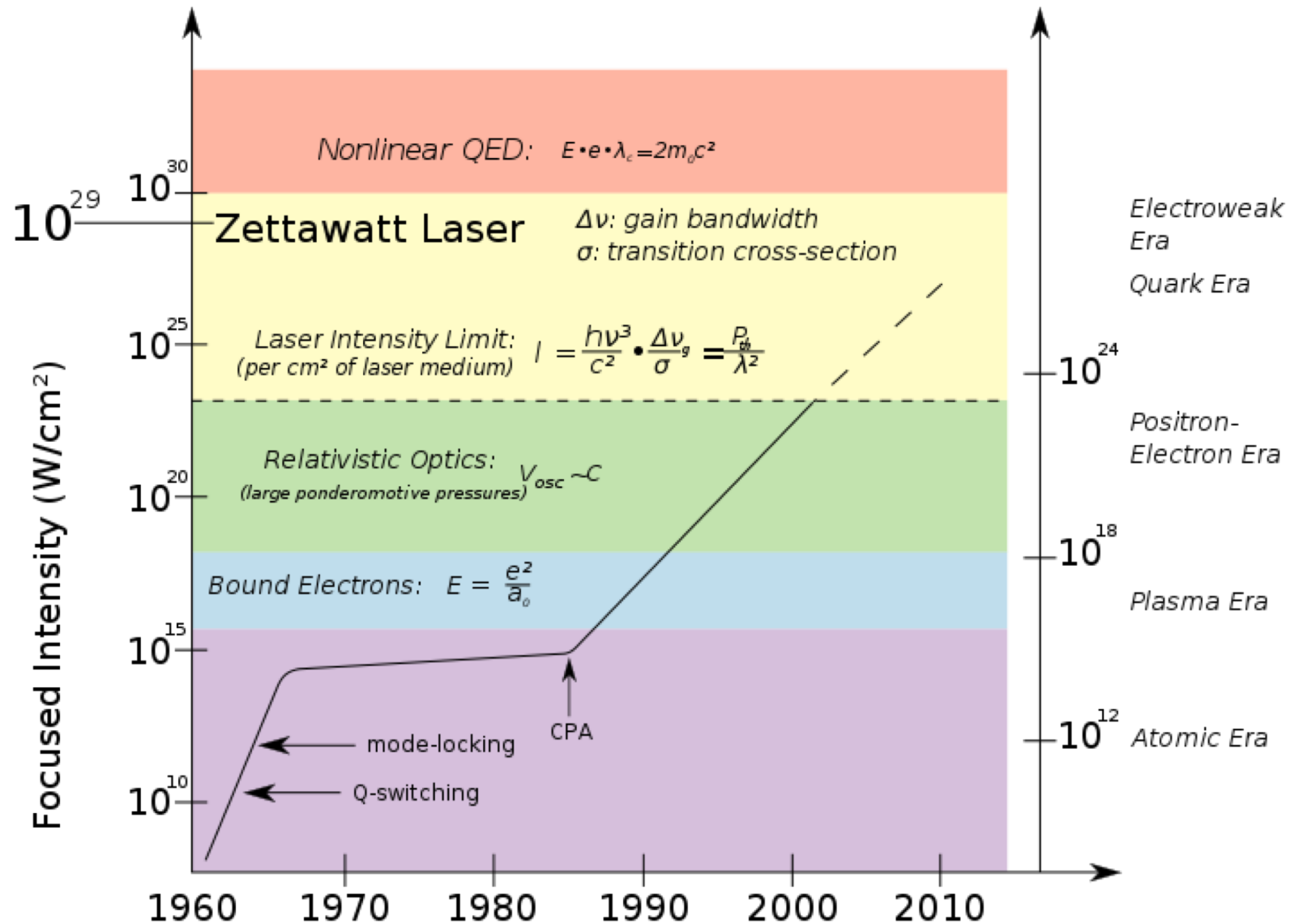
Stimulated Emission



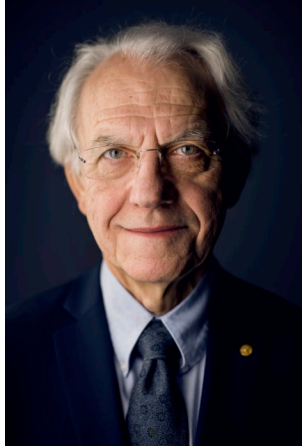
Absorption



Modern lasers



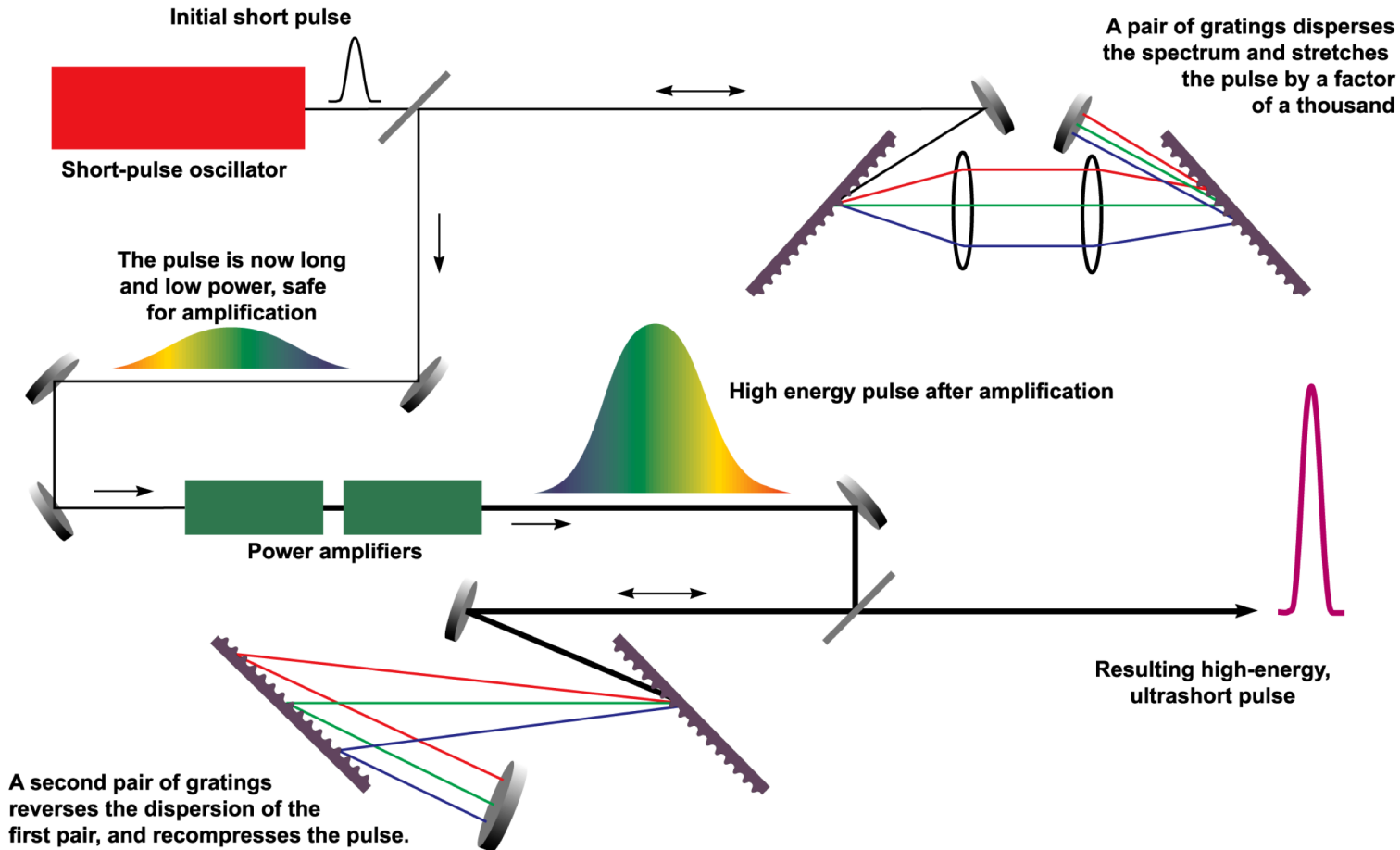
Chirp pulse amplification (CPA)



G. Mourou



D. Strickland



2018 Nobel Prize in Physics !

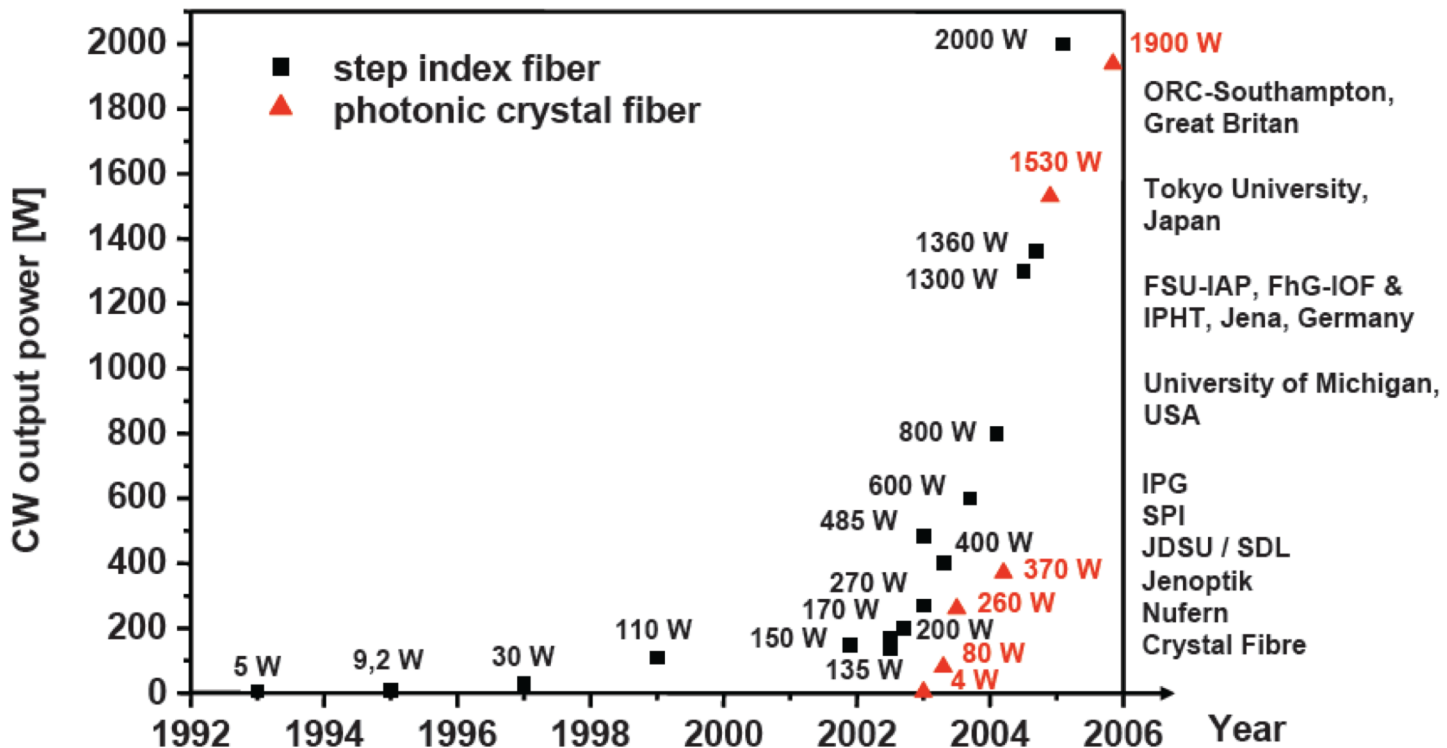
New trend: Fiber lasers

Tailored Light - Licht nach Maß

Diode-pumped double clad fiber laser (cw output)

evolution of cw fiber laser

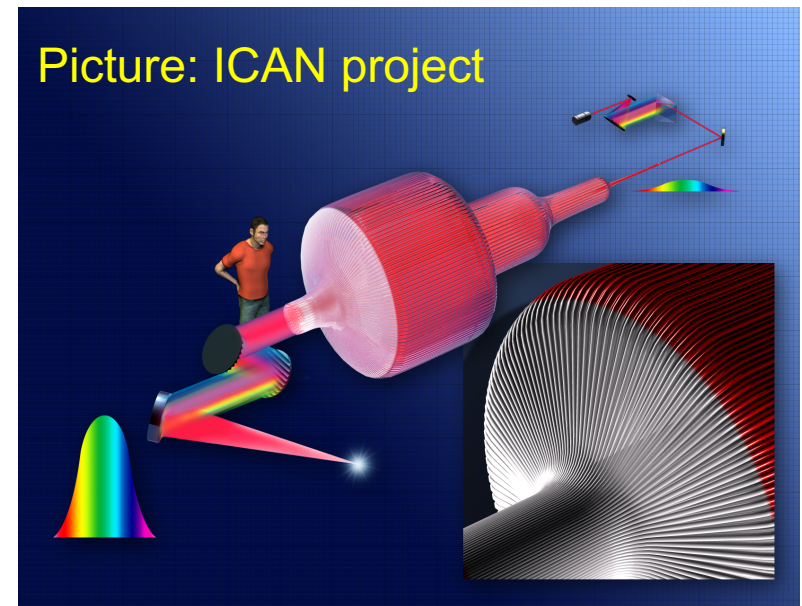
> 6 kW @ 2010



Fiber lasers

- Pro: Energy efficient, High rep-rate capable
- Cons: Power per fiber limited
- Coherent combination
 - Being studied at many places world-wide
 - Progress on DC-lasers more promising than pulsed
 - Current power levels far from interesting for GeV acceleration
- Conclusions:
 - Technology not ready yet
 - Possibly first used for pump-laser or very-low-energy LWFA

Thales Optronique is working together with academics/researchers to achieve the 61 fibre laser coherent combination



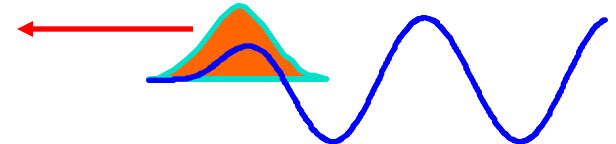
Advantages of lasers

- Most experiments around the world work on laser wakefield acceleration.
- **Lasers can be procured** in a university framework.
- With laser-generated wakefields you can **capture and accelerate plasma-electrons to generate the beam** from scratch.
- With present state-of-the-art laser one can create mono-energetic beams via LWFA!
- **No need for heavy beam infrastructure** up to some beam energy.
- The more powerful the laser, the higher the energy of the beam that one can create!

Types of plasma-based accelerators

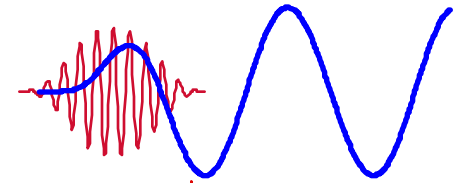
- Plasma Wake Field Accelerator(PWFA)

A high energy electron/proton bunch



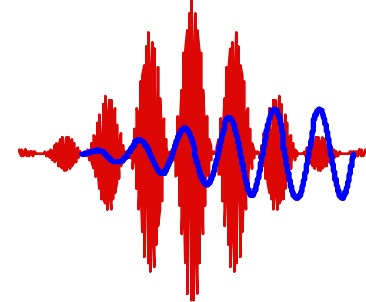
- Laser Wake Field Accelerator(LWFA)

A single short-pulse of photons



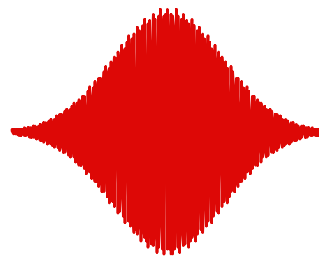
- Plasma Beat Wave Accelerator(PBWA)

Two-frequencies, i.e., a train of pulses

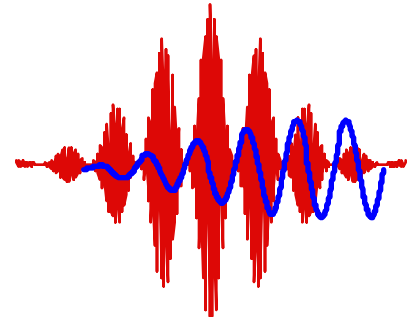


- Self Modulated Laser Wake Field Accelerator (SMLWFA)

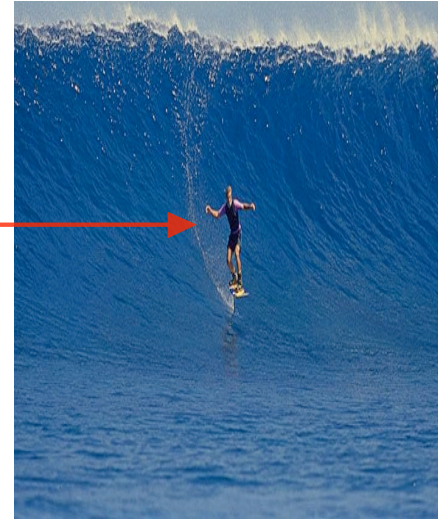
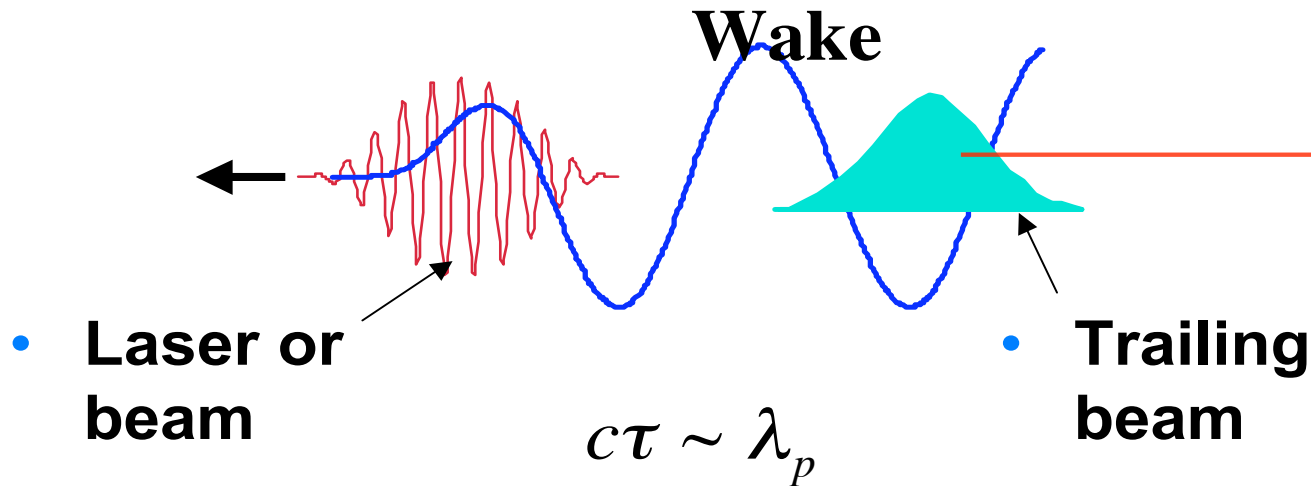
Raman forward scattering instability



evolves to



Basic principle-laser wakefield accelerators



The key is the super high accelerating gradient!

$$E_{Acc} \approx \sqrt{n_p [cm^{-3}]} V / cm$$

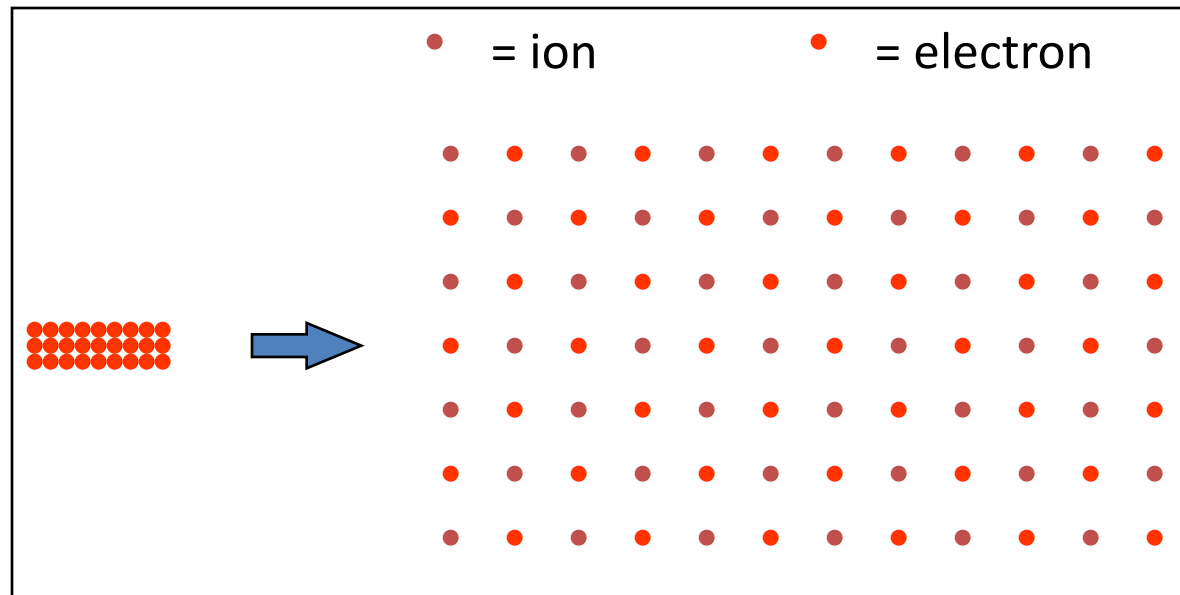
e.g. $n_p = 10^{18} \text{ cm}^{-3}$, the accelerating field will be 100 GeV/m!
3 orders of magnitude higher than the fields in conventional accelerators !

Basic principles

I) Generate homogeneous plasma channel:



II) Send laser beam or electron beam towards plasma:

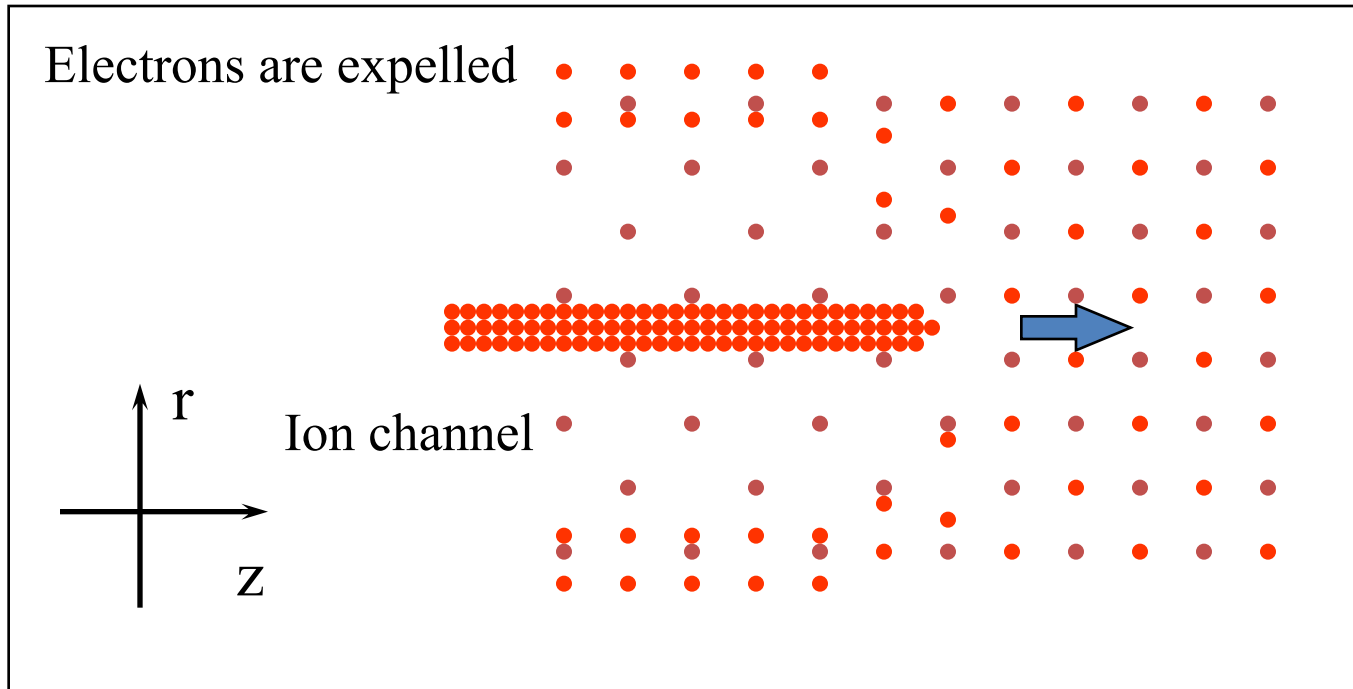


Beam density n_b
> Gas density n_0

Beam excited
plasma. Also
lasers can be
used (laser
wakefield
acceleration).

Basic principles

III) Excite plasma wakefields:

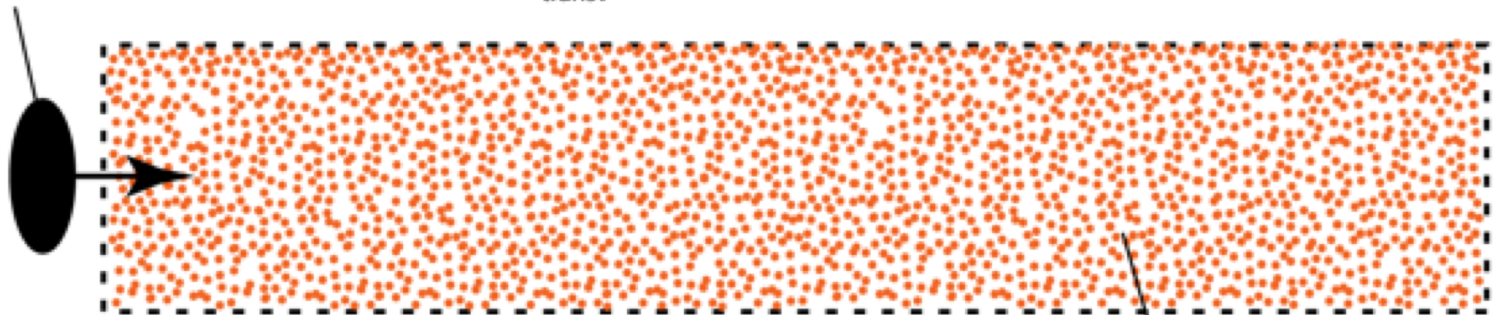


Ponderomotive force or space charge force of the beams ejects plasma electrons (ambient electrons) promptly along radial trajectories

Pure ion channel is left: Ion-focused regime, underdense plasma

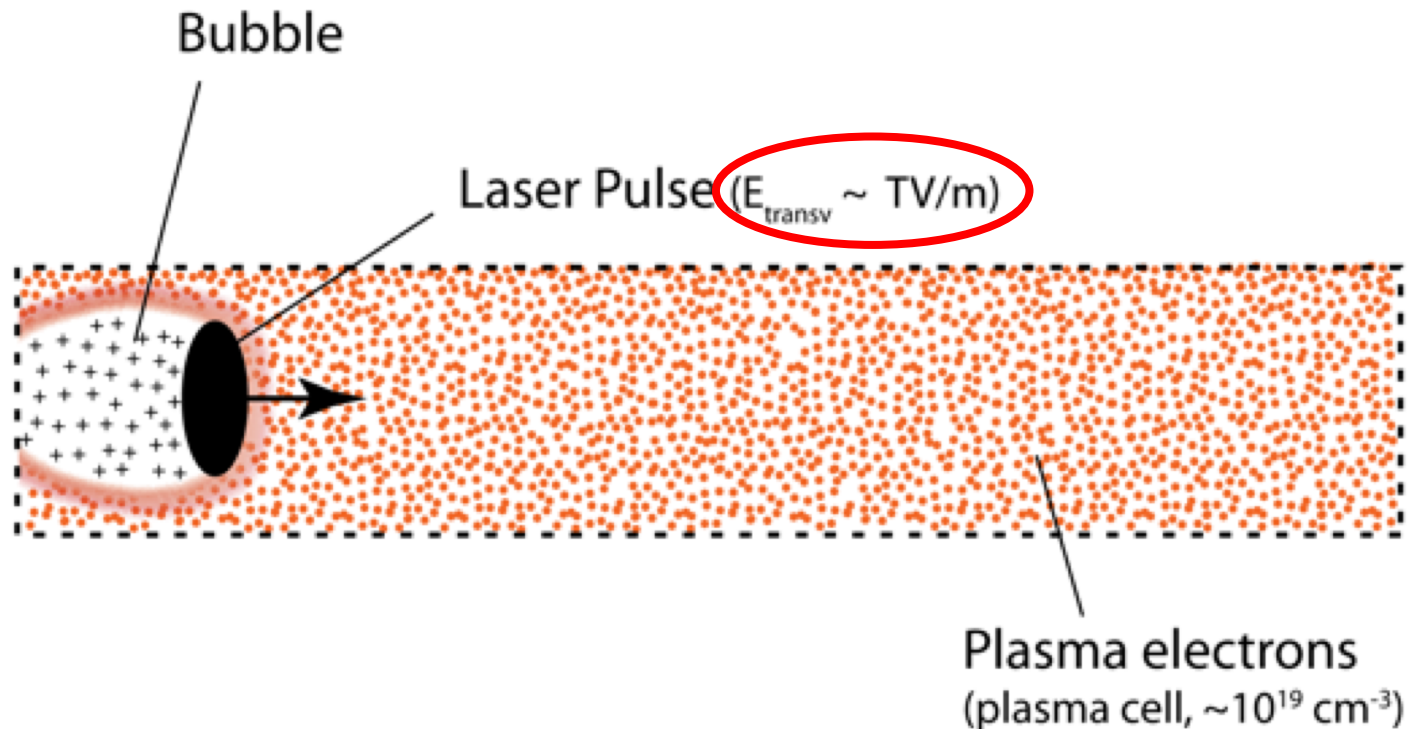
Laser plasma acceleration

Laser Pulse (200 TW, ~ 30 fs, $E_{\text{transv}} \sim \text{TV/m}$)

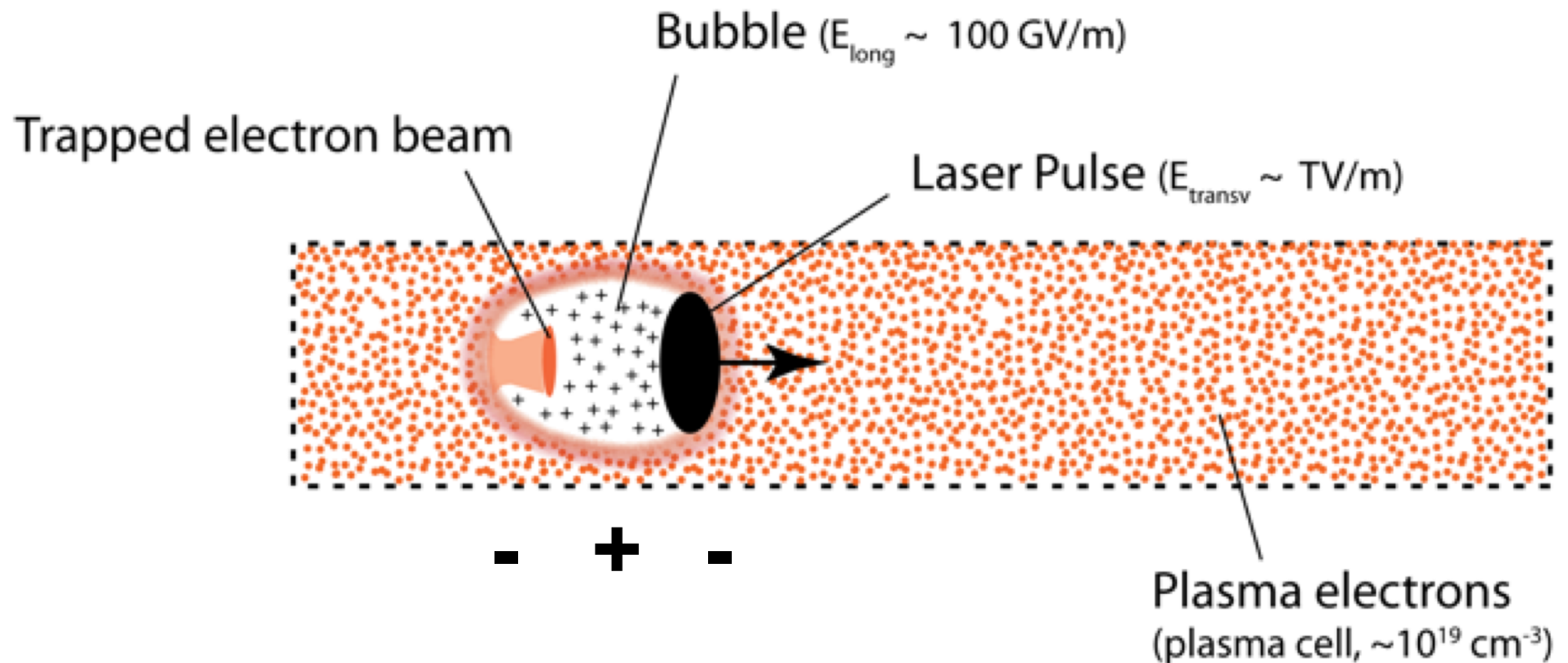


Plasma electrons
(plasma cell, $\sim 10^{19} \text{ cm}^{-3}$)

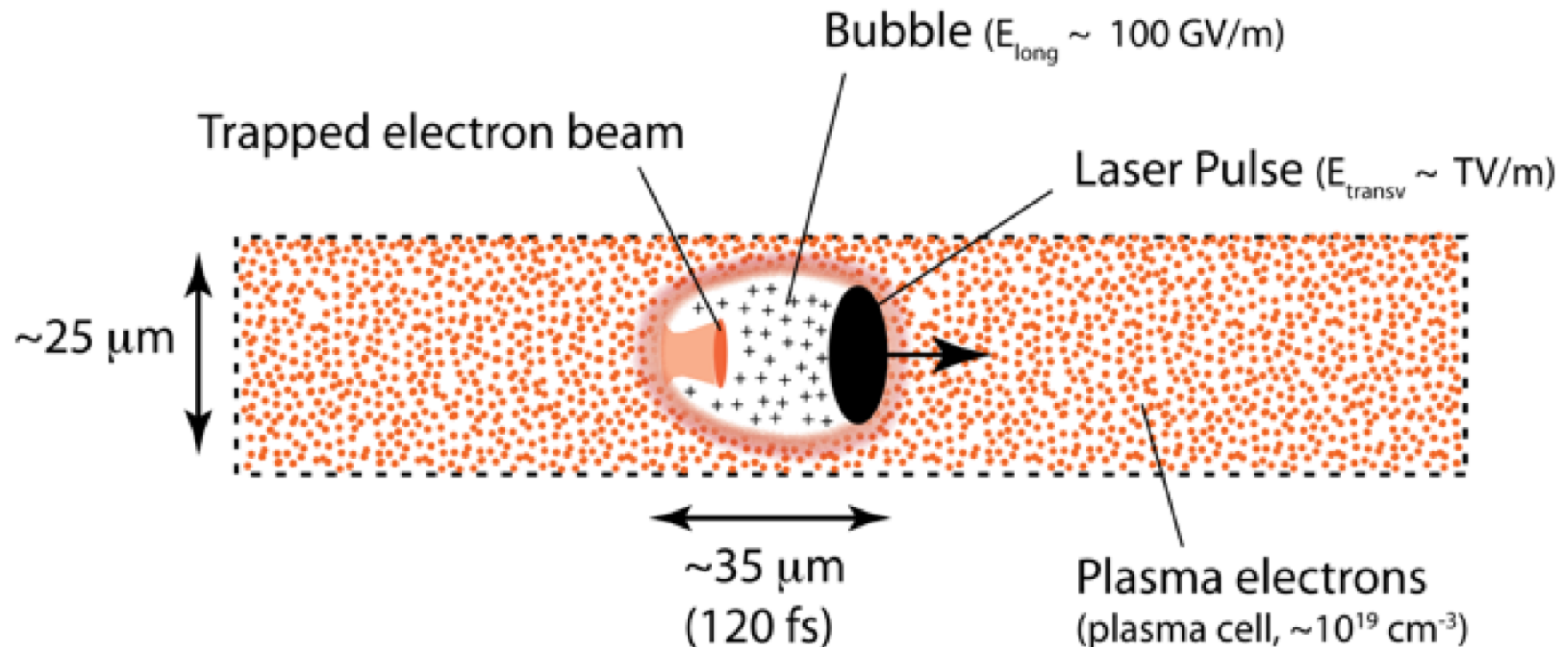
Laser plasma acceleration



Laser plasma acceleration

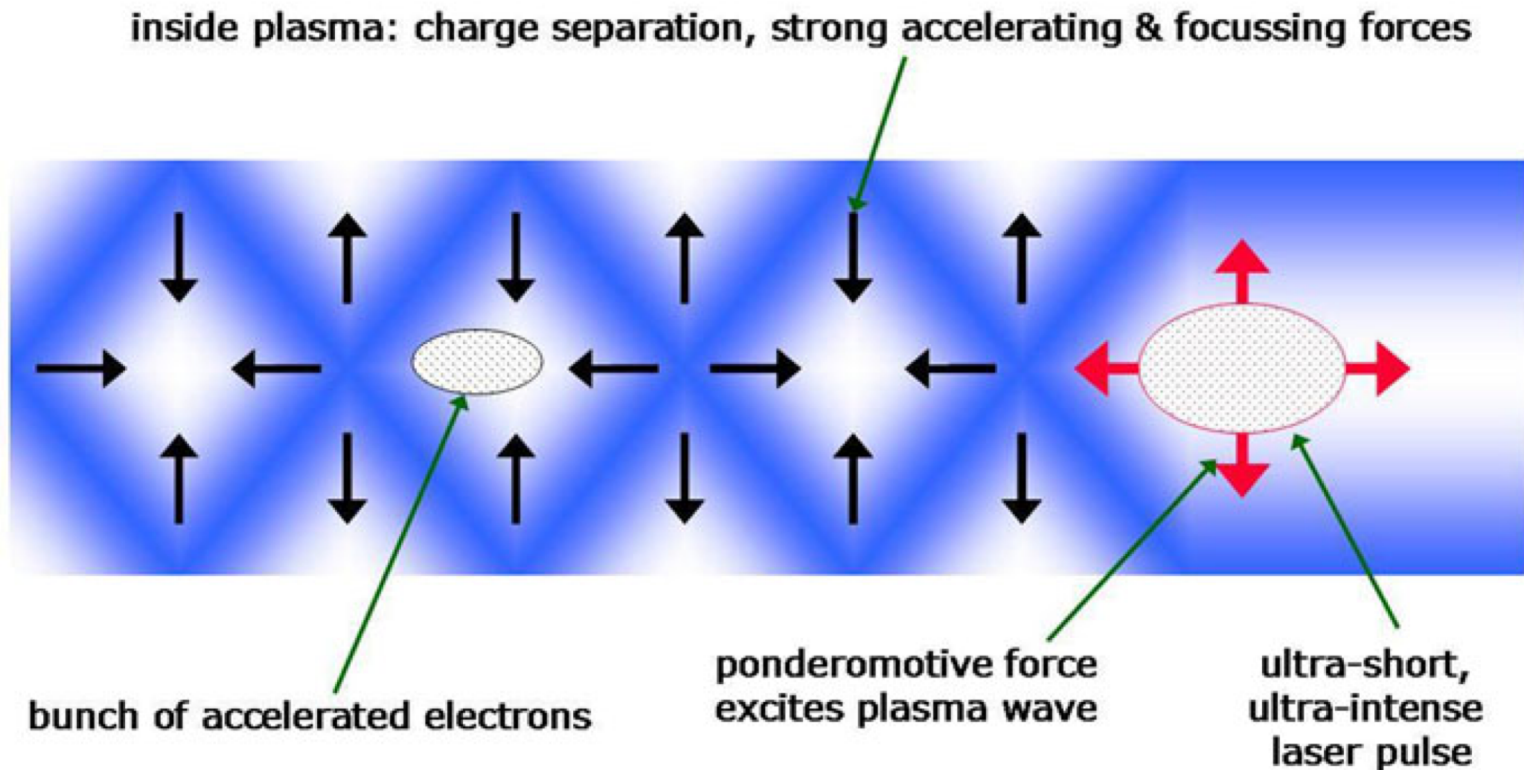


Laser plasma acceleration



This accelerator fits into a human hair!

Basic principles



A ponderomotive force (red arrows) arising from the light pressure pushes aside the plasma electrons to generate the wake. The electrostatic fields associated with this wake is utilised to produce accelerating fields which are 3-4 orders of magnitude larger than is possible in the RF cavity of a conventional accelerator.

Laser parameters

Written the laser field in term so the vector potential \mathbf{A}

$$\mathbf{E} = -\frac{\partial \mathbf{A}}{c \partial t}, \quad \mathbf{B} = \nabla \times \mathbf{A}$$

Define the normalized vector potential as

$$\mathbf{a} = \frac{e\mathbf{A}}{m_e c^2}$$

And the **laser strength parameter** is given by

$$a_0 = \left(\frac{2e^2 \lambda_0^2 I}{\pi m_e^2 c^5} \right)^{1/2} \cong 0.855 \times 10^{-9} I^{1/2} [\text{W/cm}^2] \lambda_0 [\mu\text{m}]$$

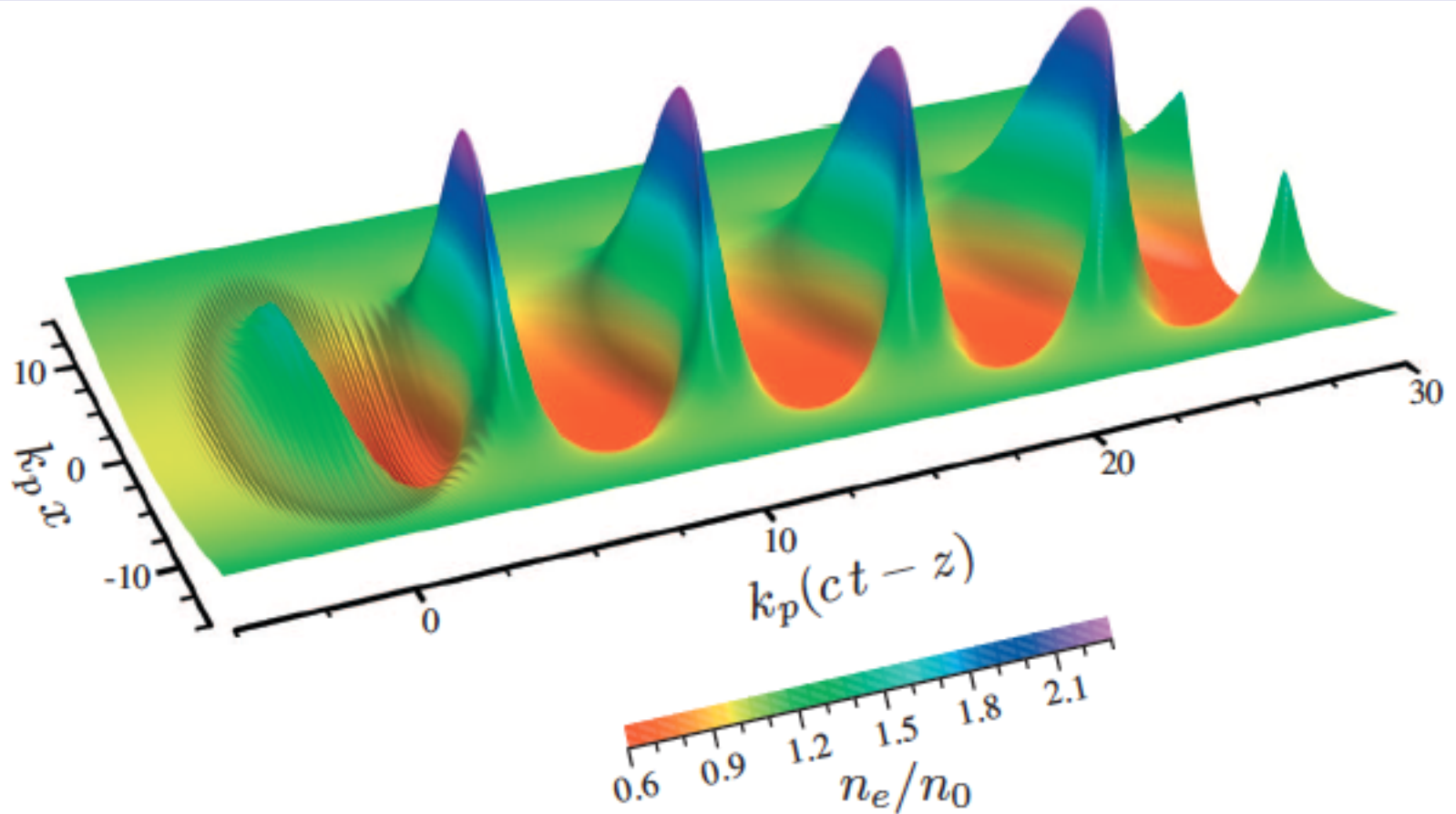
I : laser peak intensity, λ is the wavelength

The amplitude of the transverse electric field of linearly polarized laser is

$$E_L [\text{TV/m}] = \frac{m_e c^2 k}{e} a_0 \cong 3.21 \frac{a_0}{\lambda [\mu\text{m}]} \cong 2.7 \times 10^{-9} I^{1/2} [\text{W/cm}^2]$$

At $I = 1 \times 10^{18} \text{ W/cm}^2$, $E_L = 2.7 \text{ TV/m}$

Plasma density perturbation



Plasma density perturbation excited by a Gaussian laser pulse, laser pulse is travelling to the left with $a_0 = 1.5$

Linear & non-linear regimes

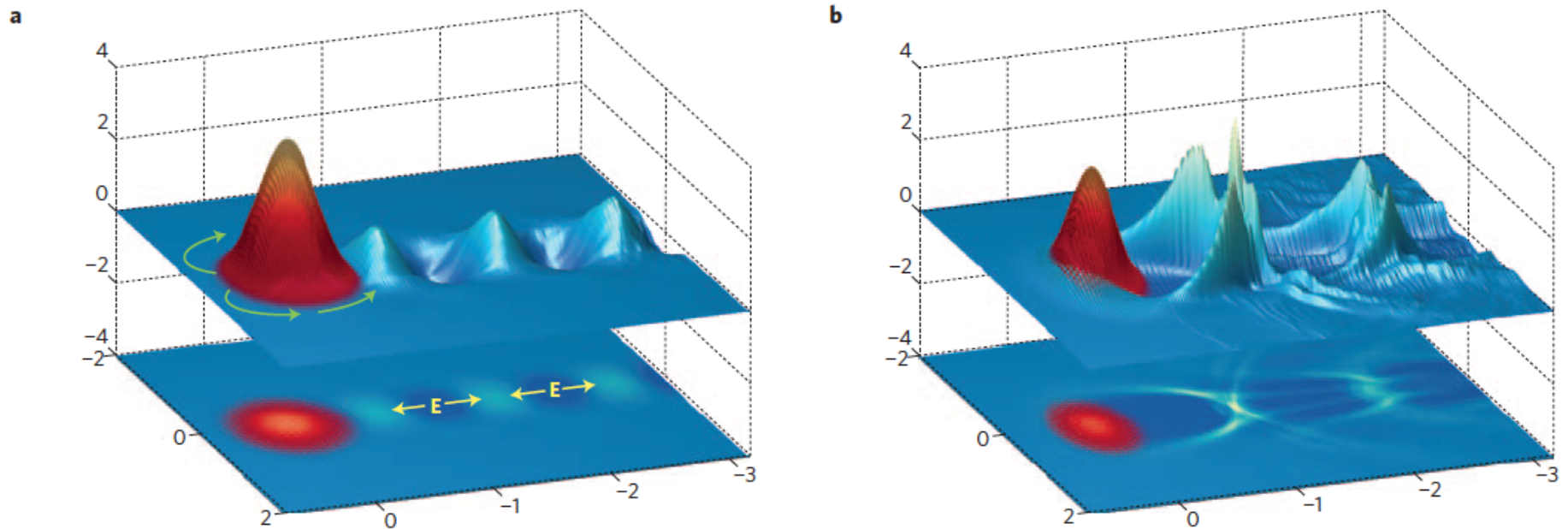
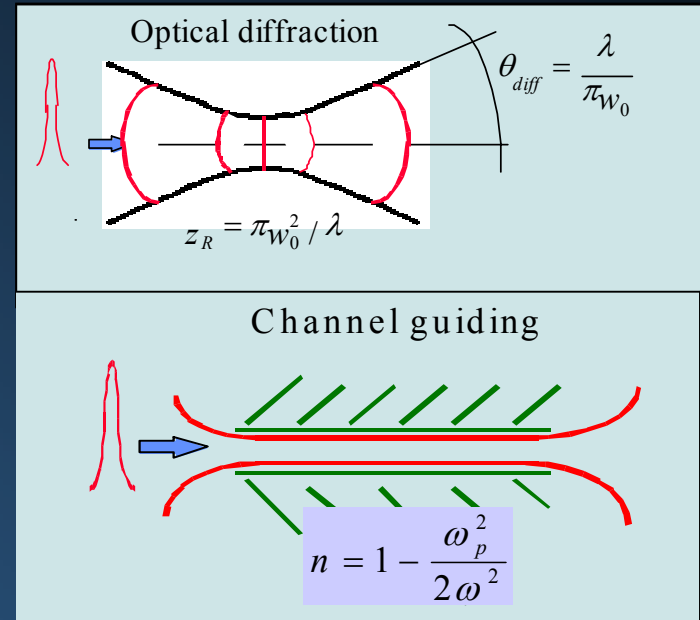


Figure 1 | Plasma waves driven by intense laser pulses. The laser pulse (red-yellow) propagates from right to left and excites a trailing plasma wave. The plasma wave amplitude (blue-green) is shown for laser pulses with initial values of the normalized laser intensity parameter of **a**, $a_0 = 0.5$, corresponding to the linear regime, and **b**, $a_0 = 4.0$, close to the bubble regime — as indicated by the excitation of a highly nonlinear plasma wave and the formation of a 'cavity' immediately behind the laser pulse. The spatial coordinates are in units of the plasma wavelength; the vertical scale is in arbitrary units, but that in **a** has been magnified by a factor of ten relative to that in **b**. In **a**, the path of plasma electrons pushed by the ponderomotive force of the laser is indicated by the green arrows and the longitudinal electric field within the plasma wave is shown in yellow. These simulations were performed using the OSIRIS 2.0 code¹⁰.

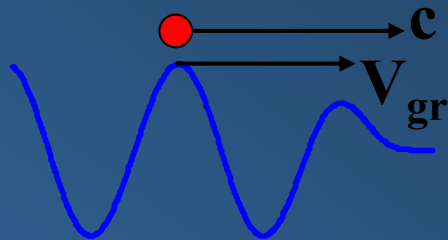
S. Hooker, Nature Photonics 2013

Limiting factors in LWFA

- **Diffraction:** order mm!
(but overcome w/ channels or relativistic self-focusing)



- **Dephasing:**



$$L_{dph} \text{ order } 10 \text{ cm} \times 10^{16}/n_0$$

- **Depletion:** For small intensity ($a_0 < 1$) $\gg L_{dph}$
For relativistic intensities ($a_0 > \sim 1$), $L_{dph} \sim L_{depl}$

Producing a mono-energetic beam

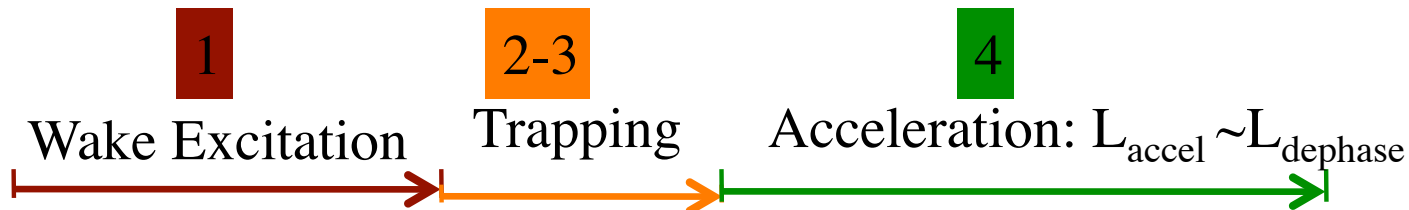
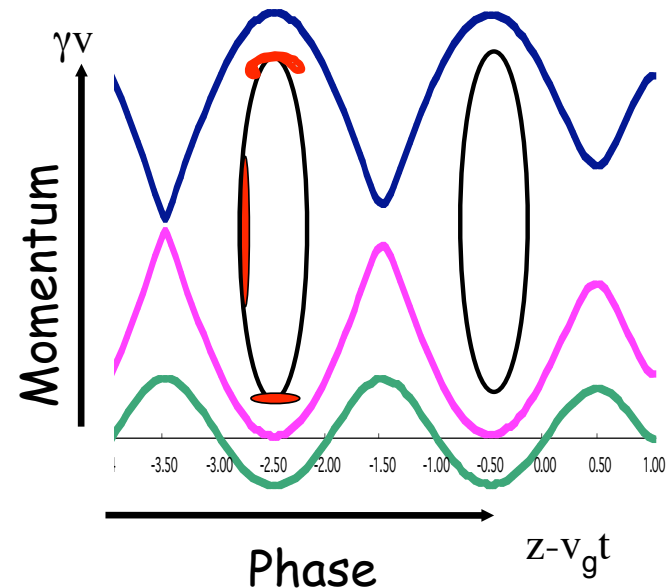
1. Excitation of wake (e.g., self-modulation of laser)
2. Onset of self-trapping (e.g., wavebreaking)
3. Termination of trapping (e.g., beam loading)
4. Acceleration

If $>$ dephasing length: large energy spread

If \approx dephasing length: monoenergetic

- Dephasing distance:

$$L_{dph} \approx \left(\lambda_p^3 / \lambda^2 \right) \propto n_e^{-3/2}$$



Useful tips

- Plasma wake field amplitude: $E_{acc} = (m_e c \omega_p / e)$
- Plasma frequency: $\omega_p = (n_e e^2 / m_e \epsilon_0)^{1/2}$
- Plasma wavelength: $\lambda_p = 2\pi c / \omega_p = 3.3 \times 10^{10} / \sqrt{n_p (cm^{-3})} [\mu m]$
- Depletion length: $L_d = (\omega_0 / \omega_p)^2 c \tau$
- Rayleigh length: $Z_R = \pi w_0^2 / \lambda$
- Dephasing length: $L_d \approx \lambda_p^3 / \lambda^2$
- Ponderomotive force: $F_p = -\nabla U_p \propto -\nabla I$

Final beam energy

- Energy gain by a particle is given as the product of electric field E , charge q and distance travelled, d :

$$W \approx qEd$$

- The phase speed of wake is (group velocity of an electromagnetic wave in a plasma)

$$\frac{v_g}{c} = \sqrt{1 - \frac{n_e}{n_c}} \approx 1 - \frac{1}{2} \frac{n_e}{n_c}$$

- n_e is the electron density of the plasma, n_c is the critical density for propagation of the electromagnetic wave (i.e. when the plasma frequency ω_p equals the frequency of the electromagnetic wave, ω_0)
- The lower the plasma density, the faster the phase speed

Final beam energy

- Dephasing will be caused due to difference between the electron velocity and the wake phase velocity

$$L_{\text{dephasing}} \approx \frac{n_e}{n_c} \lambda_p \propto n_e^{-\frac{3}{2}}$$

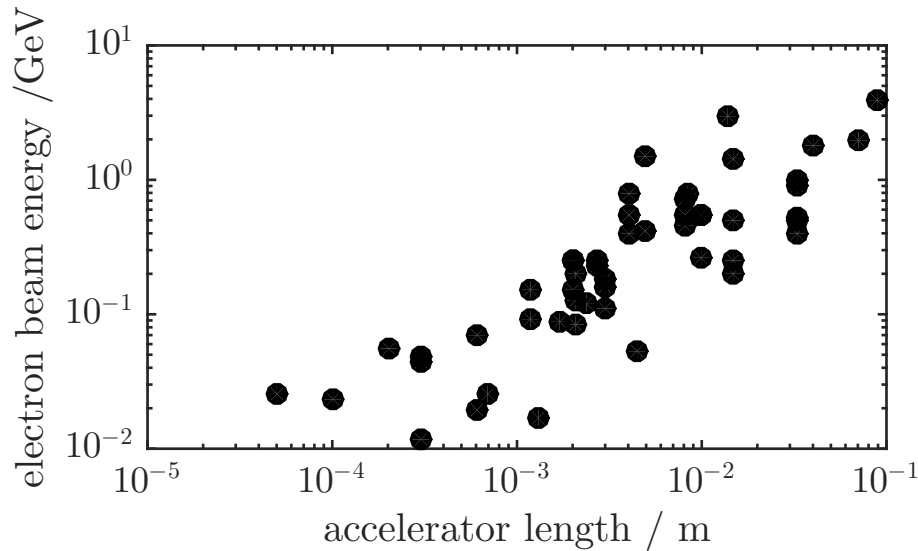
- The maximum electric field that a plasma can support increases with the plasma density

$$E_{\text{max}} \cong m_e c \omega_p / e \propto \sqrt{n_e}$$

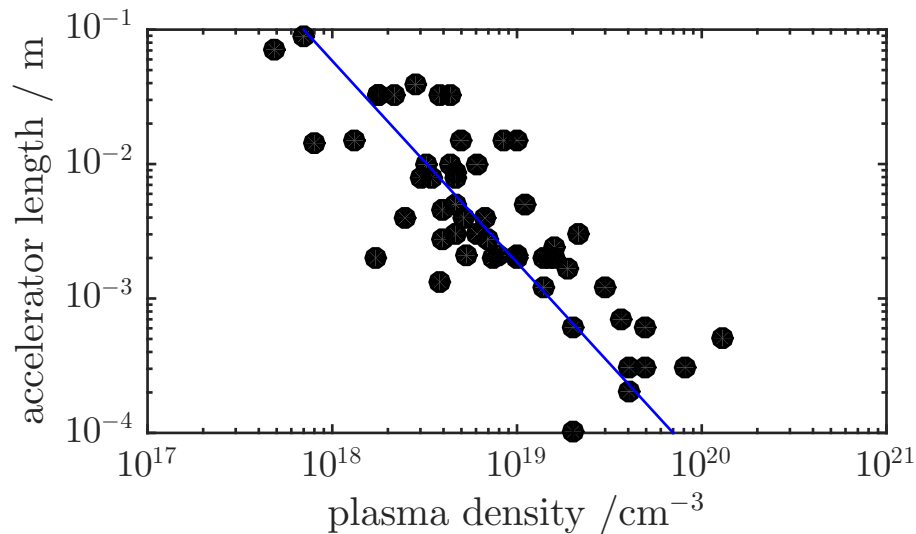
- The maximum energy that can be gained by an electron in a plasma wave as a function of plasma density is therefore written as

$$W(n_e) \approx E_{\text{max}} L_{\text{dephasing}} \propto \frac{1}{n_e}$$

Scaling laws



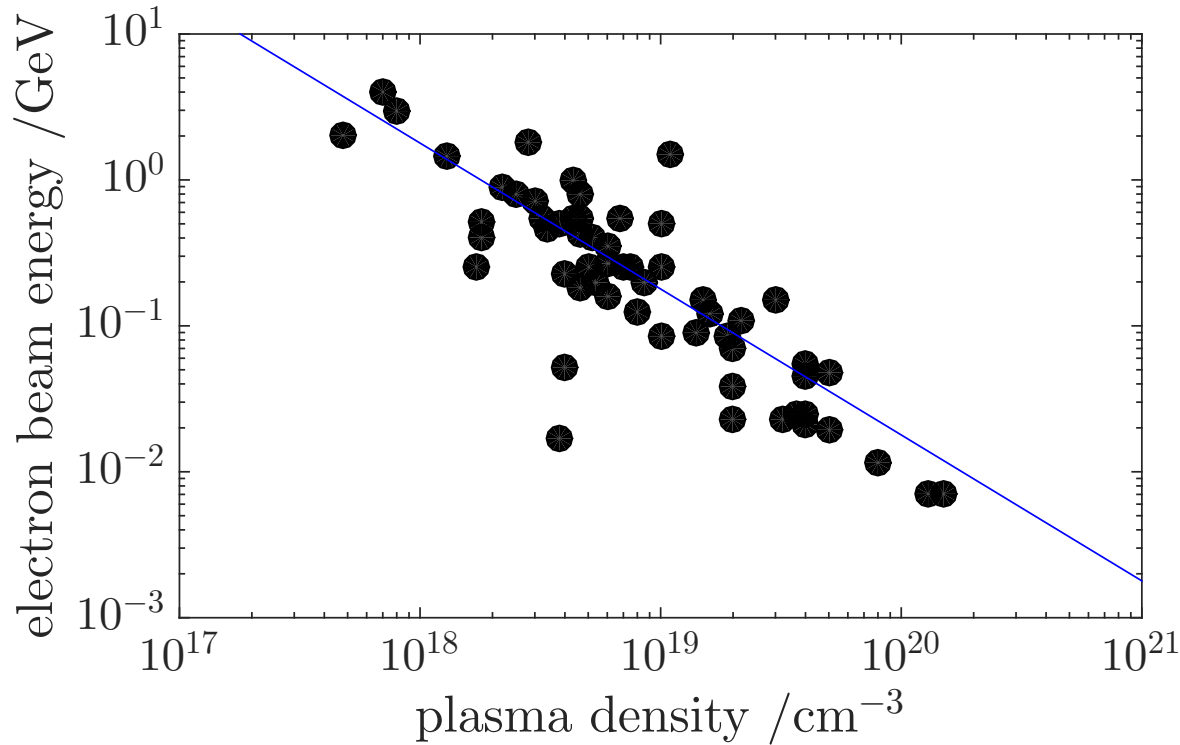
Electron beam energy vs.
accelerator length (2004-2014)



Accelerator length vs.
plasma density (2004-2014)

S.P.D. Mangles, CERN -2016-001

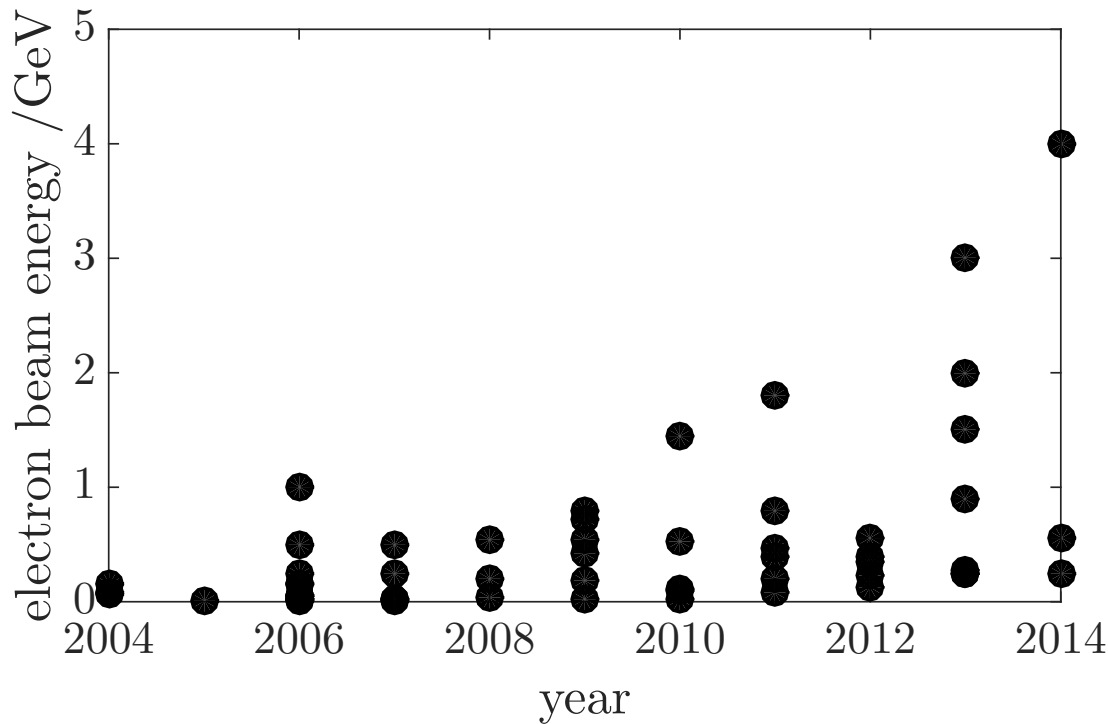
Scaling laws



Electron beam energy vs.
plasma density (2004-2014)

S.P.D. Mangles, CERN -2016-001

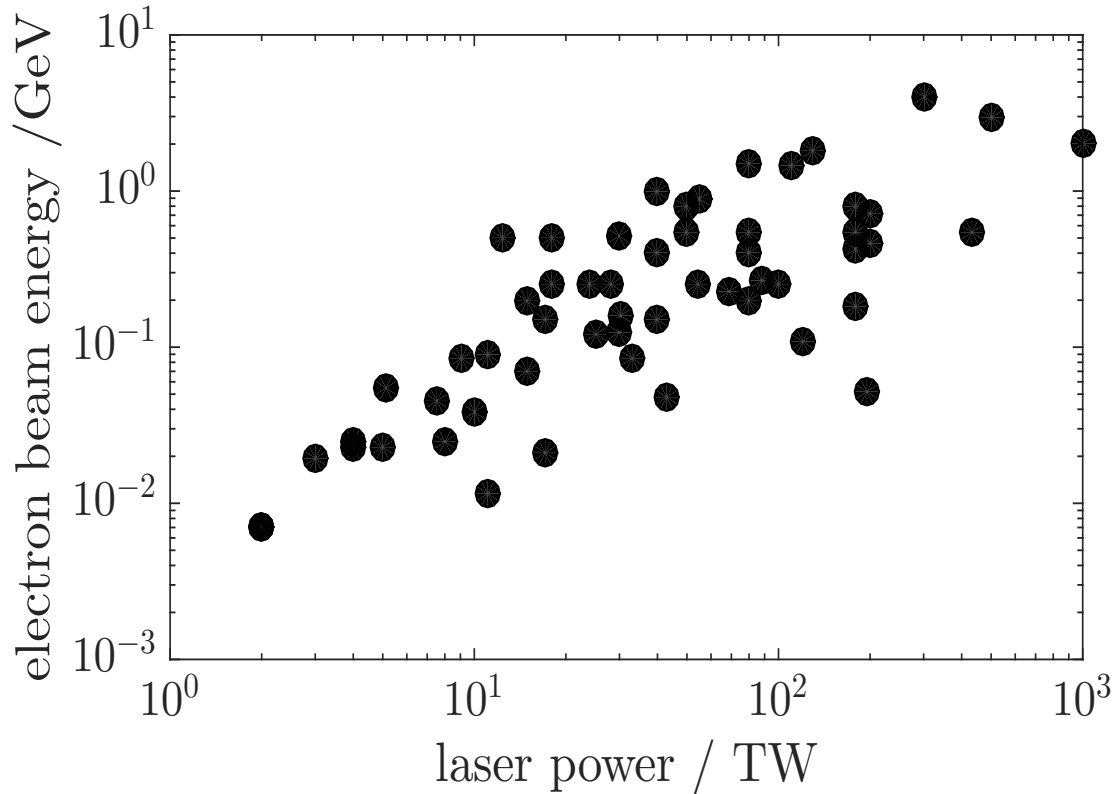
Scaling laws



Electron beam energy vs.
Years (2004-2014)

S.P.D. Mangles, CERN -2016-001

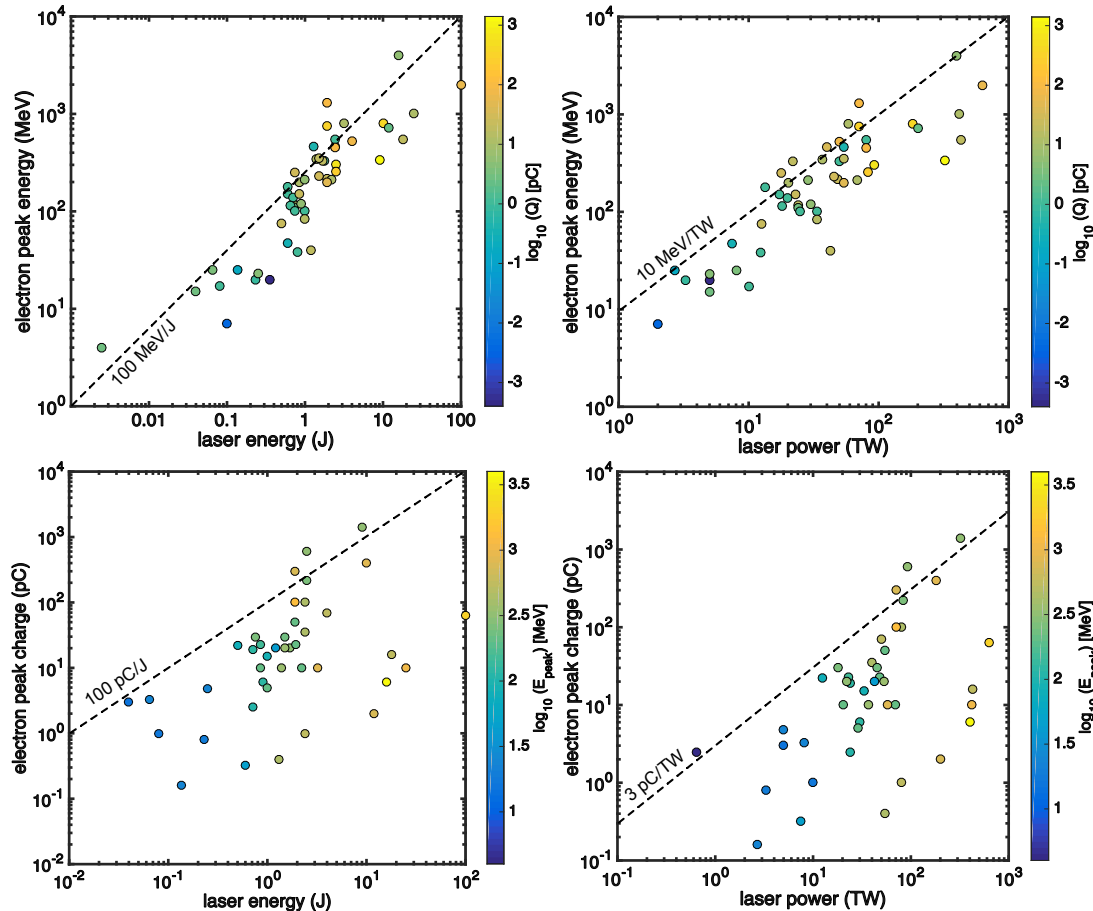
Scaling laws



Electron beam energy vs.
laser power (2004-2014)

S.P.D. Mangles, CERN -2016-001

Scaling laws



J. Wenz and S. Karsch, arXiv: 2007.04622v1 (2020)

Fig. 9: Experimental results for energy and charge: Experimentally, the best results for electron peak energy and charge closely follow extremely simple scaling laws with respect to the laser power and energy. Note that these "laws" are no fit to the data, just lines to guide the eye. Data is based on 50+ publications on LWFA during the last 15-20 years [95]

Experiments for high quality beam

30 Sep 2004 issue of *nature*:

Three groups report production of high quality e-bunches

- Approach 1: Plasma channel

- LBNL/USA: Geddes et al.

- Plasma Channel: $1\text{--}4 \times 10^{19} \text{ cm}^{-3}$
- Laser: 8-9 TW, 8.5 μm , 55 fs
- E-bunch: 2×10^9 (0.3 nC), 86 MeV, $\Delta E/E = 1\text{--}2\%$, 3 mrad

- Approach 2: No channel, larger spot size

- RAL/IC/UK: Mangles et al.

- No Channel: $2 \times 10^{19} \text{ cm}^{-3}$
- Laser: 12 TW, 40 fs, 0.5 J, $2.5 \times 10^{18} \text{ W/cm}^2$, 25 μm
- E-bunch: 1.4×10^8 (22 pC), 70 MeV, $\Delta E/E = 3\%$, 87 mrad

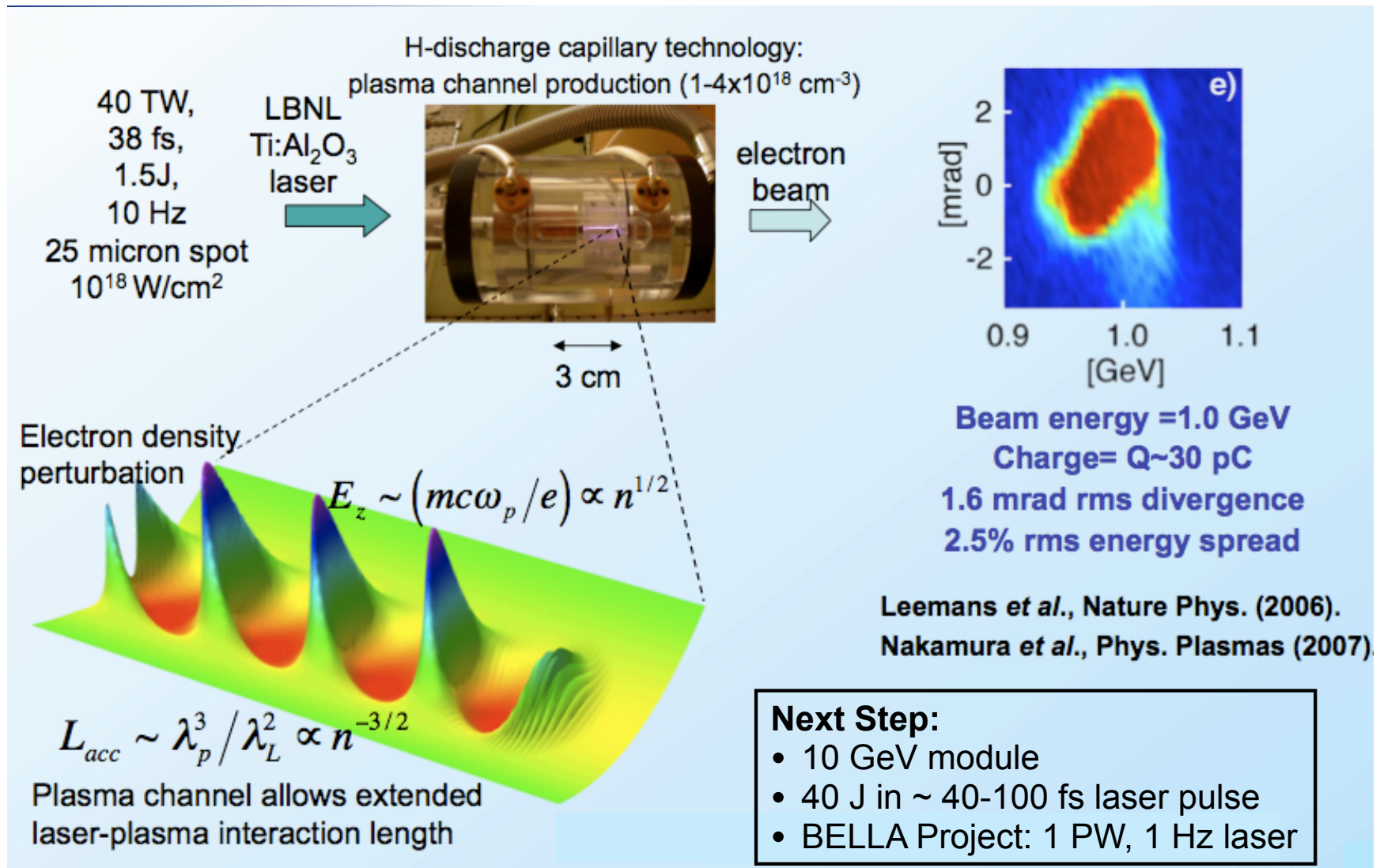
- LOA/France: Faure et al.

- No Channel: $0.5\text{--}2 \times 10^{19} \text{ cm}^{-3}$
- Laser: 30 TW, 30 fs, 1 J, 18 μm
- E-bunch: 3×10^9 (0.5 nC), 170 MeV, $\Delta E/E = 24\%$, 10 mrad

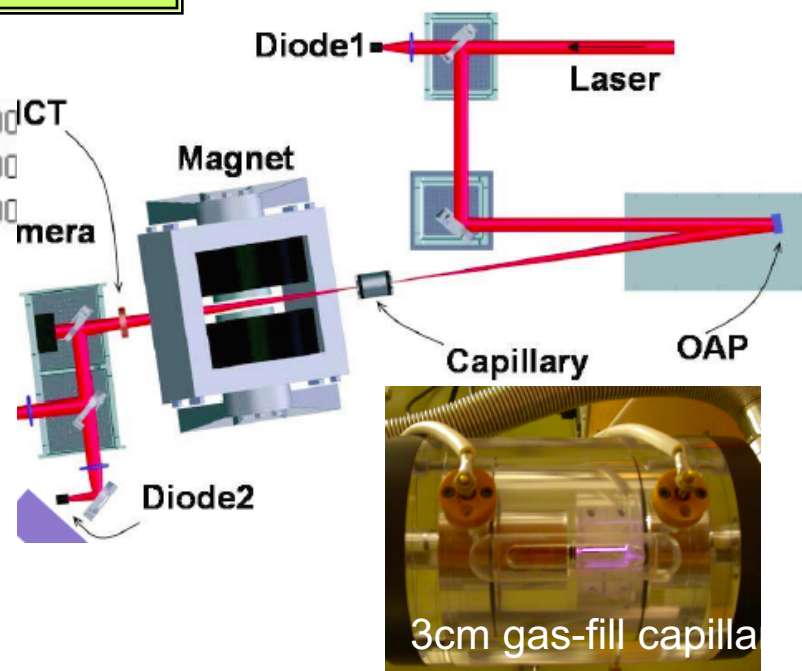
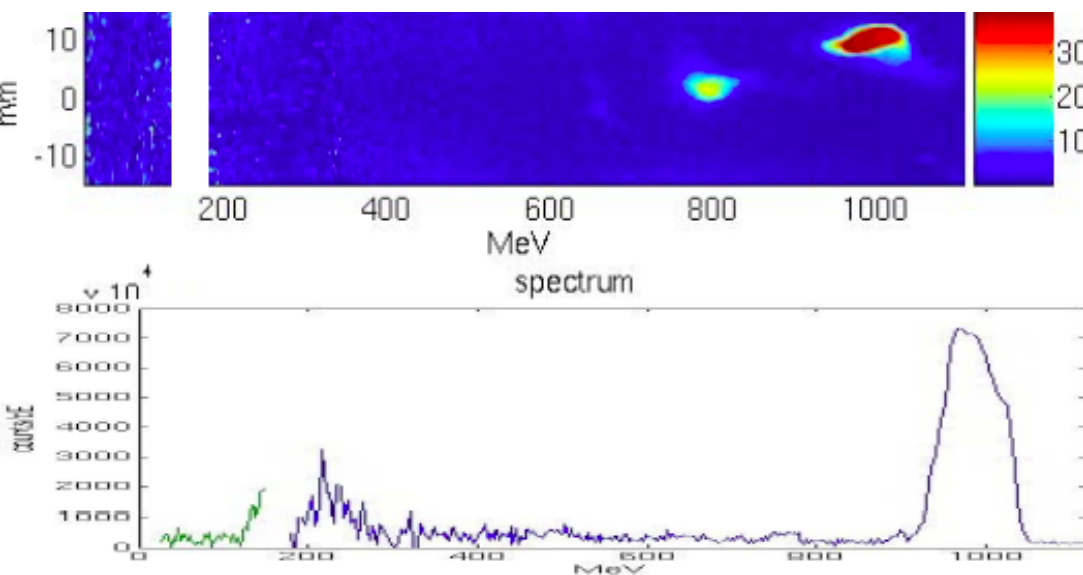
- Channel allows higher e-energy with lower laser power



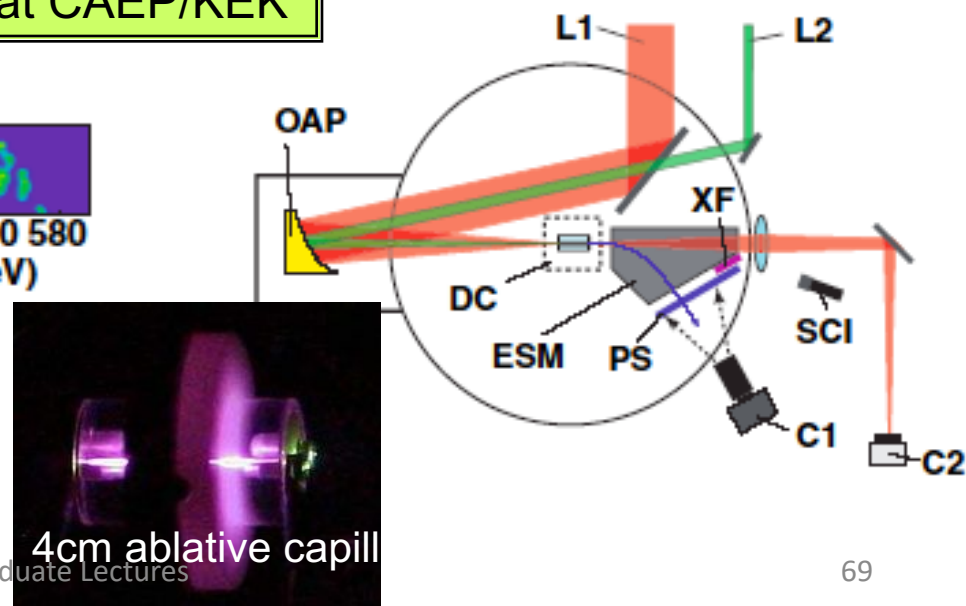
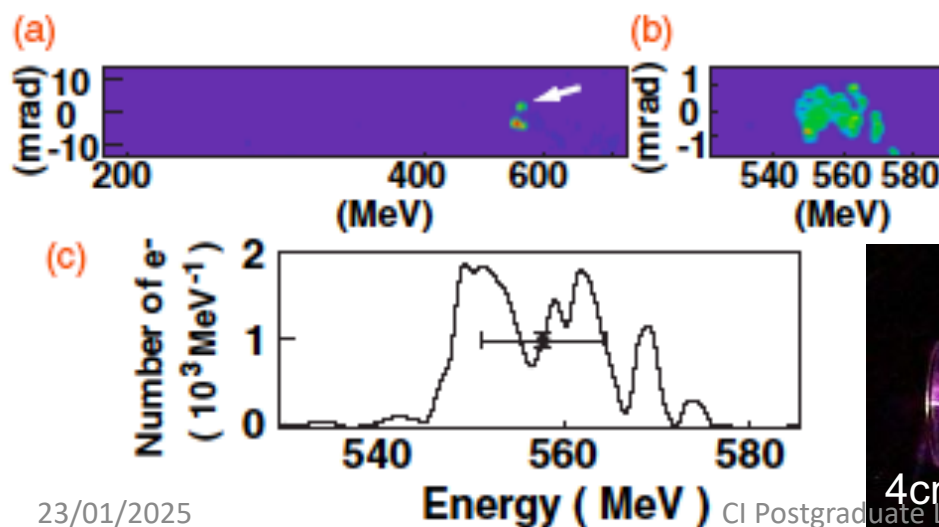
1 GeV experiment at LBNL



1 GeV capillary accelerator experiment at LBNL/Oxford U.

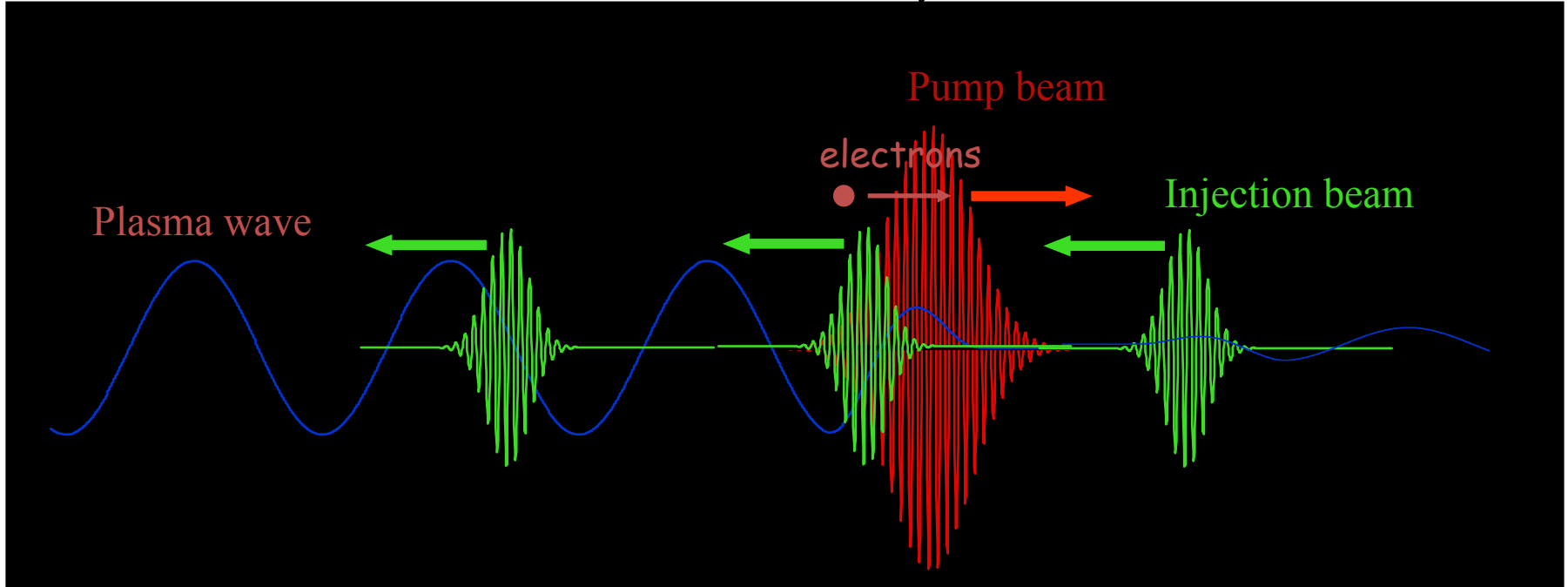
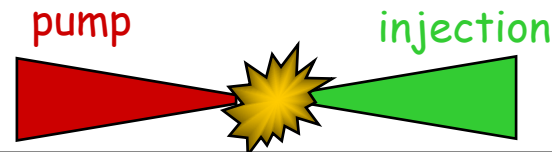


0.56 GeV capillary accelerator experiment at CAEP/KEK



Controlling the injection

Counter-propagating geometry:



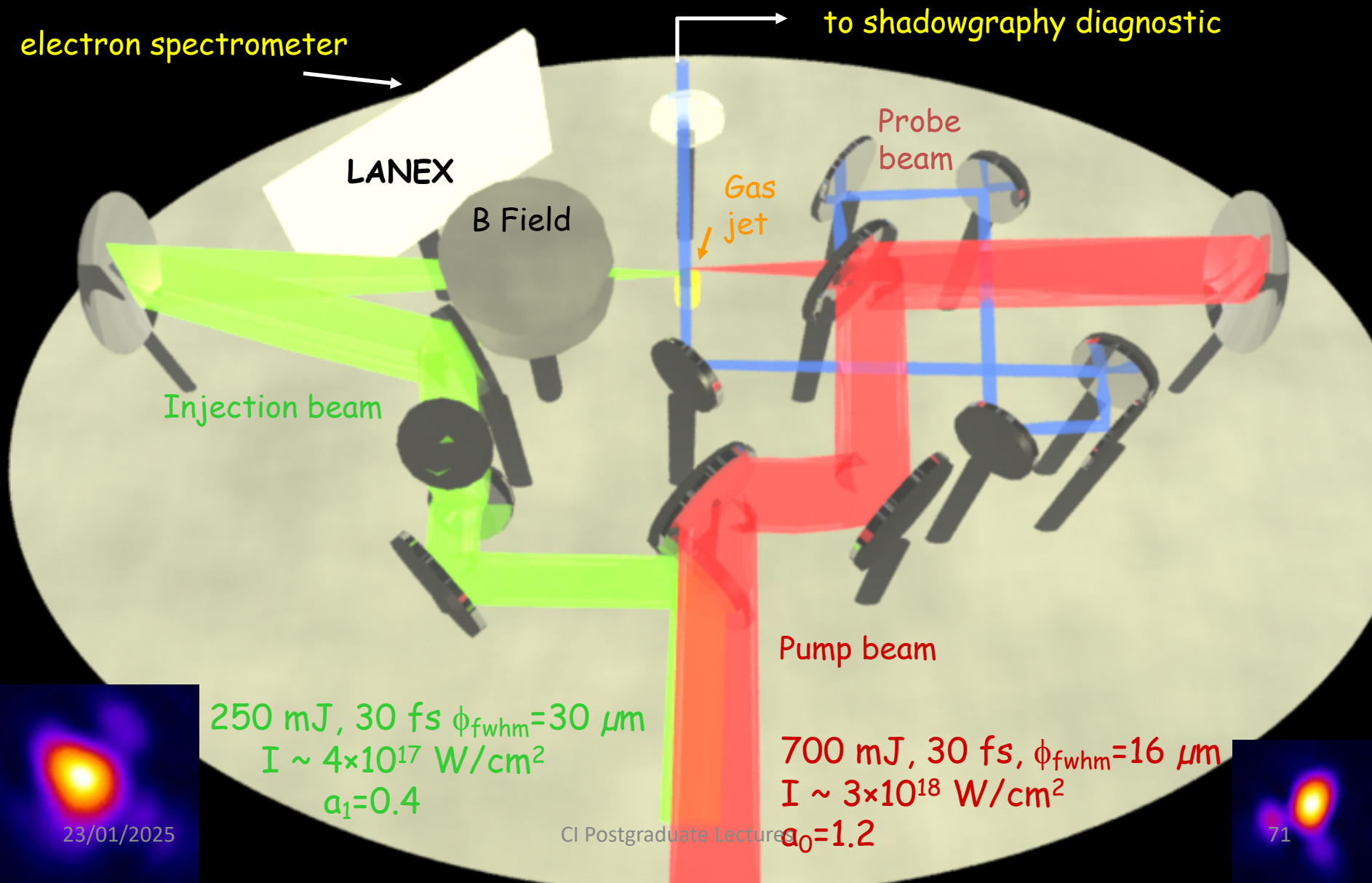
Ponderomotive force of beatwave: $F_p \sim 2a_0a_1/\lambda_0$ (a_0 et a_1 can be "weak")

Boost electrons locally and injects them:

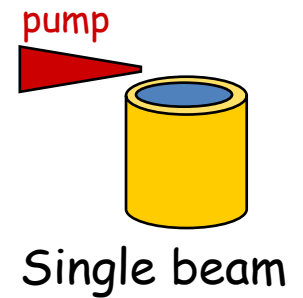
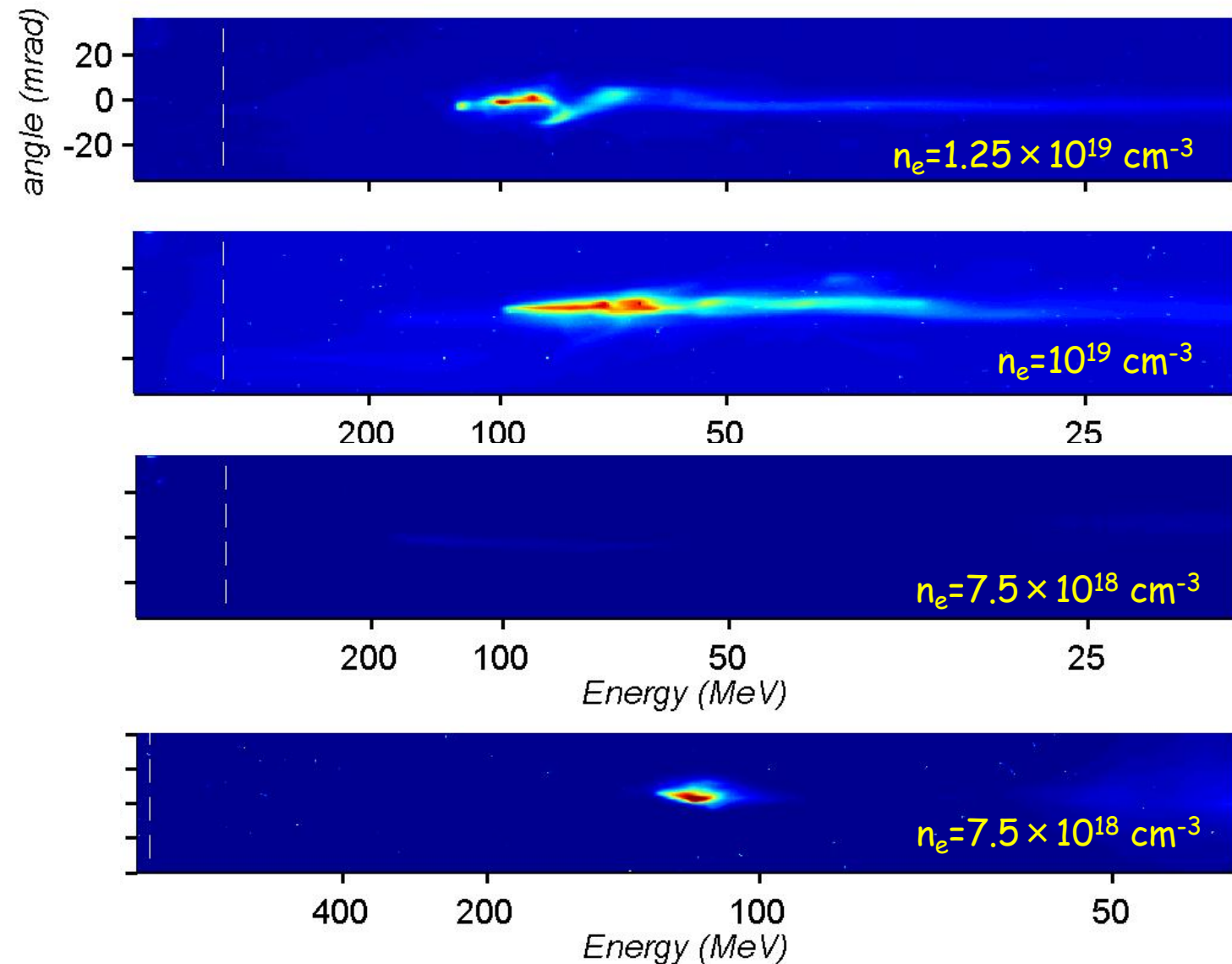
INJECTION IS LOCAL IN FIRST BUCKET

E. Esarey et al, PRL 79, 2682 (1997), G. Fubiani et al. (PRE 2004)

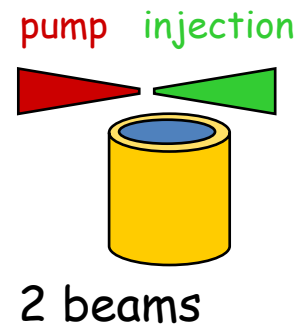
Experimental set-up



From self-injection to controlled injection



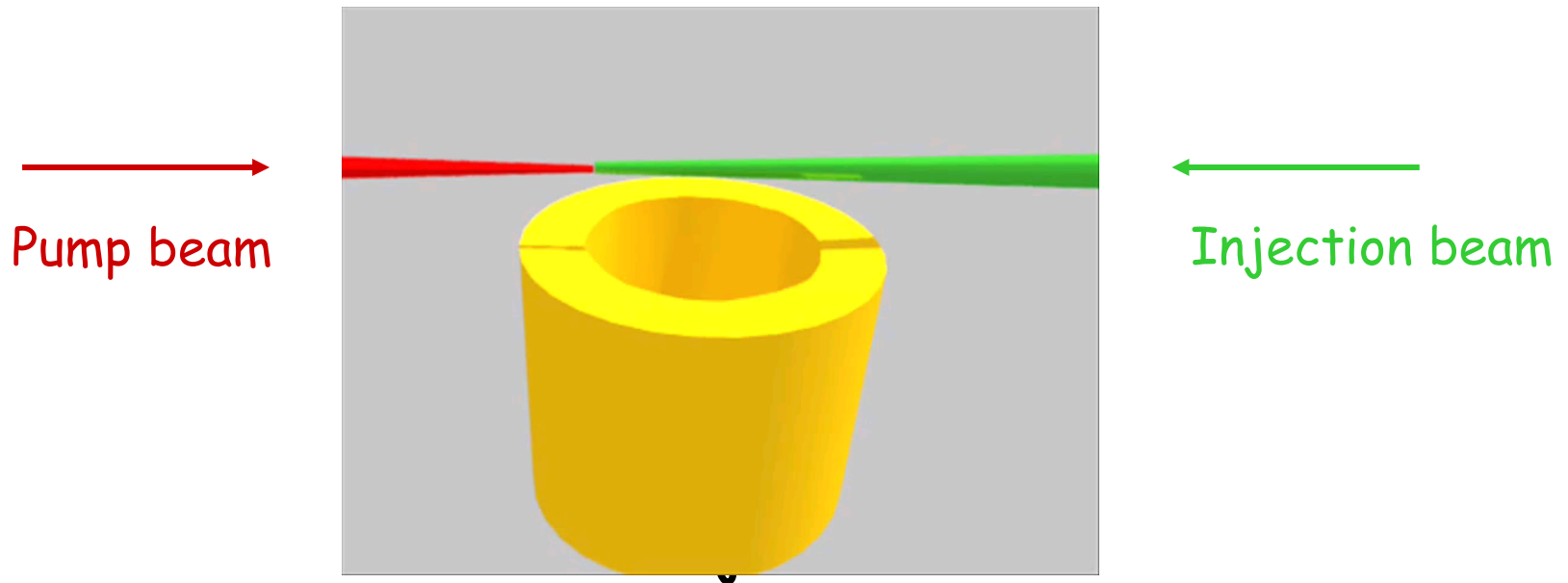
Self-injection
Threshold



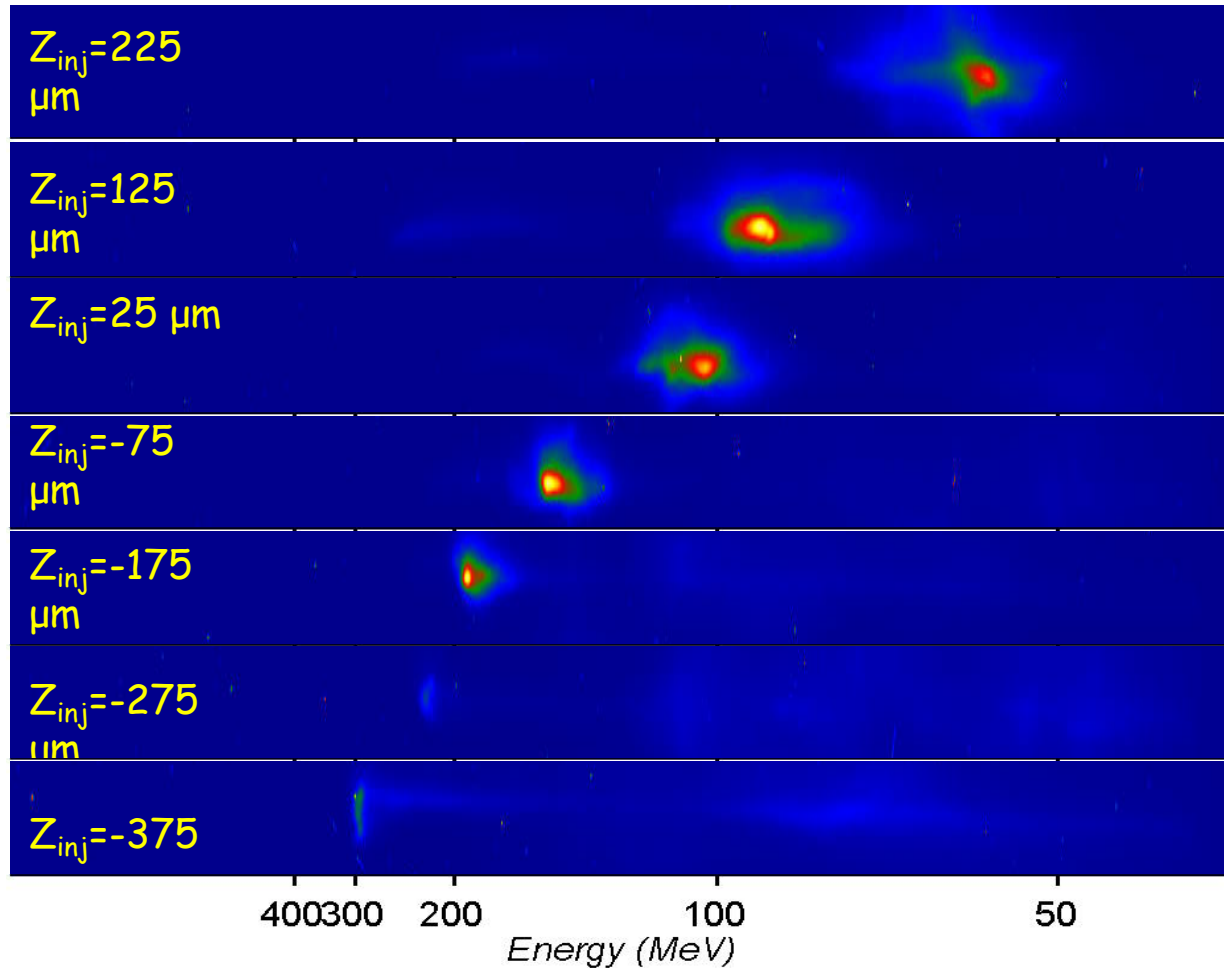
Controlling the acceleration length

By changing delay between pulses:

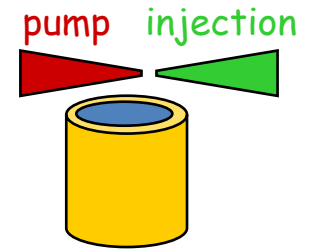
- Change collision point
- Change effective acceleration length
- Tune bunch energy



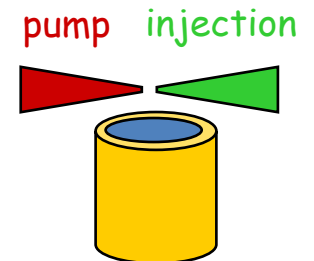
Tunable mono-energetic bunches



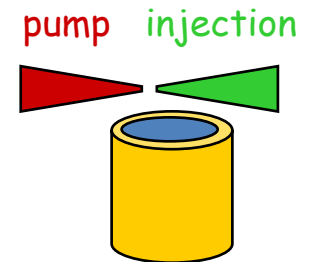
J. Faure... V. Malka (Ecole Polytechnique) Nature 444, 737 (2006)



late injection



middle injection



early injection

Dual stage LWFAs

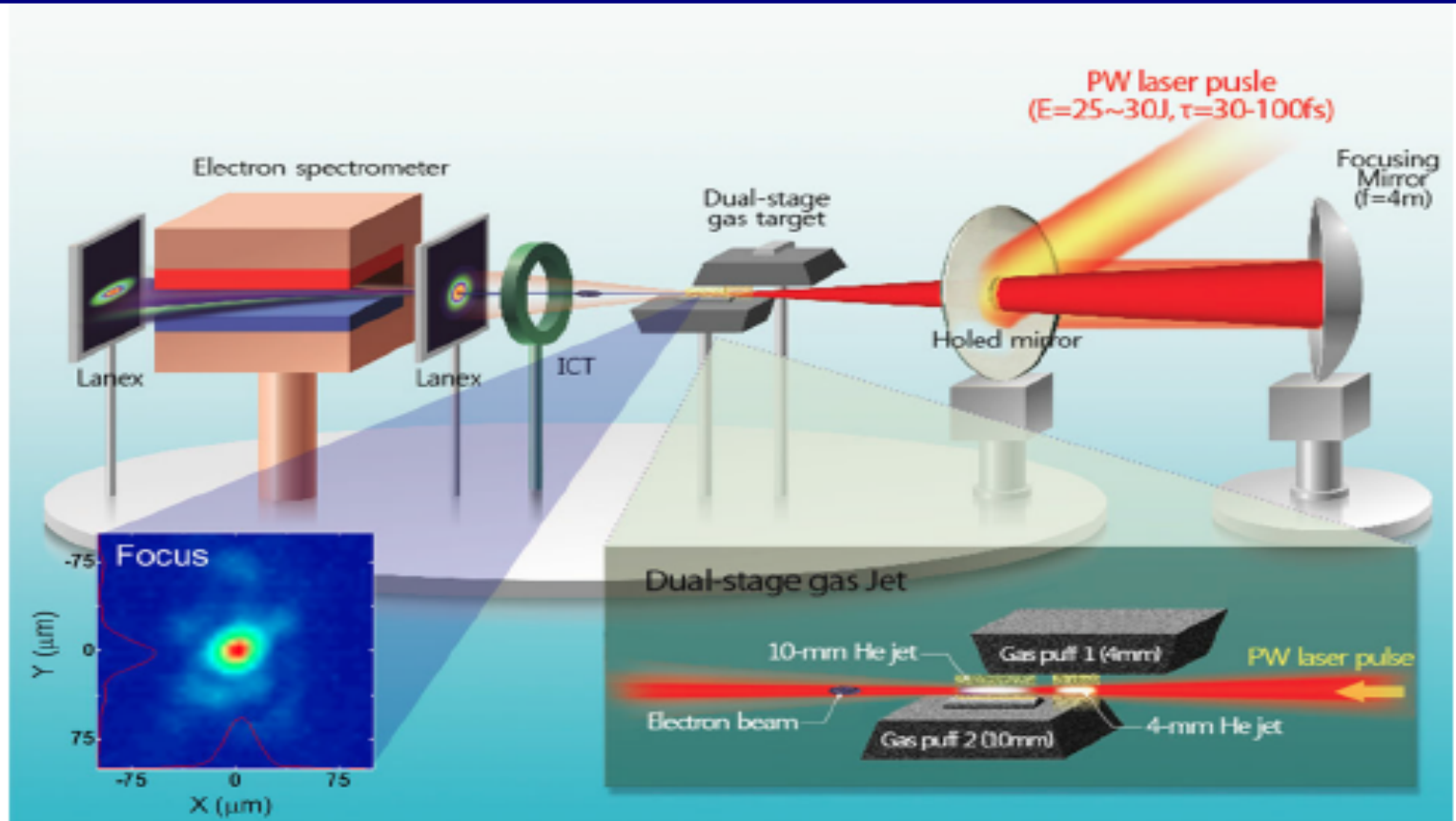


FIG. 1 (color online). Experimental layout. The dipole magnet has length of 30 cm and magnetic field strength of 1.33 T, which was installed 1 m away from the gas-jet target. Two Lanex screen have been installed at the entrance and exit of the magnet to measure electron beam profile and energy, respectively. The ICT was installed between gas jet and dipole magnet to measure the charge of the electron beam.

GIST, Korea

Dual stage LWFAs

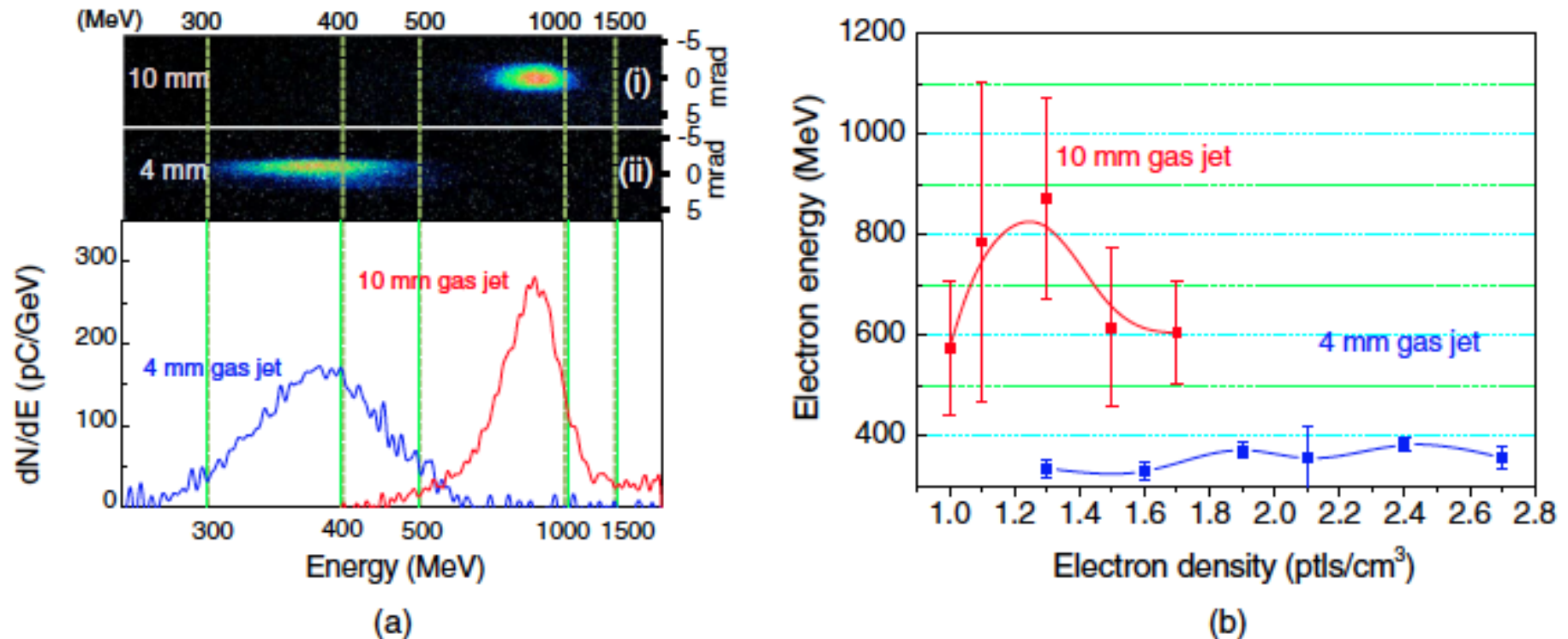


FIG. 2 (color online). (a) Electron energy spectrum for 10-mm [red line and image (i)] and 4-mm [blue line and image (ii)] gas jets. (b) Electron energy with respect to the electron density.

H.T. Kim, PRL 111, 165002 (2013)

2 GeV barrier

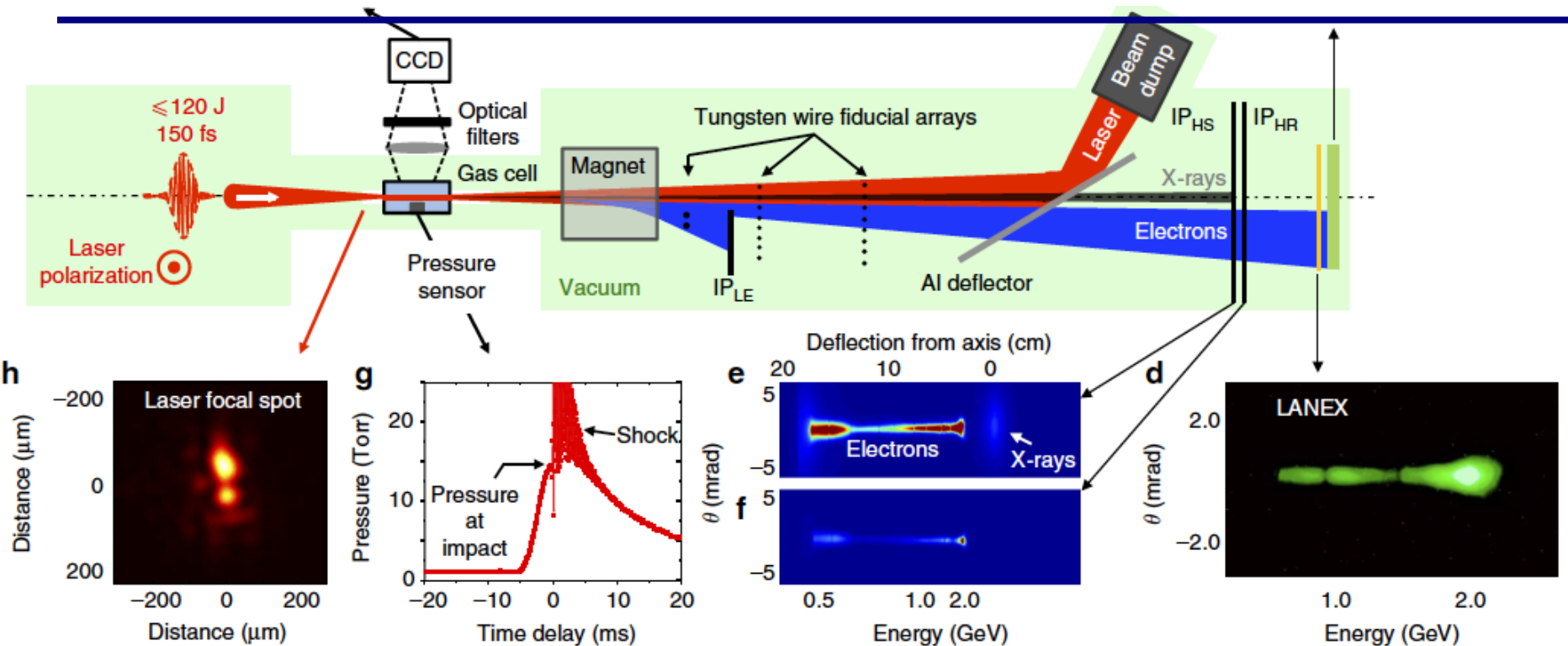
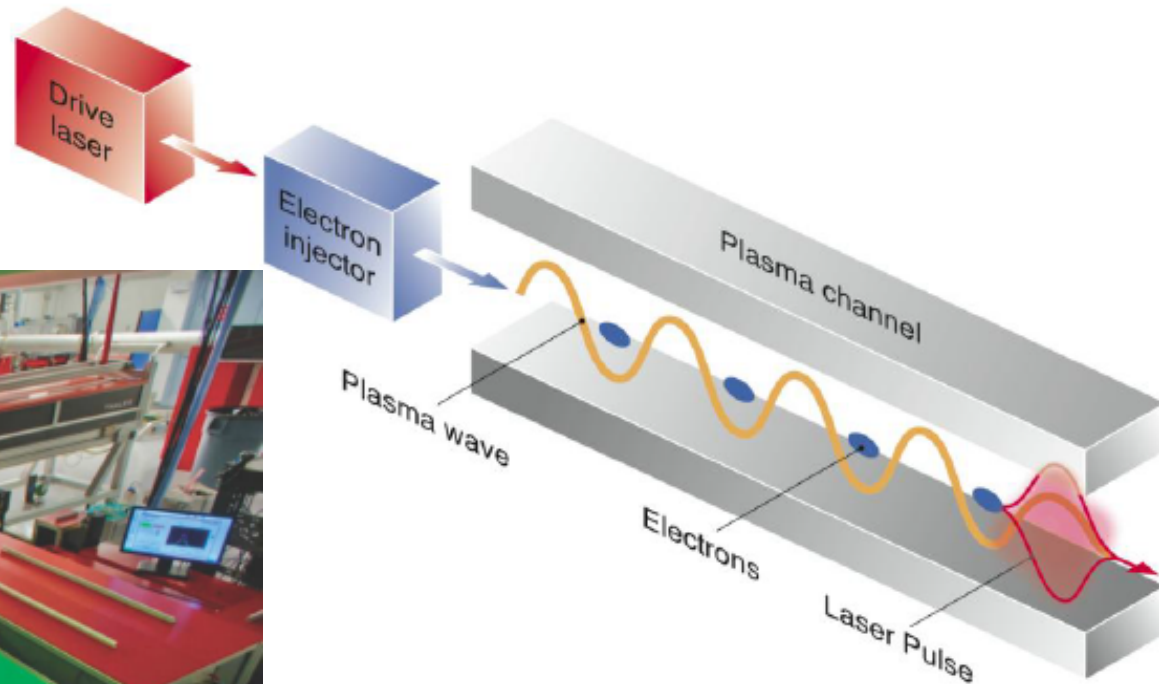


Figure 1 | Schematic diagram of PW laser-driven wakefield accelerator. The main components were enclosed in a vacuum chamber, highlighted in green, which was kept at 10^{-6} Torr. The PW laser pulse, entering from the left and linearly polarized perpendicular to the plane of the drawing, was focused into the gas cell, where it created a He plasma and wake that captured and accelerated electrons to 2 GeV. Electrons and betatron X-rays emerging from the cell exit aperture passed through a magnetic field, then through two linear arrays of eight 127 μm diameter tungsten-wire fiducials located 1.256 and 1.764 m, respectively, downstream from the cell exit. A 25- μm thick Al foil deflected the transmitted laser pulse to a beam dump. Undelected X-rays and energy-dispersed electrons above 0.5 GeV passed through this foil, and exposed in sequence a high-sensitivity (HS) imaging plate (IP_{HS}), a high-resolution (HR) IP (IP_{HR}), a phosphorescing screen (LANEX) and a plastic scintillator. An additional IP_{LE} recorded low-energy (LE) electrons (< 0.35 GeV) after they passed through a third array of fiducials. Surrounding panels highlight various diagnostics and details, clockwise from upper left: (a) transversely scattered light, spectrally filtered and imaged to a CCD camera (the dashed rectangle shows the region near the cell exit from which betatron X-rays originated, as determined by X-ray triangulation); (b) trajectories of 2 GeV electrons for shots that yielded the results in Fig. 2a,b (labelled 'a' and 'b', respectively) relative to the fiducial arrays (labelled 1-1 through to 1-8 for the first array and 2-1 through to 2-8 for the second array); (c-f), unprocessed data showing electrons up to 2.3 GeV and fiducial shadows for the shot that yielded the results in Fig. 2a, as detected on (c) scintillator, (d) LANEX, (e) IP_{HS} (also showing undeflected X-rays) and (f) IP_{HR}; (g) He pressure versus time, and an acoustic shock when the laser pulse arrived, as recorded by a fast pressure transducer; (h) a typical laser focal spot.

Petawatt laser facility at LBNL



Short pulse laser
laser guiding in plasma
(3'D' effect:
diffraction, dephasing, depletion)

2014 results-LWFA

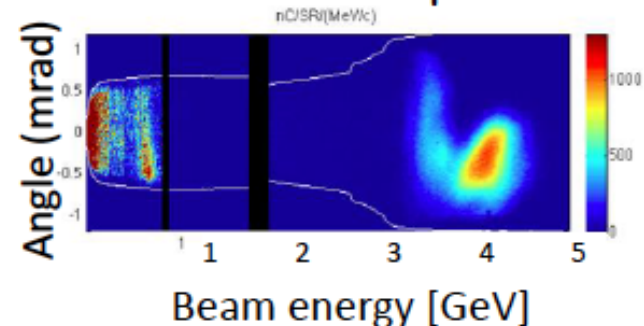
BELLA: 4.25 GeV beams from 9 cm plasma channel with 390 TW laser pulses

- With conventional technology this energy requires a 200 m long accelerator, a downsizing factor of 10,000
- Present investment in Laser Plasma Acceleration has potential to achieve ~10 GeV energy level in future experiments
- New BELLA facility commissions world-record petawatt laser for LPA science (>1 PW at 1 Hz)

9 cm long capillary discharge



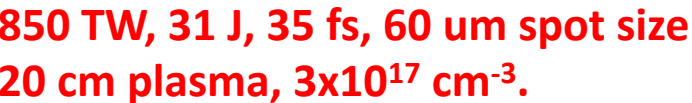
Electron beam spectrum



Impact

New technology with potential for far lower accelerator size and cost

W.P. Leemans et al., PRL 113, 245002 (2014)



80

BELLA - 7.8 GeV

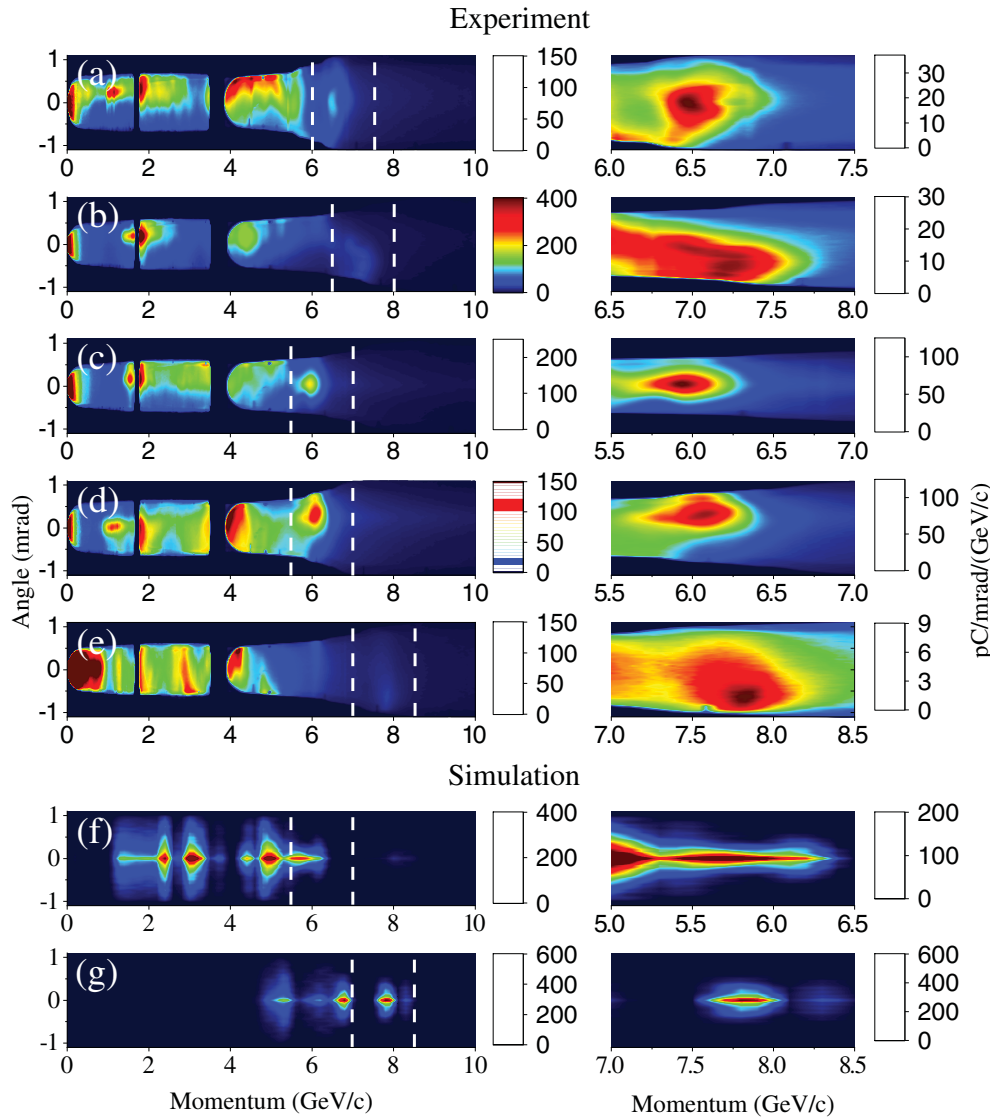


FIG. 4. (a)–(e): Electron beams measured by the magnetic spectrometer for $n_0 = 3.4 \times 10^{17} \text{ cm}^{-3}$, $r_m = 69 \mu\text{m}$ and laser power 850 TW. The driver laser pulse arrival was timed with the peak of the heater pulse. The heater pulse arrived 300 ns after the peak of the discharge current, except for (e), where the delay was 420 ns, and the heater-induced density reduction was measured to be larger, with $n_0 = 2.7 \times 10^{17} \text{ cm}^{-3}$ and $r_m = 61 \mu\text{m}$. The white dashed lines show the regions that are plotted in the right hand column, which shows the detailed spectrum of the highest energy peaks. The electron beam spectrum simulated by INF&RNO using the MARPLE-retrieved density profile (with $n_0 = 3.4 \times 10^{17} \text{ cm}^{-3}$) is shown in (f). In (g) a simulation is shown for the parameters of (e) using a transversely parabolic and longitudinally uniform density profile.

Gonsalves, et al., PRL 122, 084801 (2019)

BELLA - 10 GeV

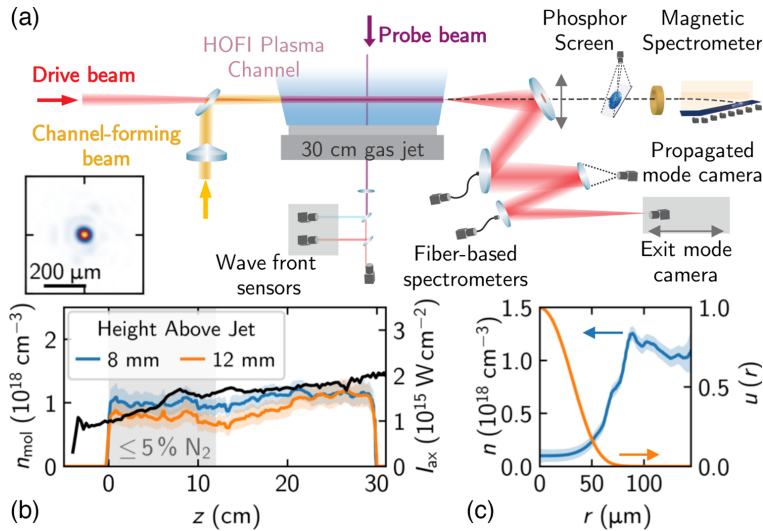


FIG. 1. (a) Schematic of the experimental setup. Inset: measured vacuum mode of the drive laser pulse. (b) Measured molecular density of the gas jet (blue and orange lines) and peak intensity of the channel-forming pulse along the length of the gas (black line). (c) Measured electron and neutral density $n = n_e + n_n$ of the HOFI plasma channel at $\Delta\tau = 6$ ns (blue) and calculated fundamental mode of the measured plasma channel (orange line).

500 TW, 21.3 J laser energy
30 cm plasma with density $1 \times 10^{17} \text{ cm}^{-3}$
hydrodynamic, optically-field-ionized (HOFI) channel
9.2-10 GeV

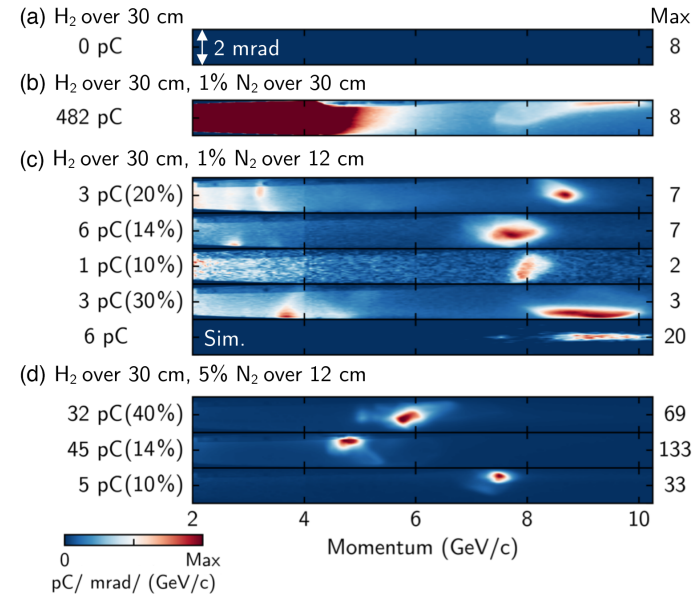


FIG. 4. Example electron beams generated in 30-cm-long HOFI channels with $\mathcal{E}_0 = (21.3 \pm 0.3)$ J. For each row, the charge measured by the spectrometer within the quasimonoegetic bunch and percent captured by the spectrometer is given. (a) $\Delta\tau = 6$ ns, no nitrogen, (b) $\Delta\tau = 7$ ns, 1% nitrogen, $L_{\text{dop}} \approx 30$ cm, (c) $\Delta\tau = 5$ ns, 1% nitrogen, $L_{\text{dop}} \approx 12$ cm, (d) $\Delta\tau = 6$ ns, 5% nitrogen, $L_{\text{dop}} \approx 12$ cm.

A. Picksley et al., Phys. Rev. Lett. 133, 255001 (2024)

Highest energy record - 10 GeV

Matter and
Radiation at Extremes

RESEARCH ARTICLE

pubs.aip.org/aip/mre

The acceleration of a high-charge electron bunch to 10 GeV in a 10-cm nanoparticle-assisted wakefield accelerator

Cite as: Matter Radiat. Extremes 9, 014001 (2024); doi: [10.1063/5.0161687](https://doi.org/10.1063/5.0161687)

Submitted: 11 June 2023 • Accepted: 22 October 2023 •

Published Online: 15 November 2023



View Online



Export Citation



CrossMark

Constantin Aniculaesei,^{1,a)} Thanh Ha,¹ Samuel Yoffe,² Lance Labun,^{1,3} Stephen Milton,³ Edward McCary,¹ Michael M. Spinks,¹ Hernan J. Quevedo,¹ Ou Z. Labun,¹ Ritwik Sain,¹ Andrea Hannasch,¹ Rafal Zgadzaj,¹ Isabella Pagano,^{1,4} Jose A. Franco-Altamirano,¹ Martin L. Ringuette,¹ Erhart Gaul,¹ Scott V. Luedtke,⁵ Ganesh Tiwari,⁶ Bernhard Ersfeld,² Enrico Brunetti,² Hartmut Ruhl,⁷ Todd Ditmire,¹ Sandra Bruce,¹ Michael E. Donovan,³ Michael C. Downer,¹ Dino A. Jaroszynski,² and Bjorn Manuel Hegelich^{1,3,b)}

AFFILIATIONS

¹ University of Texas at Austin, Austin, Texas 78712, USA

² SUPA Department of Physics, University of Strathclyde, Glasgow, Scotland G4 0NG, United Kingdom

³ Tau Systems, Inc., Austin, Texas 78701, USA

⁴ Lawrence Livermore National Laboratory, Livermore, California 94550, USA

⁵ Los Alamos National Laboratory, Los Alamos, New Mexico 87545, USA

⁶ Brookhaven National Laboratory, Upton, New York 11973, USA

⁷ Ludwig-Maximilians-Universität, Munich, Germany

Highest energy record - 10 GeV

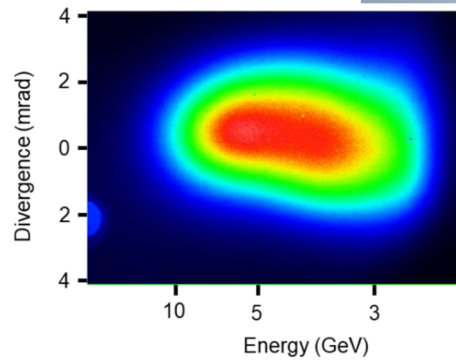
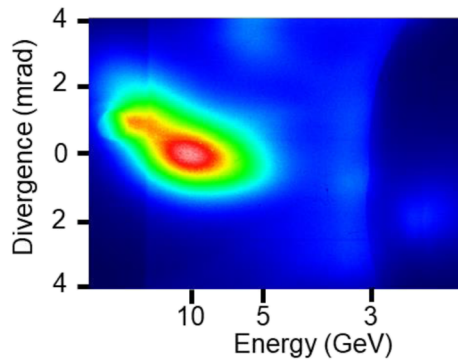
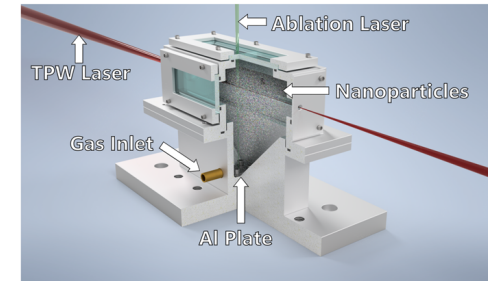
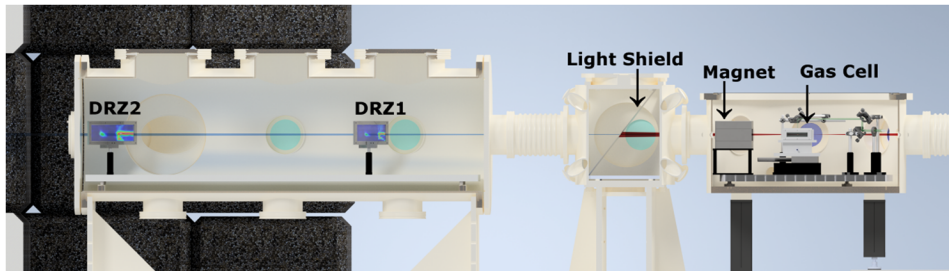


TABLE I. The laser parameters corresponding to some of the highest electron energy shots. The electron energy is taken as the centroid of the highest energy bunch. The charge is taken from DRZ2 with a lower cutoff energy of 2 GeV.

Shot	Pulse duration (fs)	Laser energy (J)	Focal plane position (mm)	Strehl ratio	Electron centroid energy (GeV)	Total charge (pC)	Pointing correction (mrad)
1	134	118	7.21	0.72	10.40 ± 1.93	1703	0
2	143	125	7.05	0.4	4.90 ± 0.42	773	0
3	136	124	7.05	0.64	6.20 ± 0.68	506	2.2
4	147	97	4.21	0.58	4.50 ± 0.36	1349	0
5	139	128	7.69	0.61	3.50 ± 0.22	419	0
6	134	126	6.29	0.47	3.40 ± 0.20	1102	0.75

C. Aniculaesei et al., *Matter Radiat. Extremes* **9**, 014001 (2024)

Application of LWFA based accelerators

LWFA based TeV collider parameters

Plasma density scalings:

Stage density scalings:

$$E_0 \propto n^{1/2}$$

$$L_{\text{stage}} \propto n^{-3/2}$$

$$W_{\text{stage}} \propto n^{-1}$$

$$U_L \propto n^{-3/2}$$

$$N_b \propto n^{-1/2}$$

Collider density scalings (for fixed luminosity):

$$f \propto n$$

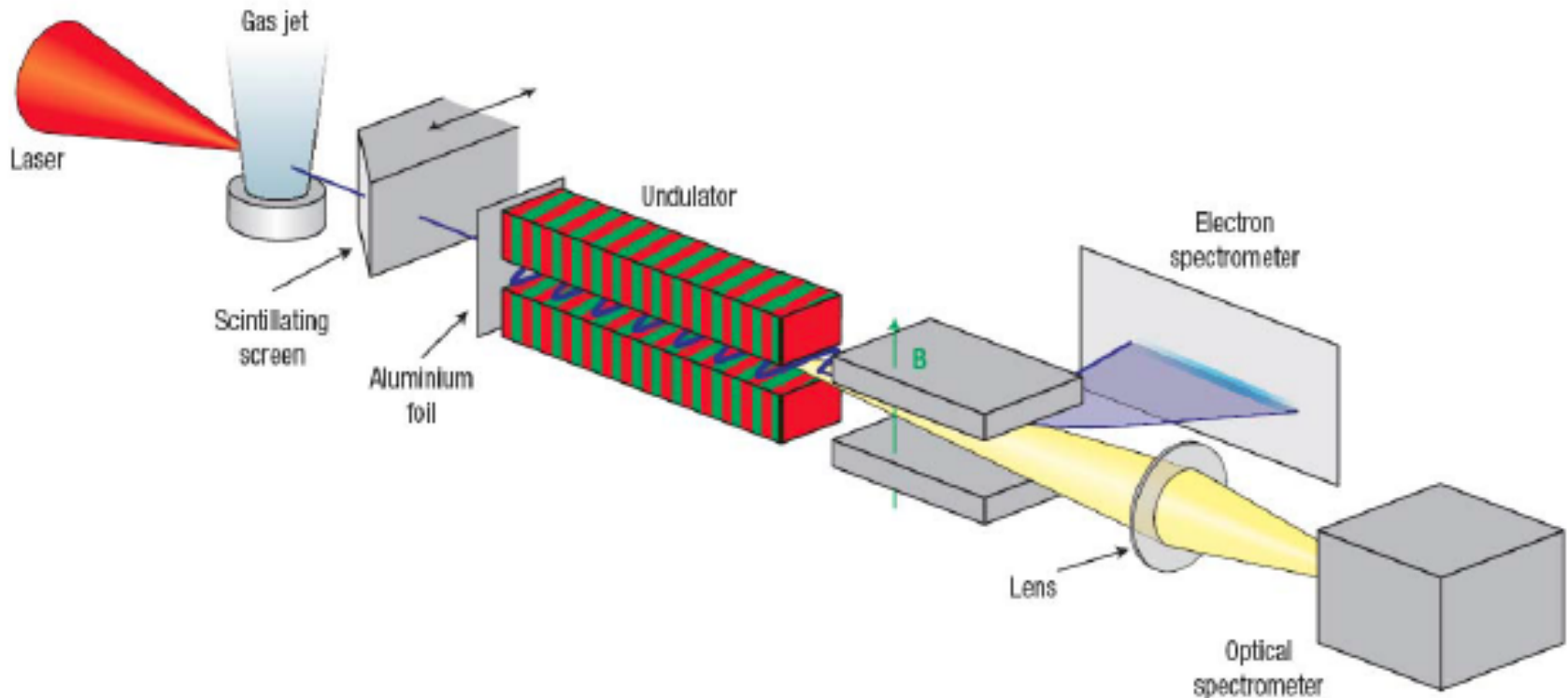
$$N_{\text{stage}} \propto n$$

$$P_b \propto n^{1/2}$$

$$P_{\text{laser}} \propto n^{-1/2}$$

Plasma number density, n_0	10^{17} cm^{-3}
Energy, center of mass, E_{cm}	1 TeV
Beam energy, γmc^2	0.5 TeV
Number per bunch, N	4×10^9
Collision rate, f	15 kHz
Beam Power, $P_b = fN\gamma mc^2$	4.8 MW
Luminosity, \mathcal{L}	$2 \times 10^{34} \text{ s}^{-1} \text{ cm}^{-2}$
Bunch length, σ_z	1 μm
Horizontal rms beam size at IP, σ_x	0.1 μm
Vertical rms beam size at IP, σ_y	1 nm
Horizontal normalized emittance, ϵ_{nx}	1 mm-mrad
Vertical normalized emittance, ϵ_{ny}	0.01 mm-mrad
Beamstrahlung parameter, Y	35
Plasma wavelength, λ_p	105 μm
Energy gain per stage, W_{stage}	10 GeV
Single stage laser-plasma interaction length	0.9 m
Drive laser coupling distance between stages	0.5 m
Laser energy per stage	40 J
Laser wavelength	1 μm
Initial normalized laser intensity, a_0	1.5
Average laser power per stage	600 kW
Number of stages	50
Main linac length	70 m
Efficiency (wall-plug to beam)	5%

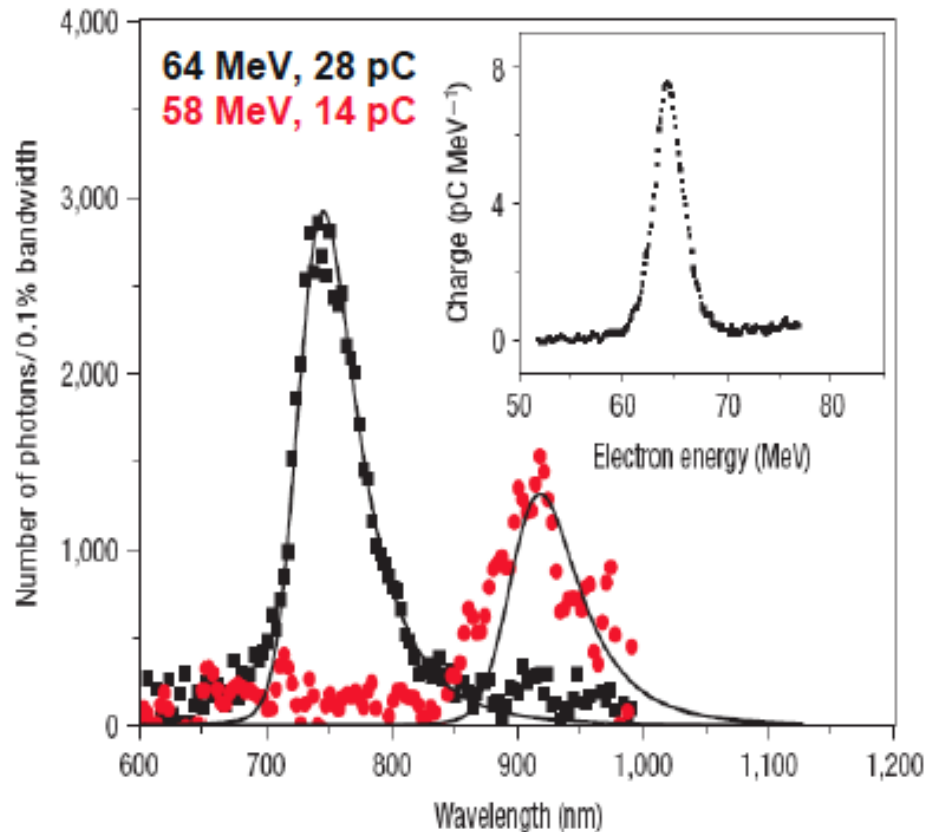
Undulator radiation



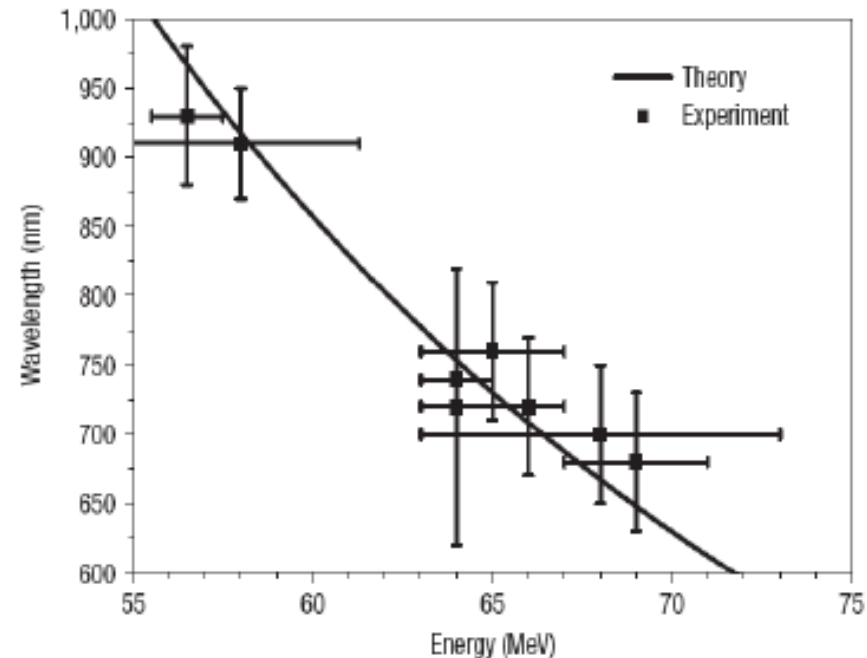
H.P. Schlenvoigt et al., **Nature Physics** 4, 130-133 (2008)-Strathclyde University

Undulator radiation

Radiation spectrum



Rad wavelength vs. beam energy



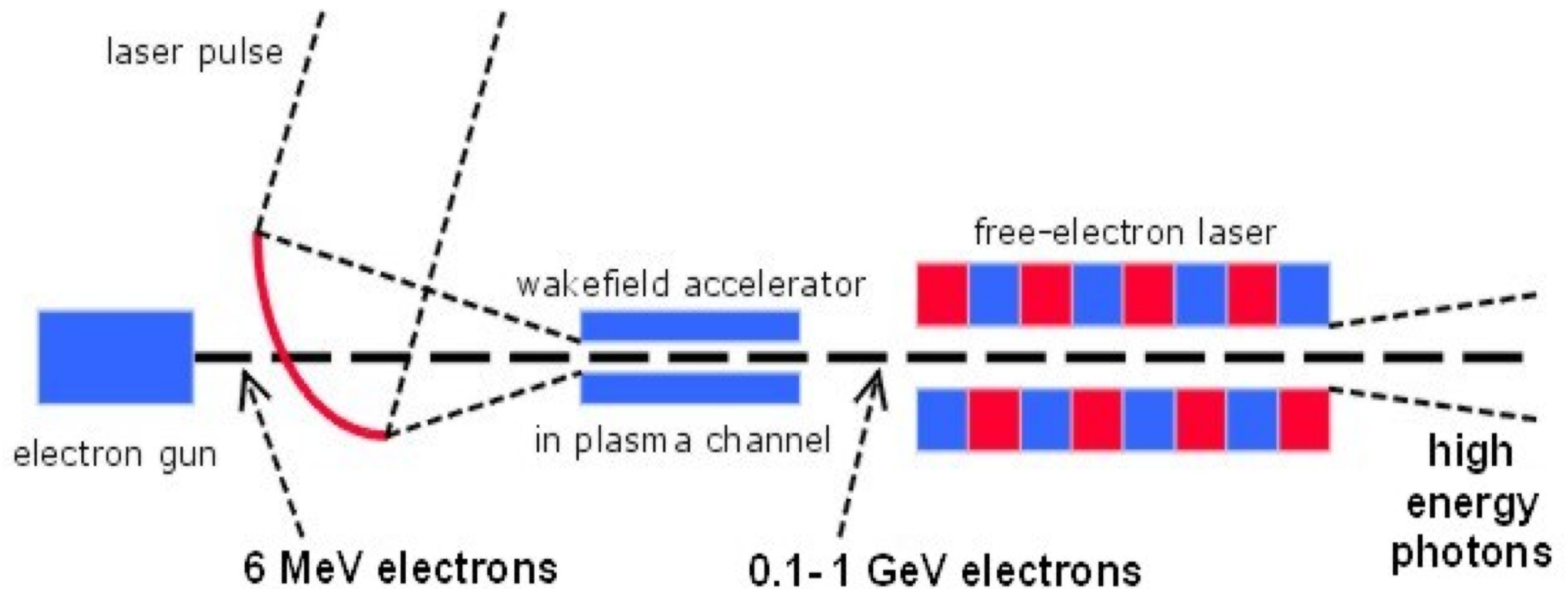
$$\lambda = \frac{\lambda_u}{2\gamma^2} \left(1 + \frac{K^2}{2} \right)$$

H.P. Schlenvoigt et al., **Nature Physics** 4, 130-133 (2008)

X-ray production at ALPHA-X

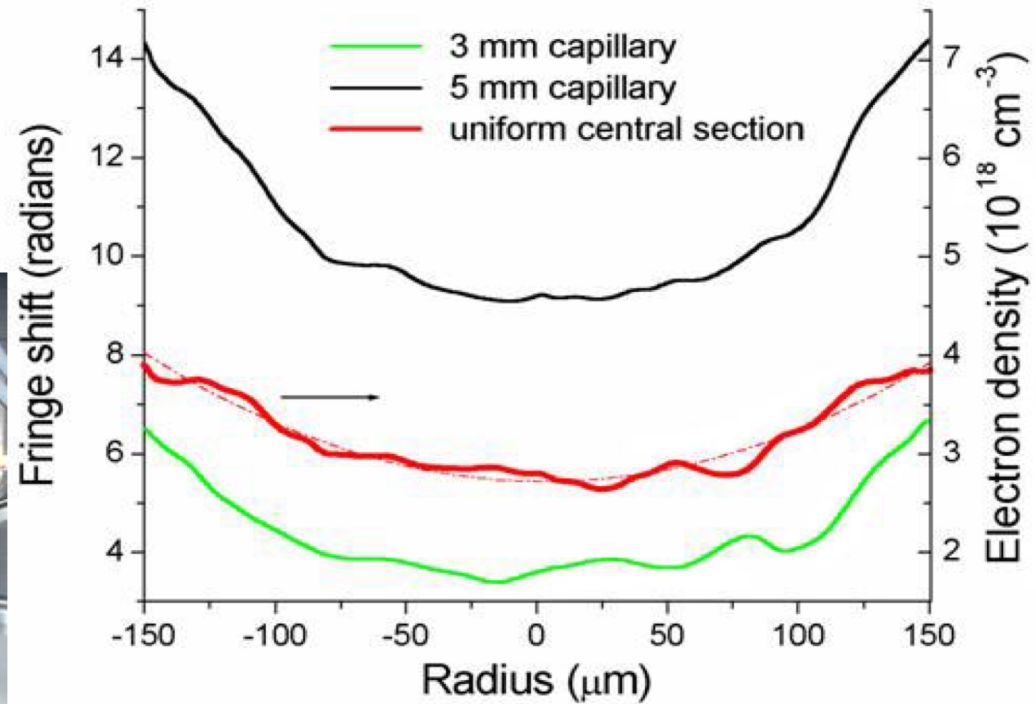
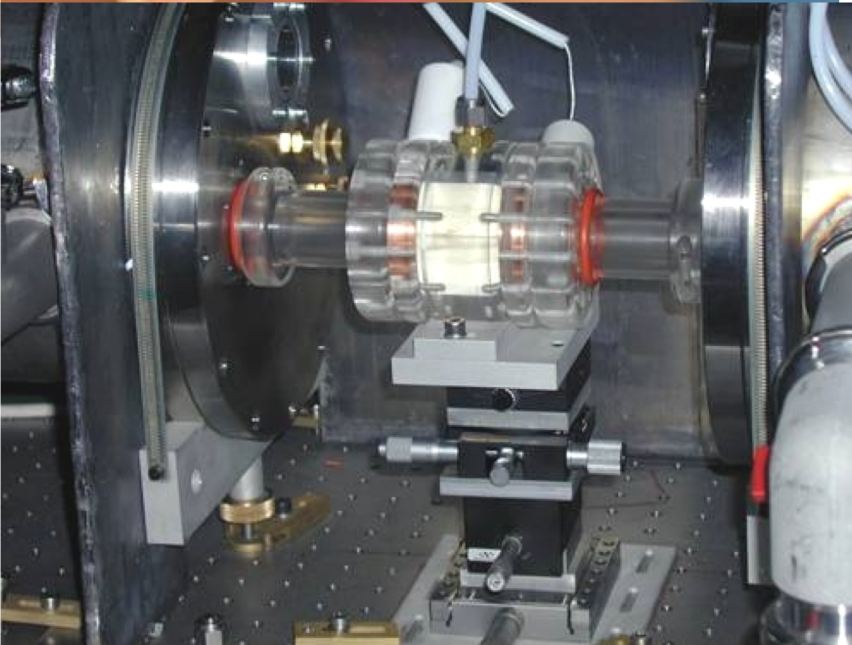
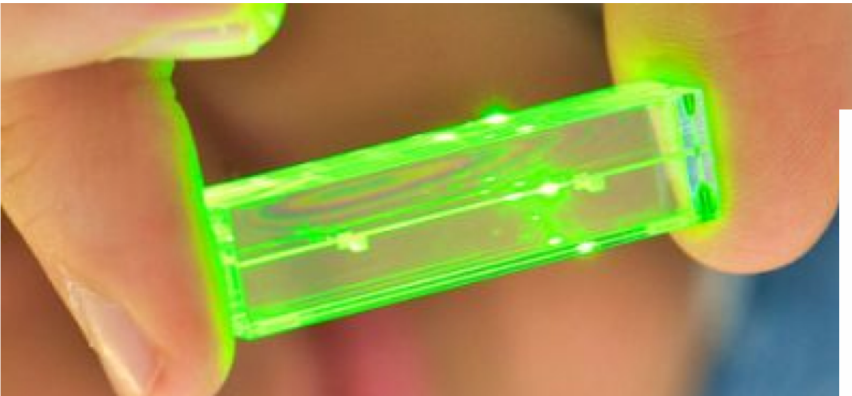
- ALPHA-X (***A**dvanced **L**aser-**P**lasma **H**igh-energy **A**ccelerators towards **X**-rays*)
- Its aim is to develop laser-plasma accelerators and apply these to producing **coherent short-wavelength radiation** in a free-electron laser. To realize these objectives an interdisciplinary programme involving advanced plasma, laser and electron beam physics has been set up. The ultra-short pulses of short wavelength radiation from these compact sources have the potential of revolutionizing time-resolved studies in a wide range of applications.
- The ALPHA-X project began in September 2002.

Layout of ALPHA-X

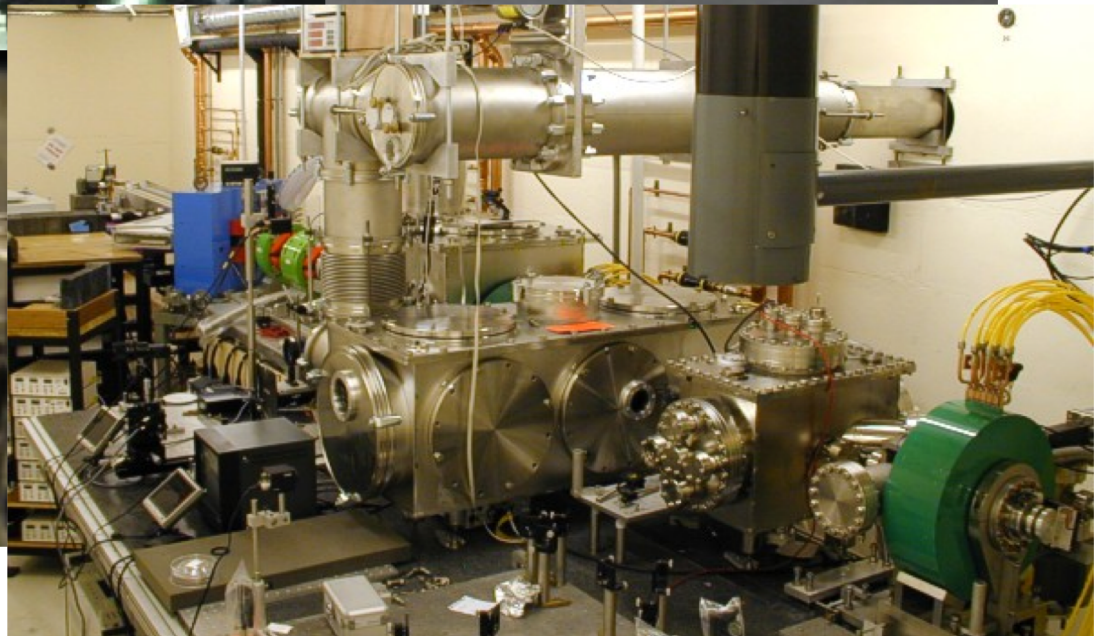
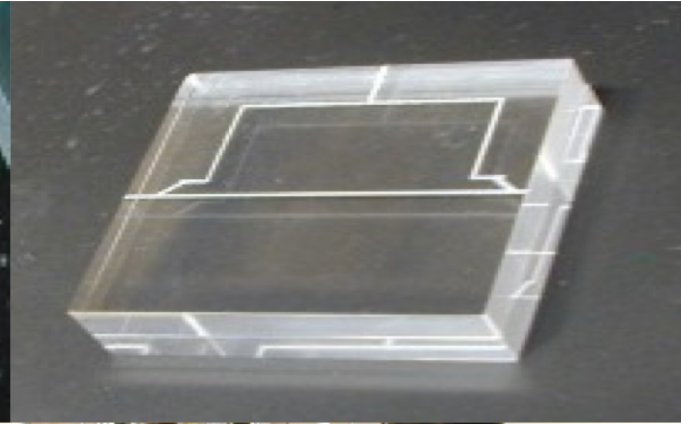
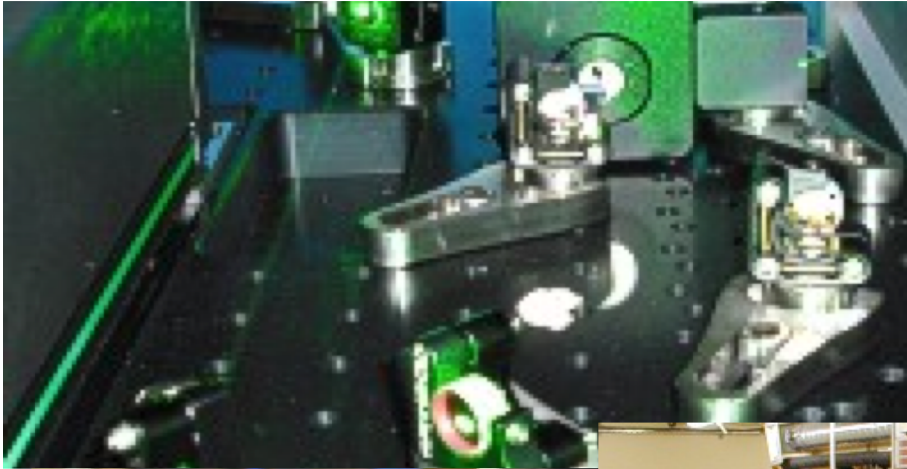


Schematic overview of the ALPHA-X set-up

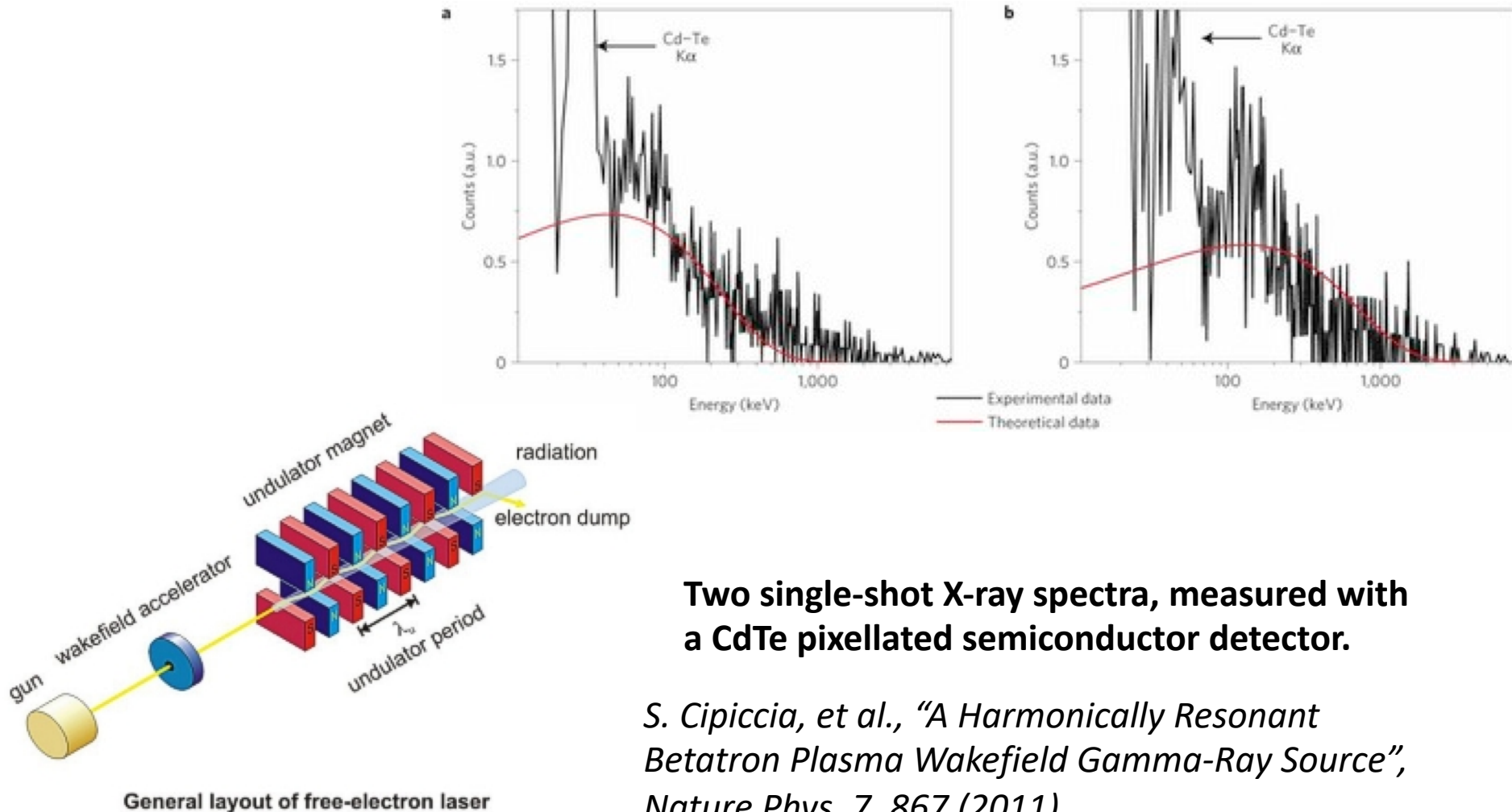
Plasma source-capillary cell



Hardware



Photons



Two single-shot X-ray spectra, measured with a CdTe pixellated semiconductor detector.

S. Cipiccia, et al., "A Harmonically Resonant Betatron Plasma Wakefield Gamma-Ray Source", Nature Phys. 7, 867 (2011)

First FEL gain (2021)

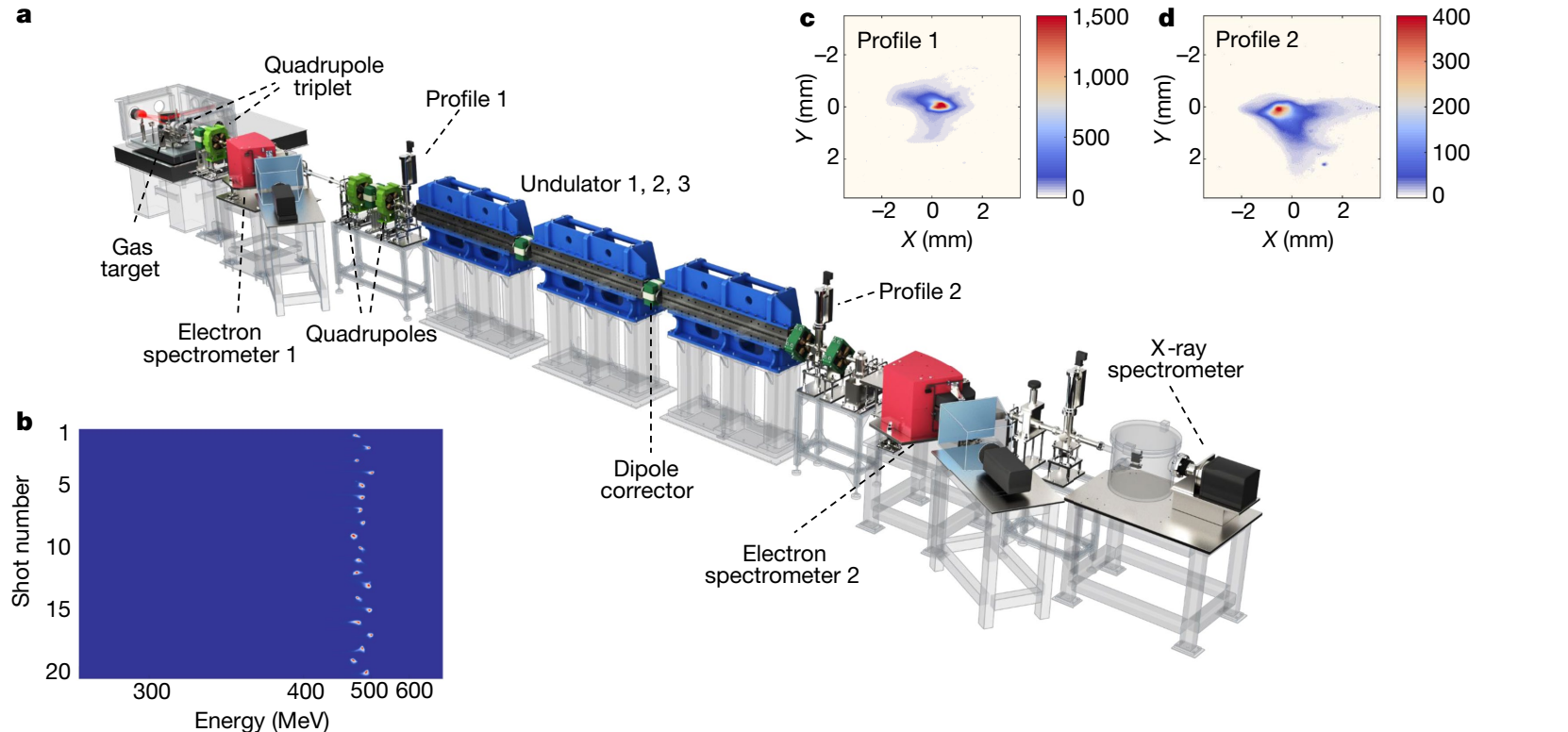
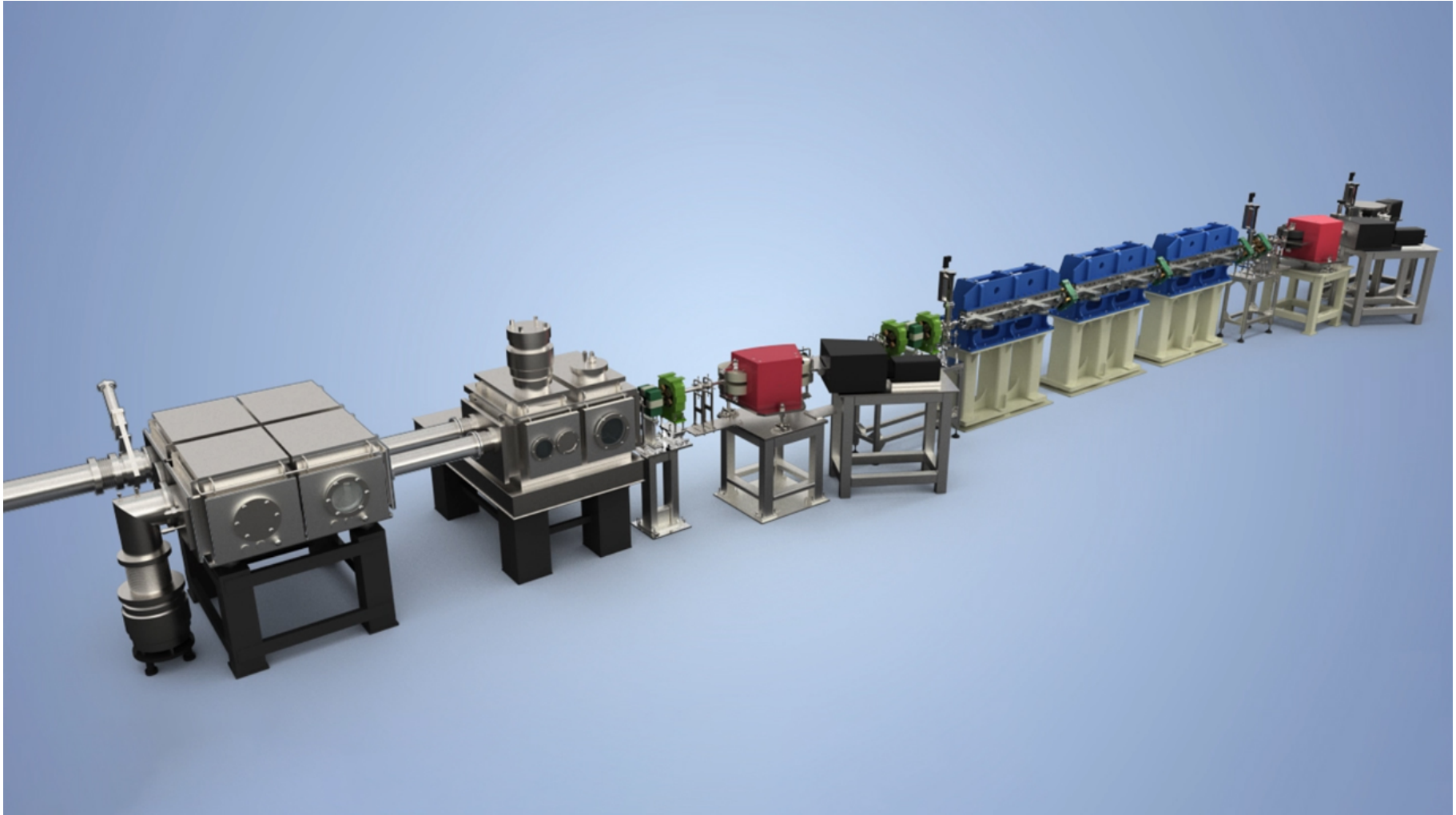


Fig.1|Schematic layout of LWFA-based free electron laser experiment.
a, Undulator beamline with a total length of approximately 12 m from the gas target for the LWFA to the X-ray spectrometer. **b**, Typical spectra of electron

beams from the LWFA for 20 consecutive shots. **c, d**, Measured transverse profiles of the electron beam at the entrance (**c**) and exit (**d**) of the undulators. The scale bars are normalized.

Wentao Wang (SIOM, Shanghai) et al., Nature 595, 516 (2021)

First FEL gain



First FEL gain

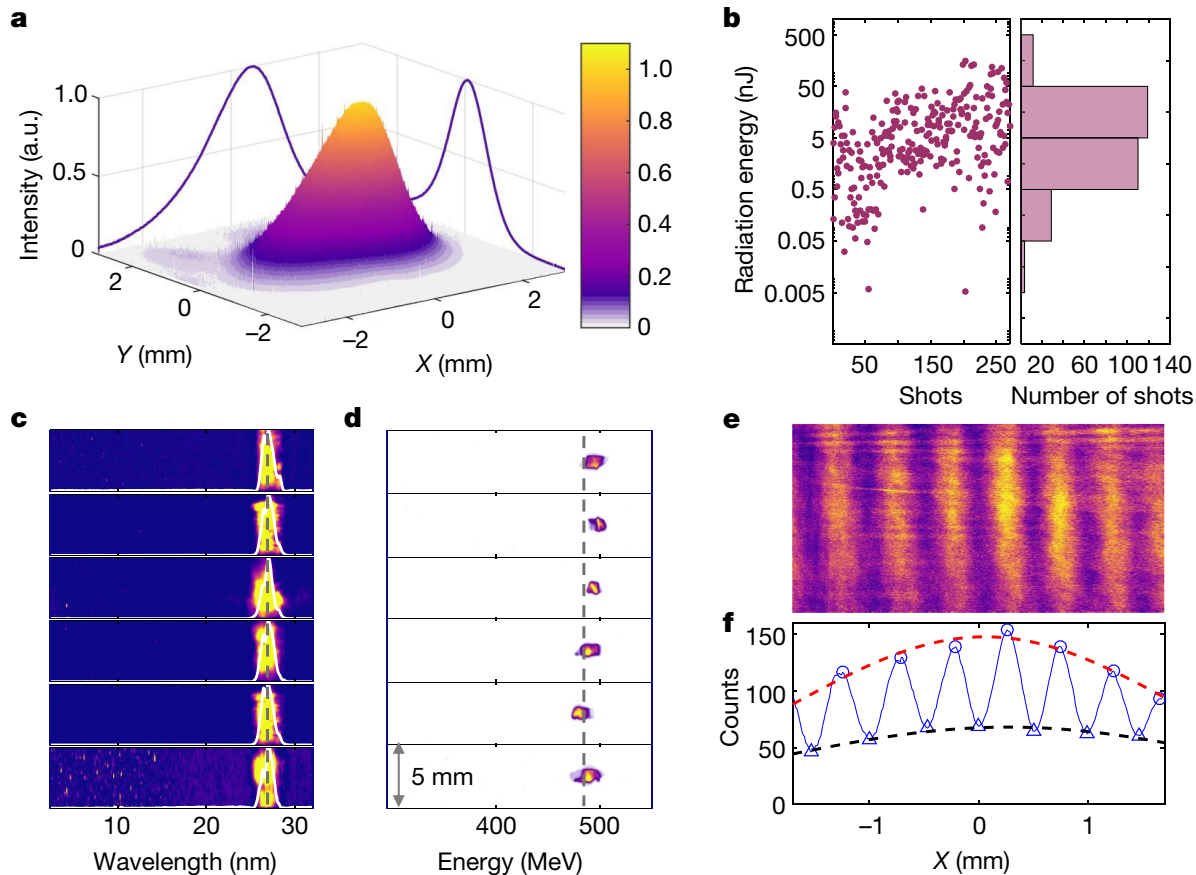


Fig. 2 | Measurement of undulator radiation. **a**, Measured transverse radiation pattern of a typical pulse on the X-ray CCD camera located 12 m downstream from the gas target. The scale bar is normalized. **b**, Shot-to-shot radiation energy over 270 pulses. **c**, **d**, Measured radiation spectra (**c**) and the

corresponding electron-beam energy spectra (**d**) detected by the second spectrometer located at the exit of the undulator. **e**, **f**, Image (**e**) and count profile (**f**) of the interference pattern generated when radiation propagates through two 10- μ m slits with a slit separation of 40 μ m.

Wentao Wang (SIOM, Shanghai) et al., Nature 595, 516 (2021)

X-rays from betatron radiation

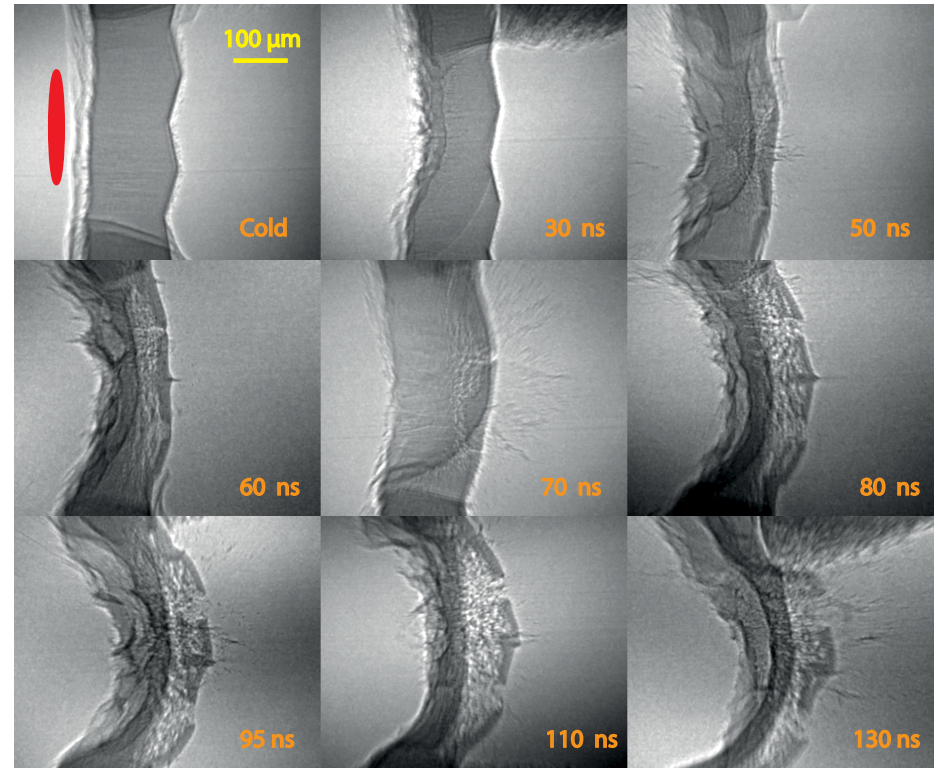
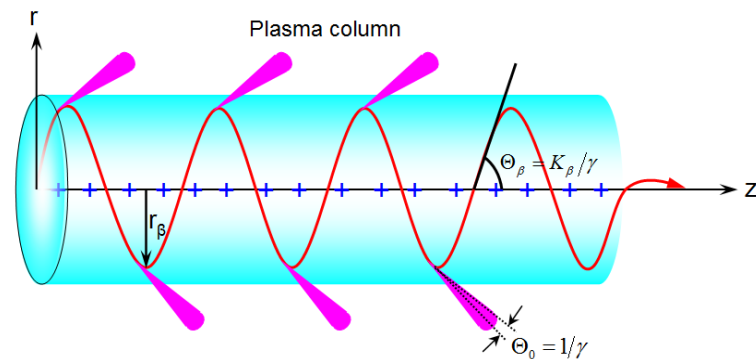
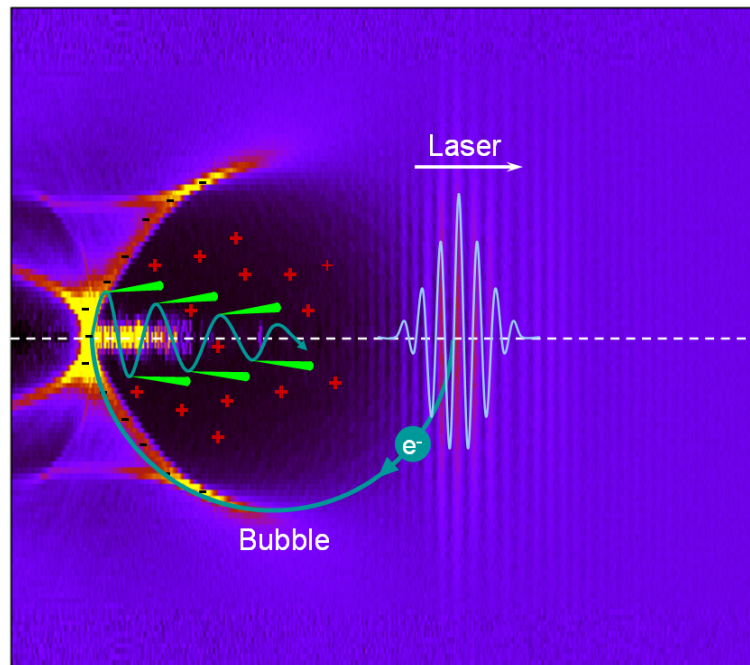
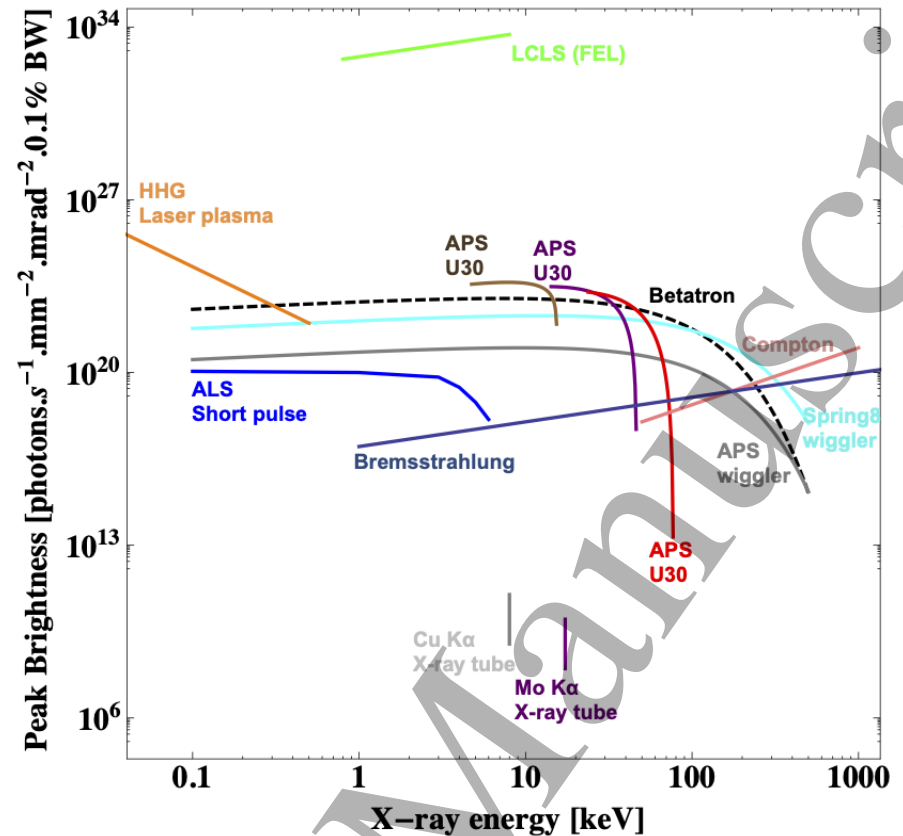
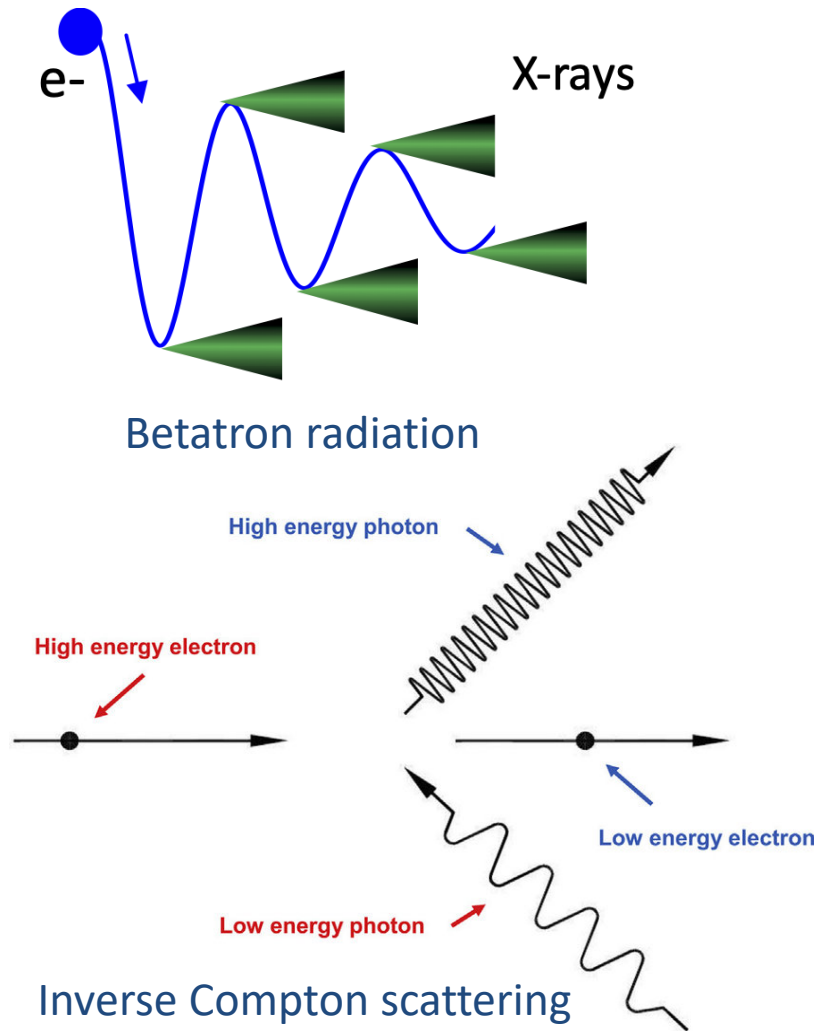


Figure 6.30: Betatron x-ray images of shocks travelling through aluminium taken at a range of delays. The red ellipse in the top left image shows the FWHM size of the drive laser spot. The orange numbers are the delay between the arrival of the shock drive laser and the betatron probe.

J. Wood, PhD thesis (2017-ICL)

X/ γ rays from betatron radiation



Felicie Albert et al 2020 New J. Phys. in press
<https://doi.org/10.1088/1367-2630/abcc62>

Proton/ion acceleration

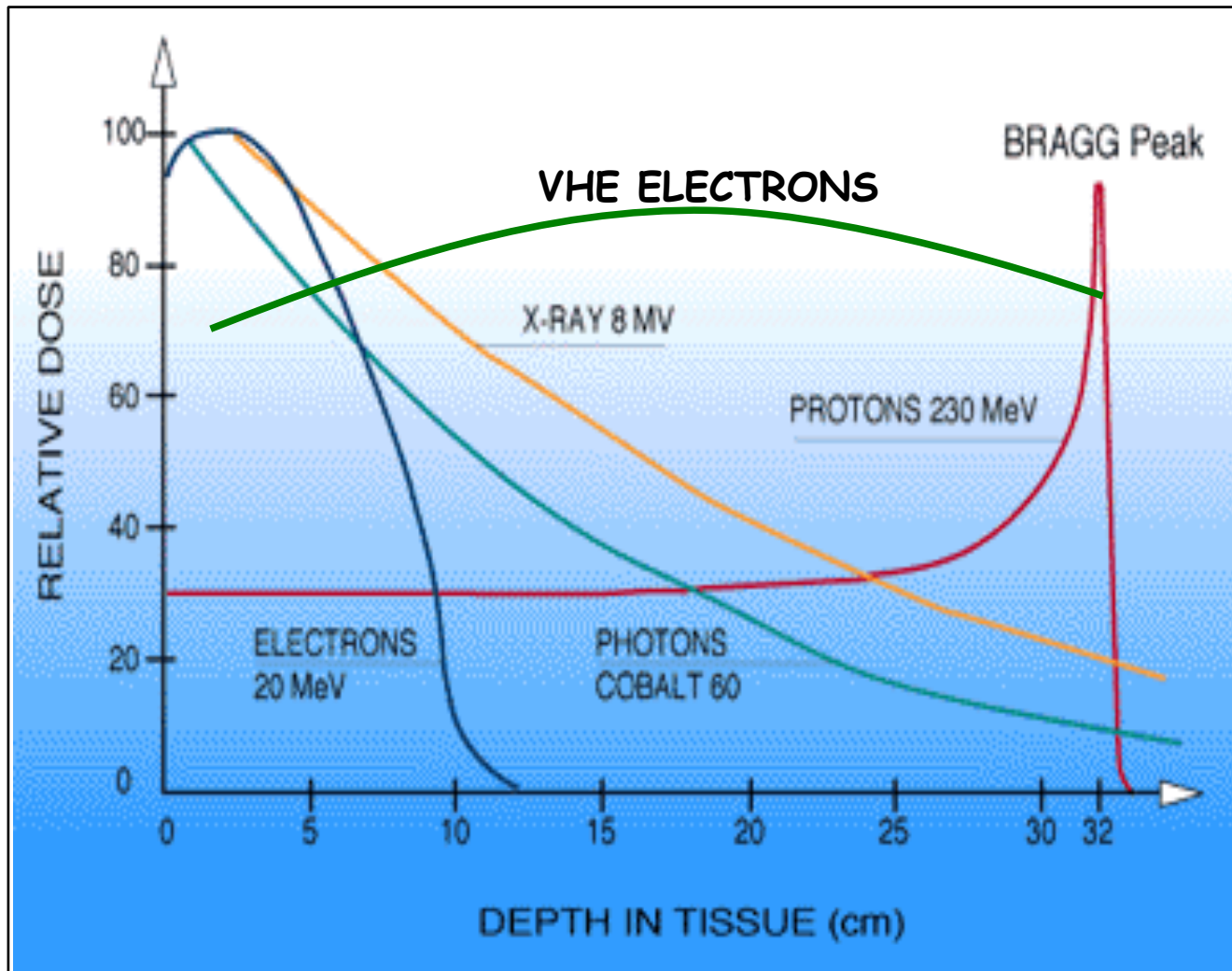
■ Proposed mechanisms

- Laser direct acceleration: light pressure (Shen, PRE 64, 056406 (2004)), needs $a=300$
- Laser driven electrostatic shock (Silva, PRL. 92, 015002 (2004)).
- Laser plasma bubble (Shen, PRE 76, 055402 (r), 2007), $a=300$
- “Target normal sheath acceleration” (B. M. Hegelich, et al., Nature 439, 441 (2006); H. Schwoerer, et al., Nature 439, 445 (2006).)

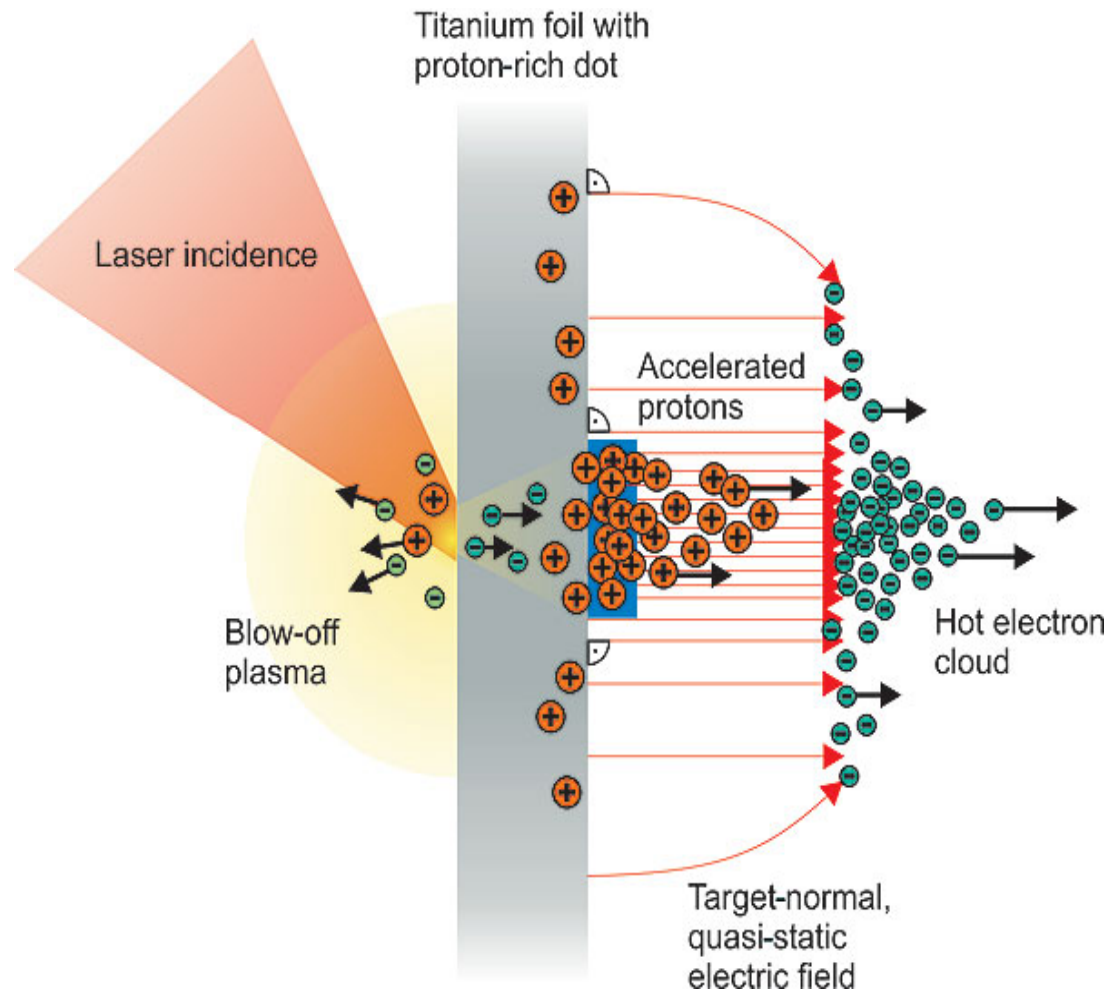
■ Demonstrated “Target normal sheath acceleration” (TNSA)

- quasi mono energetic protons of MeV/proton
- B. M. Hegelich, et al., Nature 439, 441 (2006); H. Schwoerer, et al., Nature 439, 445 (2006).

Medical application: Radiotherapy



Target normal sheath acceleration of protons

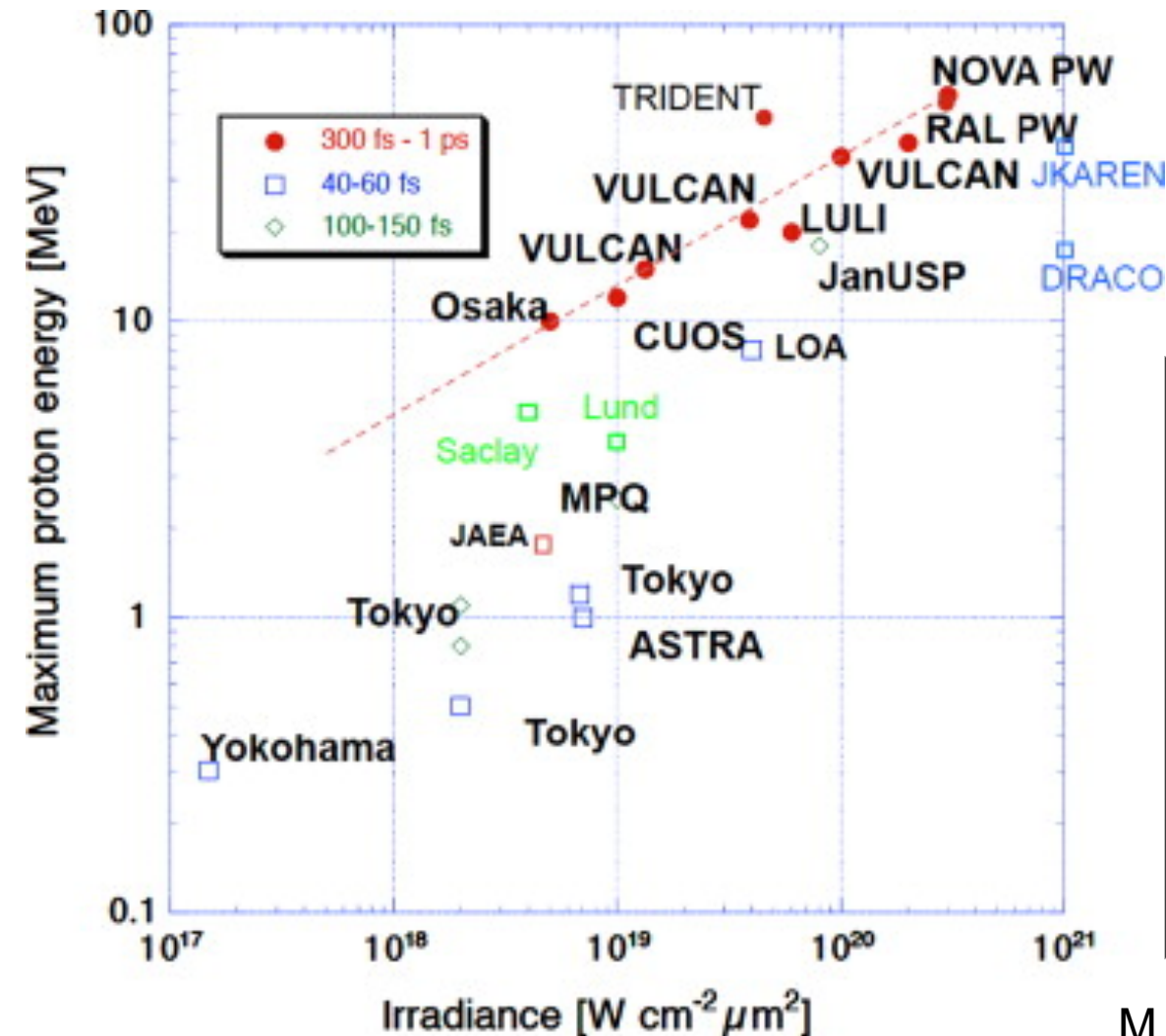


laser intensity $I_L = 3 \times 10^{19} \text{ W cm}^{-2}$

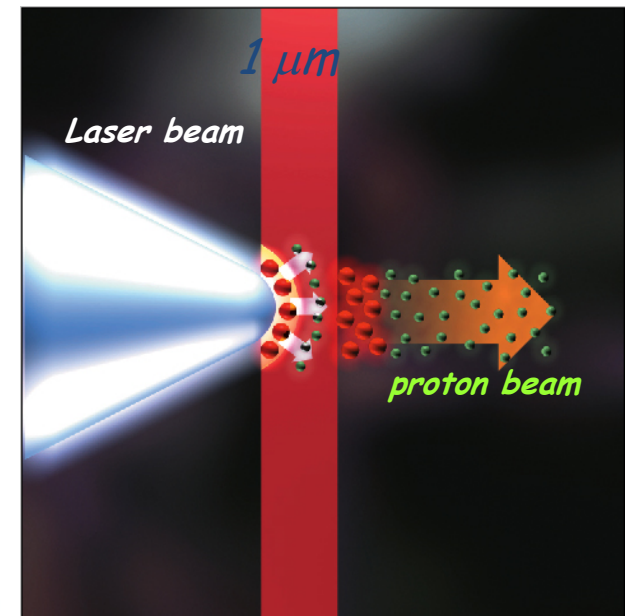
Schwoerer, et al., Nature (London) 439, 445 (2006).

A terawatt (TW)-laser pulse is focused onto the front side of the target foil, where it generates a blow-off plasma and subsequently accelerates electrons. The electrons penetrate the foil, ionize hydrogen and other atoms at the back surface and set up a Debye sheath. The inhomogeneous distribution of the hot electron cloud causes a transversely inhomogeneous accelerating field (target normal sheath acceleration—TNSA). Applying a small hydrogen-rich dot on the back surface enhances the proton yield in the central part of the accelerating field, where it is nearly homogenous. These protons constitute the quasi-monoenergetic bunch.

Proton/ion acceleration



Survey of TNSA cut-off energies measured in experiments so far, plotted vs. irradiance and labeled according to pulse duration.



M. Borghesi, NIMA 740, 6-9 (2014)

Important equations

Quantity	Definition	Engineering Formula
Gaussian Laser Beam Parameters (a_0)		
Focal Spot	$2w_0 = \frac{4\lambda_L}{\pi} \frac{f}{D} = \sqrt{\frac{2}{\ln 2}} d_{FWHM}$	$w_{\frac{1}{e^2}-0} [\mu m] = f / \# \quad @ \lambda_L = 0.8 \mu m$
Confocal Parameter	$2z_R = 2\pi w_0^2 / \lambda_L$	$\Delta z [\mu m] = 2(f / \#)^2 \quad @ \lambda_L = 0.8 \mu m$
Peak Power	$P_0 = 2\sqrt{\frac{\ln 2}{\pi}} \frac{W_L}{t_{FWHM}}$ $P_0 = \frac{\pi}{4 \ln 2} d_{FWHM}^2 I_0$	$P_0 [TW] = 940 \frac{W_L [J]}{t_{FWHM} [fs]}$ $P_0 [TW] = 0.011 d_{FWHM}^2 [\mu m] I_0 [10^{18} \frac{W}{cm^2}]$
Peak Intensity	$I_0 = \left(\frac{4 \ln 2}{\pi}\right)^{\frac{3}{2}} \frac{W_L}{t_{FWHM} d_{FWHM}^2 [\mu m]}$ $I_0 = \frac{2\pi^2 \epsilon_0 m_e^2 c^5}{e^2} \frac{a_0^2}{\lambda_L^2}$	$I_0 [10^{18} \frac{W}{cm^2}] = 83 \times 10^3 \frac{W_L [J]}{t_{FWHM} [fs] d_{FWHM}^2 [\mu m]}$ $I_0 [10^{18} \frac{W}{cm^2}] = 1.37 \frac{a_0^2}{\lambda_L^2 [\mu m]}$
Vector Potential	$a_0 = \frac{e}{\pi m_e c^2} \sqrt{\frac{I_0}{2\epsilon_0 c}} \lambda_L$	$a_0 = 0.85 \sqrt{I_0 [10^{18} W cm^{-2}]} \lambda_L [\mu m]$
Peak Electric Field	$E_0 = \frac{e a_0}{c m_e \omega_L}$	$E_0 [10^{12} V/m] = 3.2 \frac{a_0}{\lambda_L [\mu m]}$
Plasma Parameters ($n_e \propto k_p$)		
Plasma Wavelength	$\omega_p = \sqrt{\frac{n_{e,0} e^2}{m_e \epsilon_0}}$	$\lambda_p [\mu m] = \frac{33.4}{\sqrt{n_{e,0} [10^{18} cm^{-3}]}}$
Wavebreaking Field	$E_{p,0} = \frac{m_e c \omega_p}{e}$	$E_{p,0} [GV m^{-1}] = 96 \sqrt{n_{e,0} [10^{18} cm^{-3}]}$
Plasma Gamma Factor	$\gamma_p = \sqrt{\frac{n_{cr}}{n_e}}$	$\gamma_p = 33.4 \frac{1}{n_{e,0} [10^{18} cm^{-3}] \lambda_L [\mu m]}$
Critical Density	$n_{e,c} = \frac{\epsilon_0 m_e}{e^2} \omega_L^2$	$n_{e,c} [cm^{-3}] = \frac{1.1 \times 10^{21}}{\lambda_L^2 [\mu m]}$
LWFA Parameters in the Bubble Regime ($r_b = 2\sqrt{a_0}/k_p$)		
Dephasing Length	$L_d = \frac{2}{3\pi} \sqrt{a_0} \lambda_L \left(\frac{n_c}{n_{e,0}}\right)^{3/2}$	$L_d [mm] = 7.9 \sqrt{a_0} \left(\frac{\lambda_L^{-4/3} [\mu m]}{n_{e,0} [10^{18} cm^{-3}]}\right)^{3/2}$
Electric Field	$E_p = \frac{m_e c \omega_p}{e} \sqrt{a_0}$	$E_p [GV m^{-1}] = 96 \sqrt{n_{e,0} [10^{18} cm^{-3}]} \sqrt{a_0}$
Electron Energy	$W_{el} = \frac{2a_0}{3} \left(\frac{n_c}{n_{e,0}}\right) m_e c^2$	$W_{el} [MeV] \approx 380 \frac{a_0}{n_{e,0} [10^{18} cm^{-3}] \lambda_L^2 [\mu m]}$
Optimum Charge	$Q_{opt} = \frac{\pi c^3}{e^2} \sqrt{\frac{m_e^3 \epsilon_0^3}{n_{e,0}}} a_0^{\frac{3}{2}}$	$Q_{opt} [pC] = 75 \sqrt{\frac{a_0^3}{n_{e,0} [10^{18} cm^{-3}]}}$

J. Wenz and S. Karsch,
arXiv: 2007.04622v1
(2020)

LWFA- current status

Laser plasma accelerators have demonstrated:

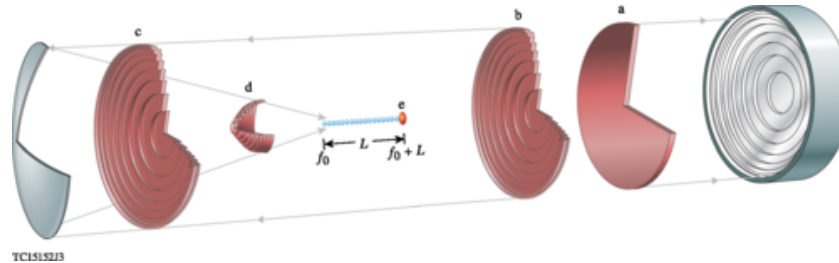
- Energy gains of 1 MeV to 8 GeV
- E-fields of 1 GV/m to 1000 GV/m
- Good e-beam quality : Emittance $\sim \pi \text{mm mrad}$
- Charge at high energy
- Quasi monoenergetic
- Very high peak current : 100 kA

LWFA advantages:

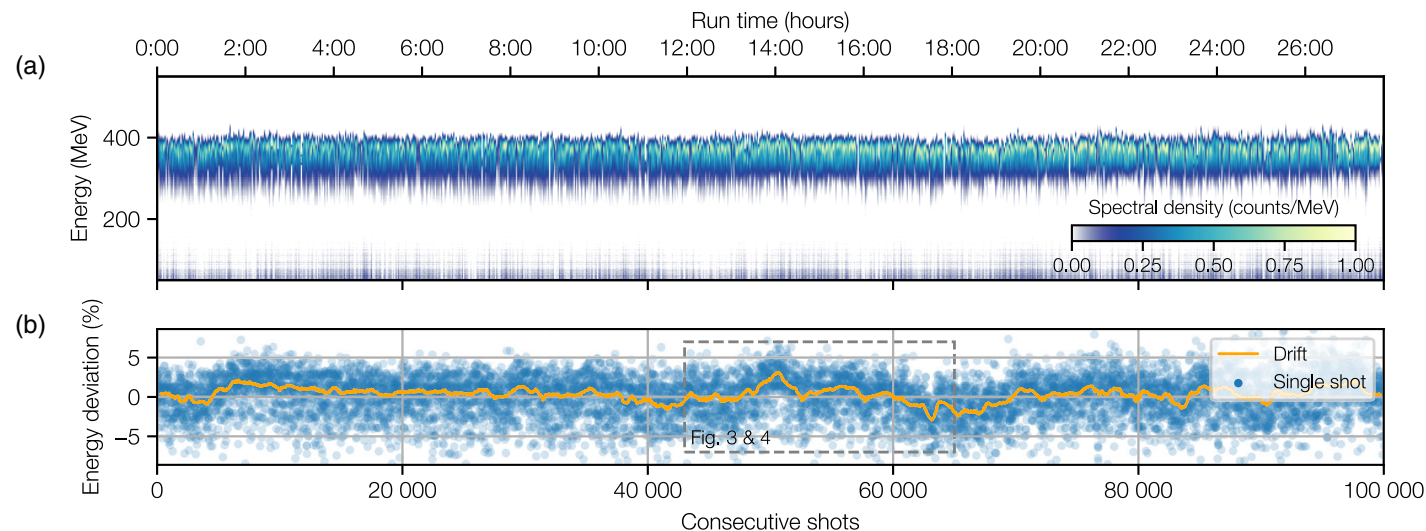
- Provide e-beam with new parameters :
 - Ultrashort
 - High current
 - Collimated
 - Compact and low cost

New developments

- Dephasingless laser wakefield acceleration (DLWFA)
(J.P. Palastro, et al., PRL 124, 134802 (2020))



- Long time operation of LPA
(A. R. Maier et al., Phys. Rev. X 10, 031039 (2020))



ICUIL World Map of Ultrahigh Intensity Laser Capabilities



C. P. J. Barty

Future perspectives

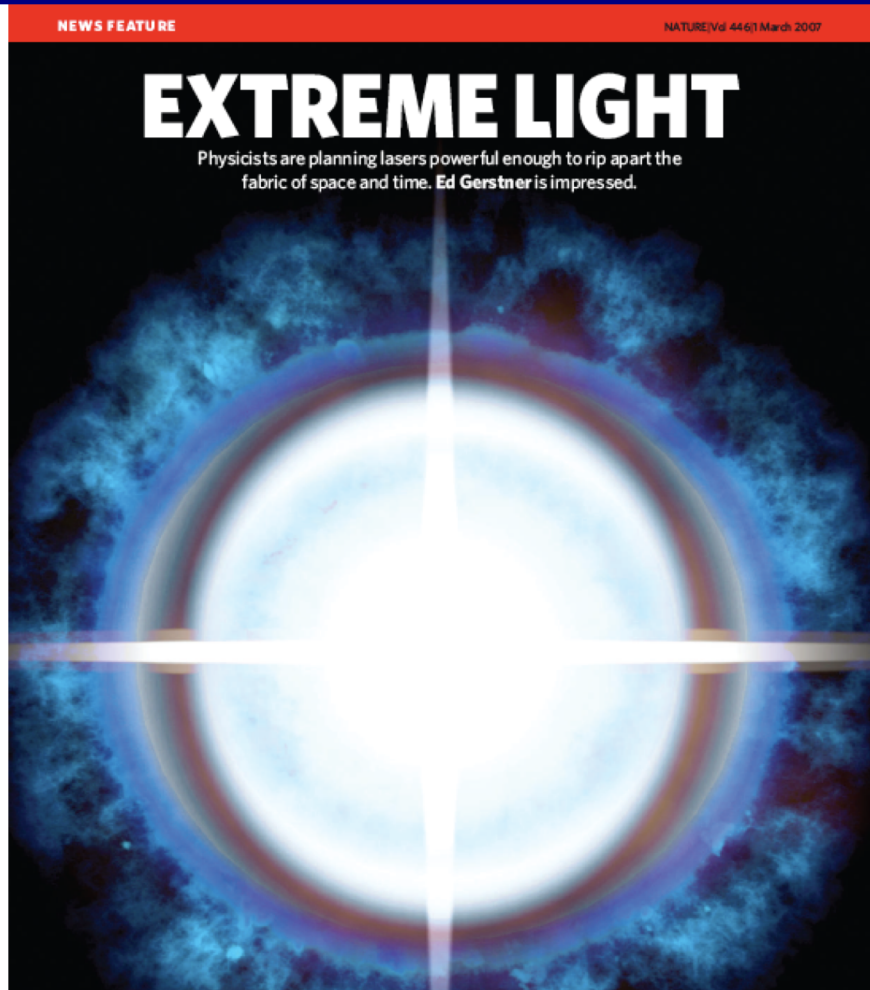
Design future accelerators based on LWFA:

- Higher charge, e.g. nC
- Low emittance ($< 1 \mu\text{m}$)
- Small energy spread
- Stable beam, long time operation
- Guiding or PW class laser system
- Multiple stage coupling/synchronization

Accelerator system development:

- Compact XFELs
- Applications (chemistry, radiotherapy, material science)
- Colliders for HEP

Extreme Light Infrastructure-ELI



**European Project
for development of
extreme light**

**Beam acceleration
is one work package**

... hundreds of GeV ...

Projection from the actual experimental and theoretical data achieved with 100 TW laser to ELI indicates that hundreds of GeV electron bunch could be generated. Indeed, the central

Future perspectives -ELI

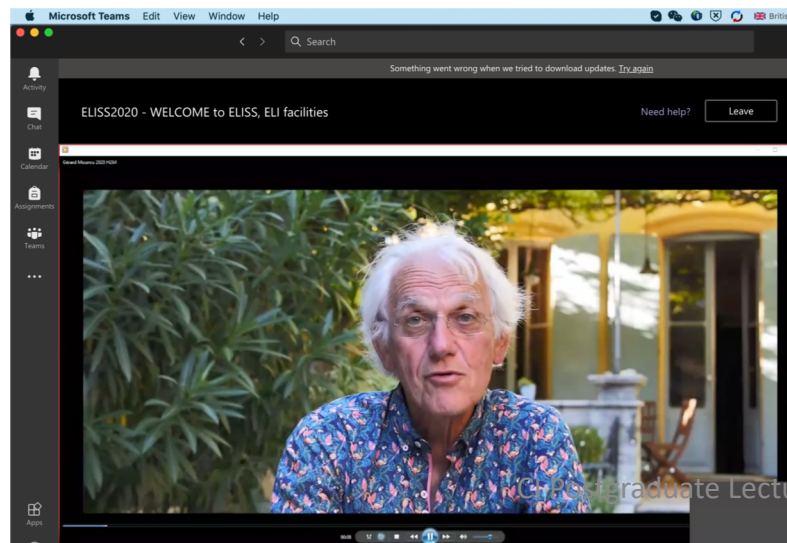
Pushing the energy frontier

ELI – Extreme Light Infrastructure

Centres in the Czech Republic,
Romania, Hungary.

10 – 200(?) PW lasers at up to
10Hz, compared to 1PW now

Goal of 10s GeV



Future perspectives-other facilities

Pushing towards applications

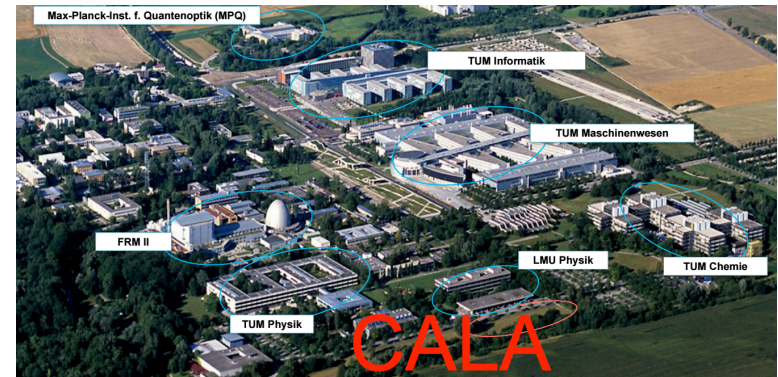
CALA - Centre for Advanced Laser Applications, Munich

3PW @ 10 Hz

SCAPA – Scottish Centre for the Application of Plasma-based Accelerators

0.35 – 1 PW

Designed for x-ray imaging and hadron therapy applications



Future perspectives

Pushing towards accelerators

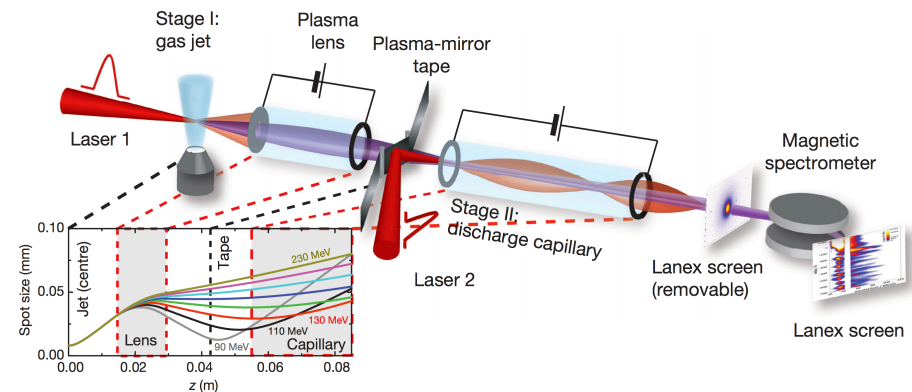
EuPRAXIA – project to develop dedicated 5 GeV LWFA facility

R. Assmann, et al., The European Physical Journal Special Topics 229 (24) 3675 (2020)

Demonstration of LWFA staging, required to beat limitations on laser pulse energy



THE MAJOR OBJECTIVE OF THE EUPRAXIA DESIGN STUDY IS THE PREPARATION OF A CONCEPTUAL DESIGN REPORT FOR THE WORLDWIDE FIRST PLASMA-BASED ACCELERATOR AT 5 GEV WITH INDUSTRIAL BEAM QUALITY AND TWO USER AREAS.



S. Steinke *et al*, Nature, 2016

Conclusions

- Short wavelength accelerators hold promise to miniaturize the future machines
- The development of laser plasma-based accelerators have achieved tremendous success in last few decades.
- The ultimate goal is to get high quality beams (high energy, low emittance , low energy spread, high current, ultrashort pulse, stable beam).
- The applications of LWFA is enormous, not only for HEP, but also many other areas, e.g. FEL, radiation sources, VHEE, proton therapy, colliders.

References

- T. Tajima and J. Dawson, Phys. Rev. Lett. 43, 267-270 (1979).
- E. Esarey, P. Sprangle et al., IEEE Trans. Plasma Sci. 24, 252-288 (1996).
- A. Modena et al., Nature 377, 606-608 (1995).
- V. Malka et al., Science 298, 1596-1600 (2002).
- W.P. Leemans et al., Nature Physics 2, 696 (2006).
- S. P.D. Mangles et al., Nature 431, 535 (2004).
- C. G.R. Geddes et al., Nature 431, 538 (2004).
- J. Faure et al., Nature 431, 541 (2004).
- H. Schworer et al., Nature 439, 445 (2006).
- E. Esarey et al., Rev. Mod. Phys. 81, 1229 (2009).
- S. Hooker, Nature Photonics 7, 775 (2013).
- W. Leemans et al., Phys. Rev. Lett. 113, 245002 (2014).
- A. Picksley et al., Phys. Rev. Lett. 133, 255001 (2024).
- AIP proceedings on Advanced Accelerator Concepts (...2008, 2010, 2012, 2014, 2016, 2018, 2020, 2022)
- Proceeding papers on LPAW Workshops(...2007, 2009, 2011, 2013, 2015, 2017, 2019, 2021)
- Proceeding papers on European Advanced Accelerator Concepts Workshop (2013, 2015, 2017, 2019, 2021)
- CERN Yellow Report, CERN-2016-001.
- J. Wenz and S. Karsch, arXiv: 2007.04622v1 (2020).
- R. Assmann, et al., The European Physical Journal Special Topics 229 (24) 3675 (2020)
- A. R. Maier et al., Phys. Rev. X 10, 031039 (2020)
- C. Joshi, S. Corde and W.B. Mori, Phys. Plasmas 27, 070602 (2020)
- Felicie Albert et al 2020 New J. Phys. in press <https://doi.org/10.1088/1367-2630/abcc62>
- W. Wang et al., Nature 595, 516 (2021).

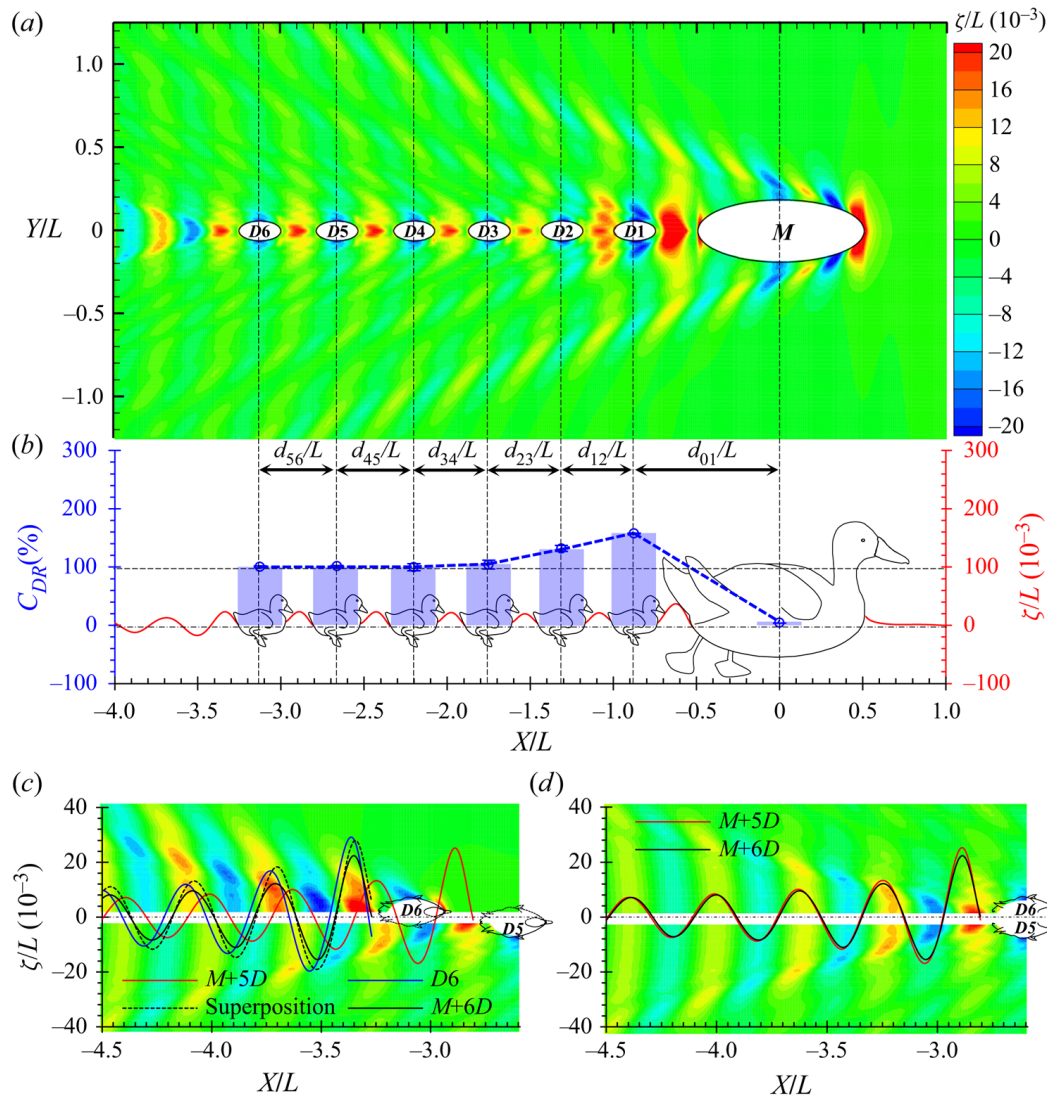
Learning outcomes-Lecture I

- ✓ Motivations for short wavelength accelerators
- ✓ How laser-plasma acceleration works
- ✓ Limitations of laser plasma accelerators
- ✓ Applications of laser-plasma accelerators

Real life examples



Real life examples



ig Noble Prize 2022!

Real life examples



a



S. J. Portugal., et al., Nature 505, 399 (2014)

Surfing waves, dreaming tiny!



Plasma accelerators to market

Physics ▾ Technology ▾ Community ▾ In focus Magazine

Jobs | [Twitter](#) | [Search](#)



APPLICATIONS | CAREERS

Taking plasma accelerators to market

7 October 2022

Newly established US firm TAU Systems aims to commercialise laser-plasma wakefield accelerators for applications ranging from medical imaging to advanced light sources.



Björn Hegelich and Jerome Paye

Eyes down TAU Systems CEO Björn Manuel Hegelich (left) and COO Jerome Paye in the lab at Texas. Credit: TAU Systems

In 1997, physics undergraduate Manuel Hegelich attended a lecture by a visiting



Advertisements



CERN Courier December 2022